Data Report for Video Plankton Recorder Cruise R/V Peter W. Anderson, February 23-28, 1999

Massachusetts Water Resources Authority

Environmental Quality Department
Report 2000-03

Data Report for Video Plankton Recorder Cruise
OSV *Peter W. Anderson*, February 23-28, 1999

Submitted to

Massachusetts Water Resources Authority
Environmental Quality Department
100 First Avenue
Charlestown Navy Yard
Boston, MA 02129

Prepared by

Cabell S. Davis
and
Scott M. Gallager

Consultants to:
SeaScan Inc., 346 Gifford St., Falmouth, MA 02540
(Under Subcontract with Battelle Ocean Sciences,
397 Washington St., Duxbury, MA 02332)

Davis, C. S. and S. M. Gallager. 2000. Data Report for Video Plankton Recorder Cruise OSV Peter W. Anderson, February 23-28, 1999. Boston: Massachusetts Water Resources Authority. Report 2000-03. 132 p.

ABSTRACT

This data report presents results from a Video Plankton Recorder survey of Massachusetts and Cape Cod Bays during February 23-28, 1999 on the EPA ship OSV *Peter W. Anderson*. The purpose of the survey was to obtain high-resolution data on the 3-dimensional spatial distribution of dominant planktonic taxa together with environmental variables (temperature, salinity, density, fluorescence, attenuation, downwelling light) during late winter. These high-resolution spatial data augment the data being collected by the on-going Harbor Outfall Monitoring (HOM) surveys of water column properties (including plankton) conducted by the Massachusetts Water Resource Authority (MWRA).

The survey was interrupted by a severe northeast storm on February 25-26, so it was carried out in two parts: pre-storm and post-storm. A total of 80 hours of video and environmental data were collected during the survey, which covered an along track distance of 472 nautical miles (873 km). Data were obtained for temperature, salinity, fluorescence, beam attenuation, downwelling light, and abundance of dominant large plankton and mesozooplankton taxa. Data for phytoplankton and zooplankton were obtained from high and low magnification video cameras, respectively.

Three characteristic water types were found in the Bays including the warm salty Massachusetts Bay Bottom Water (MBBW), the colder fresher Cape Ann Plume Water (CAPW), and very cold and fresh Barnstable Cold Plume Water (BCPW). In general, the T/S plot was characterized by upper and lower regions. Data in the upper region was located in the northern portion of Mass Bay and represented the transition from inshore MBBW to CAPW. Data in the lower portion of the T/S plot was located in both Mass Bay and in Cape Cod Bay and represented the transition from offshore MBBW and BCPW.

The different plankton taxa had different water-type affinities, thus providing some insights into their origins. A distinctive feature of the plankton was a large bloom of the diatom *Chaetoceros socialis*. The data suggest that rod-shaped diatom and *Chaetoceros socialis* colonies came from northeastern Mass Bay offshore and were transported and mixed through the middle of the bay into Cape Cod Bay. The copepods on the other hand were abundant in both eastern and western MBBW but did not penetrate into Cape Cod Bay to the extent the diatoms did. The zooplankton did penetrate into the eastern Mass Bay Bottom Water near the Nearfield region. This situation is in marked contrast with March 1998 when the water and plankton in Cape Cod Bay appeared to be a result of water flowing west and south along the coast from Cape Ann into Cape Cod Bay. The February 1999 data indicate that the route to Cape Cod Bay may have been from offshore in northeast Mass Bay down through the center of the bay, not following the coast as in 1998. Part of this difference may be due to the earlier cruise date in 1999 (February versus March), which may have preceded the strong low-salinity plume from Cape Ann that typically feeds into Cape Cod Bay later in the spring.

An initial comparison of VPR data with data from the late February 1999 HOM survey indicated that the data are in general agreement. The HOM zooplankton data indicate that the bulk of the copepods observed by the VPR are *Pseudocalanus* sp., which is a dominant prey species of the right whale. High winds precluded formation of dense copepod patches during the cruise and only one right whale was sighted. Correlation length scales of copepods from the VPR data indicate that HOM stations further apart than 20km can be treated as independent (eg. F01 and F02).

SUMMARY

This data report presents results from a Video Plankton Recorder survey of Massachusetts and Cape Cod Bays during February 23-28, 1999. The purpose of the survey was to obtain high-resolution data on the 3-dimensional spatial distribution of dominant planktonic taxa together with environmental variables (temperature, salinity, density, fluorescence, attenuation, downwelling light) during late winter. These high-resolution spatial data augment the data being collected by the on-going Harbor Outfall Monitoring (HOM) surveys of water column properties (including plankton) conducted by the Massachusetts Water Resource Authority (MWRA).

General Context — It is well known that plankton abundance varies over a broad range of temporal and spatial scales, and that this variability has proven difficult to quantify using conventional sampling equipment (eg. nets, pumps, bottles). As a result, we have a limited understanding of the underlying processes controlling plankton abundance patterns. In Massachusetts and Cape Cod Bays, there is an important societal need to understand the variations in the plankton, as this region is impacted by anthropogenic sources of contaminants. The Bays provide a rich source of seafood and serve as a principal feeding habitat for the endangered northern right whale.

In preparation for the relocation of the Boston Harbor Sewer Outfall 16 km offshore into western Massachusetts Bay, considerable effort has been mounted by MWRA to monitor many ecological components of Bays system including the plankton, benthos, and fishes. The plankton taxonomic monitoring has consisted of 11 stations sampled 6 times per year and 2 stations sampled 17 times per year, and there now exists several years of baseline data. Preliminary analysis of these data indicate that this sampling scheme provides an adequate baseline of information for determining possible changes in the plankton populations after the new outfall comes on line. Detecting change however will not necessarily provide insights into the causes of the change or what remedial action may be needed.

To augment the baseline plankton data with high-resolution distributional data on plankton and associated environmental variables, a Video Plankton Recorder survey was conducted covering the entire region of Massachusetts and Cape Cod Bays during February 23-28, 1999. These data will help provide insights into how and why the plankton are distributed in the Bays over a broad range of scales. This report describes the methods used during the cruise as well as the post-cruise data processing, visualization, and analysis.

This cruise was aboard the Environmental Protection Agency (EPA) vessel OSV *Peter W. Anderson* (AN9902) and was the third in a series of winter VPR surveys on this ship (Davis and Gallager, 1998a, 1998b, 1999, 2000). A bay-wide VPR survey on the OSV *Anderson* also was conducted in June 1998, and a local copepod patch-mapping survey was conducted using the VPR on the R/V *Halos* in March 1996 (Davis and Gallager, 2000). The present report presents the data for the February 1999 cruise only (AN9902) (Davis and Gallager, 1999). Other data are presented in Davis and Gallager (1998b) and Davis and Gallager (2000).

Results — The cruise was interrupted by a severe northeast storm on February 25-26 that had high winds and left 24 inches of snow on Cape Cod. Data were collected over the five-day period with a 24-hour hiatus in Provincetown Harbor, while we waited for the storm to abate.

A total of 80 hours of video and environmental data were collected during the survey, which covered an along track distance of 472 nautical miles (873 km) and had a spatial resolution of centimeters along the towpath of the instrument. Data were obtained for temperature, salinity, fluorescence, beam attenuation, downwelling light, and abundance of dominant plankton as determined from the video. Data from both high and low magnification video cameras were processed in the laboratory after the cruise, rather than at sea, due to the time constraints of the short survey (see below; note: real-time plankton identification is routinely done on longer VPR cruises, Davis et al., submitted).

The high magnification camera is normally used to identify dominant copepod genera such as *Oithona, Calanus, Pseudocalanus,* and *Centropages* as well as large phytoplankton taxa. On this cruise however, dense patches of the large colonial diatom *Chaetoceros socialis* (Sieracki et al, 1999; Davis et al., submitted) obscured the copepods from view in certain areas, so the low magnification camera was used for quantification of zooplankton. The high magnification camera was used to quantify abundance of large diatoms including *C. socialis*, rod-shaped diatoms, and *Chaetoceros* chains. Video from the low magnification camera was used to quantify abundance of marine snow and the following zooplankton taxa: unidentified copepods, *Pseudocalanus* with eggs, pteropods, polychaetes, unidentified large nauplii (likely barnacle nauplii), and unidentified ovals and discs.

To train the neural network, 1357 images from the high-magnification camera and 2248 images from the low magnification camera were selected as representative from several thousand unsorted images. Plankton data were obtained using our automated plankton identification system to sort over ~300,000 high magnification images of plankton captured during the survey and from ~100,000 low magnification images extracted from tapes in the laboratory after the cruise. These in-focus images were extracted by the focus detection system from a total of 17,280,000 images for each camera.

As was observed in March 1998 (Davis and Gallager, 1998b), characteristic water types were found in the Bays in February 1999. In addition to the two main types found in March 1998, which included Massachusetts Bay Bottom Water (MBBW) and Cape Ann Plume Water (CAPW), a third type, termed Barnstable Cold Plume Water (BCPW), was observed in 1999 along the southern coastal region of Cape Cod Bay. CAPW is cold and fresh and was located in the northern part of Massachusetts Bay in the upper part of the water column. MBBW is warmer and saltier and was present throughout the lower part of the water column in Massachusetts Bay. Unlike in 1998 when the T-S diagram indicated that the water in Cape Cod Bay was a mixture of CAPW and MBBW, in 1999, analysis of the T-S properties revealed a distinctive water type in southern Cape Cod Bay characterized by a plume of very cold ($< 2^{o}$ C) and fresh (<31.5 salinity) water off the mouth of Barnstable Harbor and extending westward to the mouth of the Cape Cod Canal and eastward to the region south of Billingsgate Shoal. This plume may have been generated from strong forcing by cold winter winds together with local input from snow melt runoff. In general, the T/S plot was characterized by upper and lower regions. Data in the upper region was located in the northern portion of Mass Bay and represented the transition from inshore MBBW to CAPW. Data in the lower portion of the T/S plot was located in both Mass Bay and in Cape Cod Bay and represented the transition from offshore MBBW and BCPW.

The different planktonic taxa had different water-type affinities, thus providing some insights into their origins. A distinctive feature of the plankton was a large bloom of the diatom *Chaetoceros socialis*. The concentrations were extremely high and were similar in number to the intense *Phaeocystis* bloom observed with the VPR in March 1997 in which peak

abundance was 5-10 colonies/ml (Davis and Gallager, 2000). These high concentrations saturated the VPR image processing system (for the high magnification camera only), such that, in the area of these blooms, the abundance of *C. socialis* and other large phytoplankton could be underestimated by a factor of 10 or more, and the copepods were obscured from view. Thus, we chose to not use this camera for identification of zooplankton taxa. The low magnification images, however, were unaffected by these blooms due to the difference in lighting angle compared with the high magnification camera. We were able to use the low magnification camera to obtain quantitative abundance measurements for zooplankton. The high magnification camera did provide interesting insights into the *relative* distributional patterns of the three dominant taxa of large phytoplankton. In addition to *Chaetoceros socialis*, the other dominant phytoplankton taxa included rod-shaped diatoms and *Chaetoceros* chains.

Interestingly, the patterns of high abundance of these three large diatom taxa did not correspond at all with high fluorescence; in fact, there appeared to be an inverse relationship indicating that other phytoplankton, too small to be observed with the VPR, were responsible for the high fluorescence values. The fluorescence was highest in the Cape Ann Plume Water and generally followed the near-shore coastal regions along the northern and western shores of the bays. By contrast, the abundance of large diatoms was highest away from the coast and near the mouth of Massachusetts Bay. Thus, while the water having high fluorescence followed the upper portion of the T/S plot, the water containing high abundance of the three diatom taxa followed the lower portion of the plot. Rod-shaped diatoms and *C. socialis* had similar patterns, their distributions extending from the offshore region of northern Mass Bay (especially deeper in the water column) and running through the middle of Mass Bay into central and eastern Cape Cod Bay. This pattern matched the T/S line connecting MBBW and CCBW, so there appeared to be a route of transport from northern offshore Mass Bay into central and eastern Cape Cod Bay. By contrast, *Chaetoceros* chains were most abundant in the offshore region of southern Mass Bay, and in regions of high abundance of these chains, there was lower abundance of diatom rods and *C. socialis*. A large patch of *C. socialis* was observed next to Provincetown in the right whale feeding grounds off Herring Cove.

For zooplankton, because the low magnification camera was used, the level of taxonomic identification was limited to major taxonomic groups, including copepods, unidentified large nauplii (probably barnacles), *Pseudocalanus* with eggs, pteropods, polychaetes, and unidentified ovals and disks. In addition to zooplankton groups, marine snow was quantified using this camera. The copepods large enough to be seen and quantified with this camera included individuals with a prosome length greater than 1.0 mm. At this time of year, the dominant genera of this size include the copepods *Calanus* and *Pseudocalanus*, the principal food of the right whale. The magnification of this camera is not high enough to see the typically very abundant but smaller copepod *Oithona*. Interestingly, copepod abundance appeared inversely related to chlorophyll and most closely followed the abundance patterns for the large diatoms, especially *Chaetoceros* chains. The T/S plankton plot for copepods reveals that this group was most abundant along the lower portion of the plot, along the line running from MBBW to BCPW, but was restricted largely to MBBW regions of the plot. Copepods were more abundant in the lower portion of the water column, especially in the Nearfield Region of the outfall site. At the surface, copepods were most abundant in the central regions of the Bays. Low concentrations were observed in the right whale feeding ground off Provincetown, and in general the copepod concentrations were low (<< 1 / liter) throughout the Bays with no pronounced swarms or dense patches observed. Copepod

nauplii, *Pseudocalanus* with eggs, disks, and ovals all had similar patterns to that of copepods suggesting that these groups are related. The disks and ovals likely comprised copepods in head-on or askew orientations (at this magnification it was not always possible to distinguish the antennae or urosome on the copepods), since copepods were the dominant group in this size range. Pteropods were found to be relatively abundant during this cruise. Their distributional patterns matched closely that of the copepods suggesting a common offshore origin via the MBBW. Polychaetes also were plentiful in the Bays; these may have been Tomopterids, as we have seen many of these in the shoaler regions of Georges Bank, but not in the Bays before. Marine snow was found to have highest concentrations in the southern half of Mass Bay and in the southwestern region of Cape Cod Bay, the latter region corresponding geographically, but not vertically, with the region of high beam attenuation. We also saw many unidentified fish larvae, but these were not plentiful enough to quantify in terms of their distributional patterns.

To examine the length scales for the spatial variability for the plankton and environmental variables, correlograms from the kriging process were used. The correlograms are the normalized covariance of abundance values plotted versus lagged distance. As was found in the 1998 data, the planktonic taxa exhibited a sharp loss of correlation over very short distances (< 2 km). Such a decline was not observed in the physical variables or in fluorescence or attenuation, implying taxa-specific small-scale patchiness. Unlike 1998, a large negative correlation at large scales (40-60 km) was not observed for any of the taxa or for fluorescence. Instead, no correlation was found at larger scales. On the other hand, the physical variables (T, S, density) and beam attenuation all had large negative correlations at large scales. The reason for this between-year difference may be due to the lack of a pronounced north/south gradient in plankton abundance as was observed in 1998. Instead, the plankton were distributed over long distances throughout the Bays.

These data, like those obtained in March 1998, provide insights into the spatial distribution of dominant phytoplankton and zooplankton taxa as a function of their physical environment. The data suggest that rod-shaped diatom and *Chaetoceros socialis* colonies came from northeastern Mass Bay offshore and were transported and mixed through the middle of the bay into Cape Cod Bay. The copepods on the other hand were abundant in both eastern and western MBBW but did not penetrate into Cape Cod Bay to the extent the diatoms did. The zooplankton did penetrate into the eastern Mass Bay Bottom Water near the Nearfield region. This situation is in marked contrast with March 1998 when the water and plankton in Cape Cod Bay appeared to be a result of water flowing west and south along the coast from Cape Ann into Cape Cod Bay. The February 1999 data indicate that the route to Cape Cod Bay may have been from offshore in northeast Mass Bay down through the center of the bay, not following the coast as in 1998. Part of this difference may be due to the earlier cruise date in 1999 (February versus March), which may have preceded the strong low-salinity plume from Cape Ann that typically feeds into Cape Cod Bay later in the spring.

These data, together with data from other VPR surveys, need to be examined in relation to historical data, data from the HOM surveys, as well as from moorings, satellites, and the weather service, to obtain a more complete picture of the mechanisms of transport of plankton through the Bays. Further statistical analysis comparing VPR data with MWRA net tow data is recommended. The VPR data may be useful in determining underlying statistical distributions of the plankton, which could aid in design of statistical models for determining differences between pre- and post-discharge plankton abundance using the HOM data. The initial analysis done here reveals that the correlation length scale for copepods during this

cruise was about 20 km, which suggests the stations spaced further than this distance in the HOM survey, e.g. F01 and F02 in Cape Cod Bay, provide independent samples of the copepod populations.

TABLE OF CONTENTS

ABSTRACT 3

SUMMARY 4

LIST OF TABLES 11

LIST OF FIGURES 11

1.0 INTRODUCTION 14

2.0 OBJECTIVES 16

3.0 METHODS 16

3.1 The VPR 16
3.1.1 Underwater Unit 16
3.1.2 Cable and Winch 16
3.1.3 Deployment/Retrieval 17
3.1.4 Environmental Data Logging, Processing, and Display 17
3.1.5 Video Recording, Processing, and Display 17
3.2 Survey Design and Tow Pattern 18
3.3 Post-Cruise Data Processing, Display, and Analysis 19
3.3.1 Video Processing / Focus Detection 19
3.3.2 Plankton Identification 19
3.3.3 Classification accuracy 20
3.3.4 Data visualization 21
3.3.5 Correlation Length Scales 22
3.3.6 Temperature-Salinity-Plankton Plots 22
3.3.7 Satellite Imagery 22

4.0 RESULTS AND DISCUSSION 22

4.1 Overview 22
4.2 Distributional Patterns of Environmental Variables 23
4.2.1 Temperature 23
4.2.2 Salinity 24
4.2.3 Seawater Density 24
4.2.4 Temperature-Salinity Relationships 25
4.2.5 Down-welling Light 26
4.2.6 Fluorescence 26
4.2.7 Attenuation 27
4.3 Distributional Patterns in Plankton Taxa 27
4.3.1 General Abundance Values 27
4.3.2 Rod-Shaped Diatoms 27
4.3.3 Temperature-Salinity-Plankton Relationships 28

4.3.4 Chaetoceros Chains 29
4.3.4 Chaetoceros socialis colonies 30
4.3.5 Copepods 31
4.3.7 Unidentified Disks and Ovals 31
4.3.8 Nauplii 32
4.3.9 Pseudocalanus with eggs 32
4.3.10 Polychaetes 33
4.3.11 Pteropods 33
4.3.12 Marine Snow 34
4.4 Correlation Length Scales 34
4.4.1 Physical Variables 34
4.4.2 Fluorescence and Attenuation 35
4.4.3 Planktonic Taxa 35
4.4.3.1 Diatoms 35
4.4.3.2 Zooplankton and Marine Snow 36
4.5 HOM-VPR Data Comparison 37
4.5.1 Temperature-salinity comparisons 37
4.5.2 Comparison of Temperature-Salinity-Phytoplankton relationships. 38
4.5.2.1 T – S – Fluorescence 39
4.5.2.2 T – S –Phytoplankton taxa 39
4.5.3 HOM-VPR Zooplankton Data Comparison 40
4.5.3.1 Copepod Species Composition 40
4.5.3.2 Comparison of Copepod Abundance 41
4.5.3.3 Correlogram for VPR “Simulated Plankton Tows” 41

LITERATURE CITED 42

APPENDIX 45

Cruise Narrative 45
VIDEO TAPE INVENTORY 50
Watch Schedule 51
Cruise Participants, Scientific Party 51
Ship's Officers/Crew 51

FIGURES 52

LIST OF TABLES

Table 1. Plankton taxa observed in video. 20
Table 2. Abundance (#/liter) of plankton observed during 5-s time-bins. 27
Table 3. Phytoplanton species identified in the HOM samples and grouped for comarison with the VPR data. 38
Table 4. HOM data used in the T-S-P plots. 39

LIST OF FIGURES

Figure 1A. Pre-Storm VPR Survey Track – OSV *Peter W. Anderson* February 23-25, 1999
Figure 1B. Post-Storm VPR Survey Track – OSV *Peter W. Anderson,* February 26-28, 1999

Figure 2A. Temperature (^{o}C): Along-track curtain plot of VPR data.
Figure 2B. Temperature > 1.5 ^{o}C: Along-track curtain plot of VPR data.
Figure 2C. Temperature (^{o}C): AVHRR Satellite Image
Figure 2D. Temperature (^{o}C): Stacked kriging plots of VPR data at 10m depth layers.
Figure 2E. Temperature > 1.5 ^{o}C: Stacked kriging plots of VPR data
Figure 2F. Temperature (^{o}C): Barnstable to Gloucester Transects: Pre- vs. Post-storm

Figure 3A. Salinity: Along-track curtain plot of VPR data.
Figure 3B. Salinity: Stacked kriging plots of VPR data at 10m depth layers.

Figure 4A. Density (σ_t): Along-track curtain plot of VPR data.
Figure 4B. Density (σ_t): Stacked kriging plots of VPR data at 10m depth layers.
Figure 4C. Density (σ_t):. Barnstable to Gloucester Transects: Pre- vs. Post-storm

Figure 5A. Temperature – Salinity Plot
Figure 5B. Color-coded Temperature – Salinity Plot
Figure 5C. 3-D dot-plot of data locations, with T-S color coded as in Fig. 5A.

Figure 6. Downwelling Light (W/m^2): Along-track curtain plot of VPR data.

Figure 7A. Fluorescence (µg Chl a / liter): Along-track curtain plot of VPR data.
Figure 7B. Fluorescence (µg Chl a / liter): Stacked kriging plots of VPR data
Figure 7C. Fluorescence (µg Chl a / liter): Barnstable to Gloucester Transects: Pre- vs. Post-storm

Figure 8A. Attenuation (beam-C): Along-track curtain plot of VPR data
Figure 8B. Attenuation (beam-C): Stacked kriging plots at 10m depth layers

Figure 9A. Rod-Shaped Diatoms: Sample of images used for training.
Figure 9B. Rod-Shaped Diatoms (#/liter): Along-track curtain plot of VPR data.
Figure 9C. Rod-Shaped Diatoms (log10[(#/liter+1)]): Along-track curtain plot.
Figure 9D. Rod-Shaped Diatoms (#/liter): Stacked kriging plots at 10m layers

Figure 10A, B, C. Temperature-Salinity-Plankton Plots (Plankton abundance in #/liter)

Figure 11A. *Chaetoceros* Chains: Sample of images used for training
Figure 11B. *Chaetoceros* Chains (#/liter): Along-track curtain plot of VPR data.
Figure 11C. *Chaetoceros* Chains (#/liter): Stacked kriging plots at 10m layers

Figure 12A. *Chaetoceros socialis* colonies: Sample of images used for training.
Figure 12B. *Chaetoceros socialis* colonies (#/liter): Along-track curtain plot
Figure 12C. *Chaetoceros socialis* colonies (#/liter): Stacked kriging plots

Figure 13A. Copepods: Sample of images used for training
Figure 13B. Copepods (#/liter): Along-track curtain plot of VPR data.
Figure 13C. Copepods (#/liter): Stacked kriging plots of VPR data at 10m layers.

Figure 14A. Disks, Unidentified: Sample of images used for training.
Figure 14B. Disks, Unidentified (#/liter): Along-track curtain plot of VPR data.
Figure 14C. Disks, Unidentified (#/liter): Stacked kriging plots at 10m layers.

Figure 15A. Ovals, Unidentified: Sample of images used for training .
Figure 15B. Ovals, Unidentified (#/liter): Along-track curtain plot of VPR data.
Figure 15C. Ovals, Unidentified (#/liter): Stacked kriging plots at 10m layers.

Figure 16A. Nauplii: Sample of images used for training the automatic classifier.
Figure 16B. Nauplii (#/liter): Along-track curtain plot of VPR data.
Figure 16C. Nauplii (#/liter): Stacked kriging plots of VPR data at 10m layers.

Figure 17A. *Pseudocalanus* with eggs: Sample of images used for training
Figure 17B. *Pseudocalanus* with eggs (#/liter): Along-track curtain plot of VPR data.
Figure 17C. *Pseudocalanus* with eggs (#/liter): Stacked kriging plots at 10m layers.

Figure 18A. Polychaetes: Sample of images used for training the automatic classifier.
Figure 18B. Polychaetes (#/liter): Along-track curtain plot of VPR data.
Figure 18C. Polychaetes (#/liter): Stacked kriging plots at 10m depth layers.

Figure 19A. Pteropods: Sample of images used for training the automatic classifier.
Figure 19B. Pteropods (#/liter): Along-track curtain plot of VPR data.
Figure 19C. Pteropods (#/liter): Stacked kriging plots at 10m depth layers.

Figure 20A. Marine Snow: Sample of images used for training the automatic classifier.
Figure 20B. Marine Snow (#/liter): Along-track curtain plot of VPR data.
Figure 20C. Marine Snow (#/liter): Stacked kriging plots at 10m depth layers.

Figure 21A. Correlograms for Temperature
Figure 21B. Correlograms for Salinity
Figure 21C. Correlograms for Fluorescence
Figure 21D. Correlograms for Attenuation

Figure 22A. Correlograms for Rod-Shaped Diatoms
Figure 22B. Correlograms for *Chaetoceros* Chains
Figure 22C. Correlograms for *Chaetoceros socialis* colonies
Figure 22D. Correlograms for Copepods
Figure 22E. Correlograms for Disks, Unidentified
Figure 22F. Correlograms for Ovals, Unidentified
Figure 22G. Correlograms for Nauplii
Figure 22H. Correlograms for *Pseudocalanus* with eggs
Figure 22I. Correlograms for Polychaetes
Figure 22J. Correlograms for Pteropods
Figure 22K. Correlograms for Marine Snow

Figure 23A. Locations of stations used in HOM-VPR T-S comparisons.
Figure 23B HOM T-S plot (black dots) superimposed on VPR T-S plot.
Figure 23C. HOM T-S-P plots for phytoplankton superimposed on VPR T-S plot.

Figure 24A. HOM copepod species composition and abundance.
Figure 24B. HOM (red) and VPR (blue) copepod abundances plotted together.

Figure 25. Correlogram for VPR data grouped as “simulated plankton tows”

1.0 INTRODUCTION

Processes controlling plankton population abundance in the sea operate over a wide range of spatial and temporal scales (Haury et al., 1978). Multi-scale sampling of plankton abundance and associated environmental variables can provide insights into the causes of plankton patchiness (e.g. Gallager and Davis, 1994). Historically, spatial heterogeneity in plankton abundance has been studied for a long time (Haeckel, 1890; Hardy and Gunther, 1935; Hardy, 1936; Cushing, 1975; Fasham, 1978; Haury et al, 1978; Okubo, 1980; Longhurst, 1981; Angel and Fasham, 1983; Mackas et al., 1985; Owen, 1989; Davis et al., 1991; Denman, 1992; Denman and Gargett, 1995). It has been well established that plankton patchiness is strongly correlated with physical variability (e.g., Cassie, 1959a,b, 1960) over a broad range of scales (e.g., Gallager et al., 1996), and that many mechanisms are responsible for the observed patterns (Haury et al., 1978).

In Massachusetts and Cape Cod Bays, historical data on plankton abundance are primarily from widely spaced discrete samples which do not provide adequate multi-scale spatial information (Bigelow, 1926; Toner, 1984; Horst et al., 1984; Bridges et al., 1984; Jossi and Goulet, 1990; Turner, 1994). High-resolution acoustical sampling on Stellwagen Bank revealed a close association of acoustical backscatter and internal waves (Haury et al. 1983), but the extent to which the backscatter was due to plankton, detritus, or physical microstructure remains uncertain, and this study was limited to a small region near the bank.

Since 1992, an extensive Harbor and Outfall Monitoring (HOM) program has been conducted to develop a baseline of information on the ecology of the bays prior to relocation of the MWRA sewer outfall from Boston Harbor to Massachusetts Bay. As part of this monitoring, plankton net hauls have been made 6 times per year at 11 stations spread throughout the bays and 17 times a year at 2 stations near the bay effluent outfall. The MWRA HOM plankton data are sparse by design, and are thought to be sufficient for testing for relocation effects, given the standard assumptions about the statistical distributions of the plankton are correct, i.e. that the plankton are effectively lognormally distributed.

Analysis of variance in the HOM data reveals that the variability is divided approximately evenly between interannual, seasonal, and spatial effects (Cibik et al., 1998). Thus, although high-resolution spatial sampling will increase the statistical power of the tests to a certain extent, natural interannual variability may require that several years of post-relocation data be collected to achieve high enough statistical power for detecting outfall-related changes in the plankton populations.

Even when the power is sufficient, given the sparse nature of the HOM data, understanding causal relationships between significant changes in plankton abundance and the outfall may be difficult. High-resolution sampling may provide needed insights into the spatial relationships between plankton and associated environmental variables, so that strong inferences can be made about causes of observed post-discharge plankton patterns, even during the first year post-discharge.

In sum, high-resolution sampling can help to provide:

- a better estimate of the underlying statistical distribution of the plankton in the bays,
- increased statistical power by quantifying better the plankton spatial variability
- insights into the association of plankton and environmental variables and causes of observed plankton patterns

Toward this end, four broadscale Video Plankton Recorder surveys of the bays have been conducted over the past three years (March 1997, March 1998, June 1998, and February 1999). The objective of these cruises was to characterize the distribution of the major planktonic taxa together with environmental variables. In each year, an intense phytoplankton bloom was observed, but with a different dominant species each time. In 1997, a dense bloom of the noxious alga *Phaeocystis* occurred in Cape Cod Bay and no dense copepod patches were observed. As a result, right whale foraging in the region that year was the most limited on record. In March 1998, a dense bloom of rod-shaped diatoms was observed, and again no dense copepod swarms were observed during the survey (Davis and Gallager, 1998b). Although right whale foraging was extensive in 1998 (Mayo, pers. comm.), we did not observe any over the short period of our March survey. During the June 1998 cruise, the region was surveyed to examine the plankton distributions during the stratified season. Data from the March 1997 and June 1998 surveys are discussed in a separate report to EPA (Davis and Gallager, 2000). To augment the 1997 and 1998 VPR survey data, the fourth VPR survey was conducted in February 1999, thus providing an interannual context to these surveys.

This report describes data from the 1999 VPR survey conducted between February 23-28 using the EPA research vessel *Peter W. Anderson*. The survey consisted of VPR towyo transect lines covering the two bays. As on the prior two VPR surveys on the OSV *Anderson*, the objectives were to:

1) determine the distributional patterns (and dominant length scales of variation) of zooplankton and large phytoplankton taxa and

2) determine the relationship of plankton distributions to associated environmental variables over a broad range of scales to better understand the causes of the observed plankton patterns and to provide a broadscale context within which to interpret the MWRA HOM data

2.0 OBJECTIVES

The objectives of this report are to:

1) present high-resolution distributional data on the plankton and environmental variables from the VPR survey in February 23-28, 1999.

2) quantify the correlation length scales of the plankton and environmental variables

3) examine the spatial relationships between plankton and environmental variables in an effort to understand the causes of the plankton distributional patterns.

3.0 METHODS

3.1 The VPR

3.1.1 Underwater Unit

The Video Plankton Recorder is a towed underwater video microscope that images plankton and seston in the size range from 0.1 - 20 mm (Davis et al., 1992a,b, 1996; Gallager et al., 1996). The VPR included two video cameras, high and low magnification, with fields of view of 7 and 25 mm, respectively. The cameras were synchronized at 60HZ with a xenon strobe (~2 μs pulse duration). The VPR system also included a CTD (Seabird), fluorometer (Wetlabs), transmissometer (Wetlabs), light sensor (Licor 192SA), flow meter (General Oceanics), altimeter, and pinger. The VPR sensors including cameras were mounted on a steel frame attached to the underside of a 3.5' V-fin.

3.1.2 Cable and Winch

The data were telemetered to the surface via 0.68" armored fiber optic tow cable. Fiber optic receivers in the winch drum converted the signals back to analog electric (coax for video, and copper conductors for other data) which were sent through copper slip-rings to the ship's main lab. The winch (Dynacon with level wind) was placed on the starboard quarter of the fantail facing toward port, and the tow cable was fair-led through an aluminum block (30" sheave) suspended from the end of the crane boom.

3.1.3 Deployment/Retrieval

The VPR was towed from the crane boom off the port side of the ship to avoid sampling in the ship's wake. A detailed account of deployment/retrieval methods is given in the cruise report (Davis and Gallager, 1999) and in the cruise narrative (see Appendix).

3.1.4 Environmental Data Logging, Processing, and Display

Environmental data from the VPR underwater unit together with GPS data (position, date, time in GMT), bottom depth data from the ship and time of day (GMT) from a video time-code generator were input to a data-logging PC (486) via multiple serial ports. A C++ program was used to read and parse the incoming data and write it to files on a Zip drive as well as on a hard drive of a Toshiba notebook PC (Tecra 8000 266Mhz Pentium II running Windows NT 4.0) via network file system mount at 10Mbit.

The Toshiba notebook was linked to the image processing system (a 200MHZ Dual-processor Pentium-Pro running MS Windows NT workstation 4) via a 100 megabit local area network. A 10-100Mbit switching box was used to allow communication at 10 and 100Mbit. Environmental data was processed and displayed in real time on the Toshiba notebook using C and Matlab routines. The C routine (called from within the main Matlab controlling program) was used to read and parse data from the active logging file and output the data to a binary Matlab (.mat) file. This file then was loaded into Matlab and the data processed. The environmental data were displayed as 3-D color dot plots using latitude, longitude, and VPR depth as the axes. Dot color was proportional to the value of the variable using a blue-red color map to represent low-high values, respectively.

Because of a fundamental limitation of Microsoft operating systems, the logging file could not be read from while it was being written to. To plot the data (at 2 minute invervals), we had to stop the logging program, copy the file to a temporary file, and then start logging again. The temporary file then was read into the parsing/plotting program. This method caused interruptions in data acquisition which became progressively worse as the logging file grew in size. We thus closed the logging file and opened a new one every few hours. (On subsequent cruises we have switched from NT to Linux as the operating system on the notebook.)

3.1.5 Video Recording, Processing, and Display

The raw video coming from the slip rings via coaxial cables was time-stamped with time code from the time-code generator, displayed on video monitors, and recorded on SVHS tape recorders. Video from the high magnification camera also was sent to the image processing system. Image processing consisted of focus detection, feature extraction, and classification.

The high magnification video was input into the Imaging Technologies Inc. Model 150/40 image processing board contained in the Pentium-Pro computer. A C++ program running on this computer was used for focus detection. On average, about 0.1-1 in-focus objects (i.e. regions of interest, ROI) were observed per second (out of 60 video fields per second) in each camera.

These ROIs were saved to disk as tagged image format (TIF) files using time of day in milliseconds as the filename. The ROI files were saved in subdirectories corresponding to hour and year-day (with Jan 1 = day 0). To avoid differences in time of day between the computer clock and the time code generator, time code was sent to the computer's serial port. When the focus detection program was started, it read the initial time code and then incremented this time, in milliseconds, (using the computer clock) as the ROIs were extracted. Hundreds of thousands of these ROI files were generated during the course of the cruise. A Matlab program running on the Toshiba extracted diagnostic features from the ROIs. These features were saved in files corresponding to each ROI file.

Before automatic identification of the plankton could be done, the neural net classification program needed to be trained. This training is typically performed at the beginning of each cruise to accommodate cruise-specific illumination conditions resulting from camera/strobe alignment and general water clarity. The potential for using an archived set of classifiers for different cruises was investigated, but lighting conditions change markedly from cruise to cruise due to changes in water clarity, so that re-training before each cruise is needed. This training period requires manual sorting of ~2000 images after some period of collection has taken place. We have found that this training period can take 2-3 days to complete given the personnel available and watch schedule for VPR operations. Since most of our cruises are 2 weeks in duration, the initial time required for training is not a problem. On the short Mass Bay VPR surveys, we have completed most of the survey before the training can be done. It was therefore decided to extract the ROIs at sea but to do the training and classification after we returned to the laboratory. After the cruise, training data sets were created for the high magnification camera by copying selected hours of ROIs into a training directory and manually sorting representative ROIs into the proper taxonomic categories. The neural net training program then was run on this set of training ROIs to develop the parameter values needed for classification. The classifier then was used to begin automatically sorting ROIs into taxonomic categories. Low magnification tapes were processed in the laboratory after the cruise. A second training set was sorted and the feature extraction and automatic classification were performed.

3.2 Survey Design and Tow Pattern

As was the case with the prior VPR surveys on the OSV *Anderson*, it was originally planned to conduct a series of orthogonal transect lines running the length and width of the bays. We initially steamed along parallel track lines in Mass Bay but were forced into Provincetown Harbor by a major northeast storm. After the storm, due to persistent high winds and seas and the narrow width of the ship, we had to adjust our track lines so that we were no more than 30 degrees from a line orthogonal to the wave troughs. Nonetheless, the entire area was surveyed. The VPR was towyoed from near surface to

near bottom at a ships speed of 5 knots. The OSV *Anderson* technicians operated the winch while the VPR team monitored and controlled the VPR system from the main lab (using 4 hour shifts). The VPR was towyoed continuously during the 80 hours of survey time. The average distance between towyos was ~500 meters. Since our winch payout and haulback rates are the same for all towyos, the towyo spacing is shorter in shallower water and longer in deeper water. In Cape Cod Bay the median towyo spacing was 460m.

3.3 Post-Cruise Data Processing, Display, and Analysis

3.3.1 Video Processing / Focus Detection

The low magnification video tapes were processed in the laboratory using optimal parameter values for focus detection. The ROIs were saved as a separate camera number since the features and neural network classifiers would be different for the two cameras. Phytoplankton and zooplankton taxa were quantified using high and low magnification cameras, respectively. The phytoplankton data are know to be underestimates of absolute abundance levels (for reasons given below), but the data do provide accurate estimates of the relative distributional patterns for these taxa. The VPR did provide accurate absolute estimates of zooplankton abundance (e.g. see Benfield et al., 1996).

3.3.2 Plankton Identification

Once the ROIs were generated, image features were extracted. A large subset of ROIs for each camera was copied to corresponding training directories for manual sorting. The training ROIs were sorted manually into the various taxonomic groups. Representative ROIs were sorted into a given taxon until that taxon contained a sizable number of ROIs.

The list of taxa identified, the corresponding number of ROIs manually sorted, and the taxa selected for automatic identification are shown in Table 1 for each camera.

Table 1. Plankton taxa observed in video.

TAXON	Number of ROIs Manually Sorted		Used in Training for Automatic Identification
	High Mag	Low Mag	
Diatom, rod-shaped	430		✓
Diatom, *Chaetoceros* chain	229		✓
Diatom, *Chaetoceros socialis*	420		✓
Diatom, sphere	278		
Copepod		426	✓
Ctenophore, lobate		23	
Ctenophore, juvenile		20	
Disk, unidentified		160	✓
Cerianthid		4	
Nauplii, unidentified		120	✓
Fish Larva		22	
Larvacean		46	
Marine snow		544	✓
Irregular, unidentified		100	
Medusa		13	
Oval, unidentified		114	✓
Pseudocalanus w/ eggs		198	✓
Clione		9	
Polychaete		198	✓
Pteropod		215	✓
Shrimp		15	
Siphonophore		13	
Total ROIs sorted	1357	2248	

Only those taxa having a relatively large number of training ROIs were selected for automatic identification. Only *Pseudocalanus* carrying eggs could be readily distinguished from the other copepods, so all other copepods were grouped together as unidentified copepods.

3.3.3 Classification accuracy

For the 11 taxonomic groups automatically identified (Table 1 shaded), the neural network classifier was found to be 87% accurate for the training set. Higher accuracy could be obtained by combining taxa (e.g. grouping the grazers) into 6 groups, but it was felt that the accuracy for the 11 taxa was acceptable and allowed important distributional data on these taxa to be obtained.

3.3.4 Data visualization

The distributional data are displayed in two types of plots. Curtain plots were used to show the along-track vertical distribution of the different variables, while kriging was used to show the horizontal distributional patterns at fixed depths using stacked plots.

The curtain plots were generated by first obtaining the values of a given variable at 5-second intervals along the VPR towpath. The corresponding latitude, longitude, and depth of these data points then were found from the navigational and pressure-sensor data.

For plankton, the number of individuals in a given taxon observed during each 5-s interval was divided by the volume imaged during the interval in liters to obtain abundance in #/liter. The volume imaged per video field by the high magnification camera was 0.5 ml, as given by the product of the field width (0.7 cm), field height (0.55 cm), and depth of field (1.3 cm). The VPR is towed in the direction of the field width, i.e. orthogonal to the camera/strobe axis. Since video fields were acquired at 60 Hz, the volume imaged per 5 s was 0.15 liters for the high magnification camera. For the low magnification camera the dimensions were 2.4 x 2.0 x 1.0 cm for width x height x depth, respectively, for a volume of 4.8 ml per field and 1.44 liters/5s.

In general, the VPR is a proven instrument in terms of its ability to quantitatively sample zooplankton. An extensive comparison between the VPR and MOCNESS samplers is given in Benfield et al. (1996).

Once the values in each 5-s interval were obtained, the cumulative distance traveled along the cruise track (in kilometers) was determined from the latitude and longitude. The values then were interpolated to a regular grid (x,z) using the NCAR graphics routine, ZGRID, which uses a cubic spline fit and Laplacian smoothing. The gridded data then was mapped to a surface defined by latitude, longitude, depth, and variable value using the Matlab surf.m function.

Horizontal kriging was performed on data for each of the five environmental variables (temperature, salinity, density, fluorescence, and attenuation) as well as for the eleven plankton taxa. Software developed in Matlab by Denzang Chu (WHOI) was used for kriging, and the results were saved to disk for subsequent customized plotting. Data first were prepared for use in the kriging program by separating the 5-s data into five 10m depth intervals: 0-10, 10-20, 20-30, 30-40, and >40. Data were saved in depth-specific files with columns for longitude, latitude, and variable value. Each of these data files for each variable was read into the kriging program one at a time. After loading a given data file, the data were decimated by a factor of 10 to speed up the computation. A variogram then was generated and a function fit via least squares to the variogram (inverse of correlogram). Standard kriging then was performed and the kriged data, together with the parameter values and correlogram data were saved to disk as a Matlab binary file. For a given variable, the five 10m-depth files were loaded into a Matlab program written to create the stacked plots. The stack plots used the same color map as the curtain plots. The locations of the decimated data points used in the kriging were overlaid as white dots on the kriging plots. Only the portion of the kriging plots that have an error less than 5% are shown in the stacked plots.

3.3.5 Correlation Length Scales

In addition to the distributional plots, the correlograms for each variable are presented so that the correlation scales of environmental data and plankton abundance can also be seen. Data for these plots were obtained from the kriging analysis for each species. A program was written to plot all correlograms for a given variable on one page. Note that the correlation analysis was performed on the 10 s data for each 10m depth layer, so the data along individual towyo paths in each layer are 10 s apart or about 30 meter averages. The data points on the resulting correlograms were plotted at lagged distances with 2 km resolution.

3.3.6 Temperature-Salinity-Plankton Plots

To further examine the association of the plankton with the different water mass types in the Bays, temperature-salinity-plankton (T-S-P) plots are presented. These plots were generated directly from the 10-s binned data by plotting plankton abundance as a colored dot at each temperature-salinity point. Dot diameter and color was linearly related to abundance.

3.3.7 Satellite Imagery

Satellite data from AVHRR were obtained from Andrew Thomas' remote sensing group at U. Maine via their web site (http://wavy.umeoce.maine.edu). The data were downloaded as .tif images of the Gulf of Maine and the Mass Bay region was cut out of the figures and pasted together with the color map on a single page using Corel Photo/Paint.

4.0 RESULTS AND DISCUSSION

4.1 Overview

This data report presents distributional patterns and correlograms of plankton and environmental variables as determined from a VPR survey that took place from February 23 (1945Z) to 28(2200Z), 1998. The survey covered the entire region of Cape Cod and Massachusetts Bay, but was done in two parts, pre-storm (Fig. 1A) and post-storm (Fig. 1B). The VPR was towyoed nearly continuously for 80 hours with the exception of the storm break covering a total along-track distance of about 472 nautical miles. Maximum towyo depth was 124 m. Also presented in this report are satellite data of sea surface temperature from AVHRR (obtained from A. Thomas' U. Maine web site: http://wavy.umeoce.maine.edu/).

4.2 Distributional Patterns of Environmental Variables

4.2.1 Temperature

Seawater temperature over the entire region ranged from 0.19 – 4.65 ^{o}C. As in 1997 and 1998, a cold surface plume of low salinity water was observed from Cape Ann, extending toward the south into northern Massachusetts Bay (Fig. 2A, B; note color scale in B is for values >1.5 ^{o}C). Colder water also was present along the south shore and in Cape Cod Bay. Warmer water was observed in the offshore region and in the central and southern regions of Mass Bay. It appeared as though the warmer saltier offshore waters from the Gulf of Maine had been moved into the central portion of Mass Bay.

The surface temperature patterns determined from the VPR are similar in a relative sense to the distribution of sea surface temperature (SST) observed from the AVHRR satellite (compare Figs. 2A, B with 2C). Generally, SST was warmer in the central portion of Mass Bay and colder along the coast (Fig. 2C). The image from February 23 is prior to the storm while those from February 27-28 are post-storm. No obvious differences were observed before and after the storm. The four images taken on February 28 appear to have been scaled differently from one another; upon close examination the small scale patterns in temperature are seen to be relatively similar. Further analysis of the AVHRR data from this region is needed and could provide some interesting insights into the motion of the water through the Bays.

The kriged VPR temperature data (Figs. 2D, E) also shows this pattern of surface temperature distribution, although the values in Cape Cod Bay are relatively lower than the corresponding AVHRR SST data for this region. Nonetheless, the relatively colder water near Cape Ann, along the coast south of Boston and in Cape Cod Bay can be seen in the kriged plots as well as in the first, second, and last panels of the satellite figure (Fig. 2C). The kriging also shows clearly the general increase in temperature with depth due to the warmer saltier water from the Gulf of Maine contributing to the MBBW.

Despite the strong winds, the VPR data reveal that the water column remained thermally stratified in the Cape Ann region (Figs. 2A, B, D, E). In this area, temperature generally was colder at the surface and warmer at depth. This stratification persisted through the strong northeast storm (Fig. 2F). The two sections shown in Figure 2F run down the middle of the Bays from near Barnstable to Cape Anne (Figs. 1A, B). (Note: The Cape Cod Bay portion of the post storm section was taken from the transect labeled with 8 and 9 in the post-storm survey track, Fig. 1B). The pre-storm transect was completed on February 23-24 and the post-storm transect was completed on February 27-28. The general pattern in temperature is very similar before and after the storm. The section is characterized by warm temperatures in the middle of the section (50-70 km) and colder temperatures toward either end. The Cape Ann Plume Water can be seen in the right portion of both sections at the surface. This plume appears to extend further south (left) in the post-storm section, as does the warm region in the middle of the section. Unlike March 1998, no warm surface layer was present in the Cape Cod Bay region.

4.2.2 Salinity

The surface plume from Cape Ann is especially evident in the salinity data (Fig. 3A). The plume appears as a bowl extending southward from Cape Ann into northern Mass Bay. Unlike March 1998, the plume did not extend west along the coast toward Boston Harbor and thus was not continuous with the lower salinity water south of Boston and in Cape Cod Bay.

The lowest salinity water (< 31.0) was found off Barnstable Harbor in southern Cape Cod Bay, and in general, the water of Cape Cod Bay was fresher than that in Mass Bay. As for temperature, this lower salinity water did not appear to be contiguous with the Cape Ann plume which extends further off shore into north central Mass Bay.

The highest salinity water was observed in the MBBW in the northern half of Mass Bay (Fig. 3A). This higher salinity water was observed in the lower half of the water column in all of the east-west transects south of Cape Ann including Stellwagen Basin.

The total range of salinity values observed during the survey was 30.62 near Barnstable to 32.74 in the offshore bottom water of northern Mass Bay.

The kriging results for salinity clearly show the freshwater plume extending south from Cape Ann as well as the unconnected low salinity water on the coast just south of Boston (Fig. 3B). In both areas, the low salinity waters occurs primarily in the upper 20 m of the water column (i.e. first two layers in Fig. 3B) and become progressively weaker with depth. As in March 1998, the entire region of Cape Cod Bay is generally fresher than southern Massachusetts Bay and offshore regions.

As was the case for temperature, a large intrusion of relatively salty water extended westward from offshore locations into Massachusetts Bay all the way to Plymouth Harbor and into the Nearfield region (Fig. 3B). This higher salinity water can be clearly observed in the upper 30 m of the water column. This plume also appears to extend southward through the middle of Cape Cod Bay, with the eastern and western parts of the bay having relatively lower salinity.

Salinity generally increases with depth throughout the region (Fig. 3B). In some areas, the water column was more isohaline. A higher salinity region northeast of Plymouth Harbor (the tip of the higher salinity tongue) persists with depth (Figs. 3A, 3B). Likewise salinity in the apices of the two transects north of Provincetown varied little with depth.

4.2.3 Seawater Density

Seawater density (σ_t) mirrored the temperature and salinity patterns, with less dense surface waters off Cape Ann in northern Mass Bay and denser water in the central region of Mass Bay (Fig. 4A). The Cape Ann surface plume is see to be restricted to the northern portion of Mass Bay. Highest density was observed in the middle part of the survey area with intermediate and low density in Cape Cod Bay (Fig. 4A). Lowest density water was found off Barnstable; even with the coldest water found in this plume, the density is lowest due to the correspondingly low salinity values. High density water from this

middle region did extend into the northwestern region of Cape Cod Bay near Plymouth (Fig. 4A).

The total range of seawater density observed during the survey was 24.54– 25.93 σ_t .

Kriging results clearly show the high salinity/density intrusion extending into the middle of Massachusetts Bay from offshore (Fig. 4B). The higher density water again was seen to extend southwestward to Plymouth in northwestern Cape Cod Bay, with both the southern and eastern regions of the bay having relatively lower density. The high density water also penetrated westward into the Nearfield region. Density generally increased with depth throughout the survey region.

The basic density structure of the Bays did not appear to be significantly affected by the northeast storm (Fig. 4C). The distribution of density along these sections was similar to that for temperature, with high density in the bottom layer extending upward to the surface in the middle of the section and lower density water on either end. The Cape Ann plume appears to have moved further south after the storm. The stratification is most intense at the northern end of the transect due to the intrusion of the Cape Ann plume.

4.2.4 Temperature-Salinity Relationships

Based on temperature-salinity (T-S) relationships (Fig. 5A), three distinct water types can be defined. Using the color coded T-S plot (Fig. 5B) as a guide, the 3-D distributional patterns of the different water masses are revealed (Fig. 5C). Interactive visualization was done (using a program written in Matlab) to examine how the different sections of the T/S plot (Fig. 5B) map into 3-space (Fig. 5C).

First, warmer-saltier water (blue 'fingers' in upper right on T-S plot; Fig. 5B) is located in bottom waters of Massachusetts Bay (Fig. 5C). As defined in (Davis and Gallager, 1998b), this water-type is termed Massachusetts Bay Bottom Water (MBBW), and in the present report it is characterized by salinity greater that about 32.25 and temperature greater than about 3.75 ^{o}C. This deep water extends shoreward from the offshore Gulf of Maine area into the bottom waters of the near-field region (note blue layer on bottom half of the east-west transects south of Gloucester, Fig. 5C). This bottom water also extends southward into the deeper regions of southern Massachusetts Bay. The upper and lower blue "fingers" on the T/S plot for the MBBW were found to map to the eastern and western portions of Mass Bay, respectively. The top finger corresponds to bottom water in the Nearfield region, while the bottom finger represents bottom water found further offshore.

The second dominant water-type is Cape Ann Plume Water (CAPW). In contrast to the warmer and saltier MBBW, the plume of colder fresher water from Cape Ann appears as a 'finger' in the left portion of the T-S plot centered at a salinity of 31.25 and a temperature of 2.5 ^{o}C (Fig. 5B). The CAPW is characterized by salinity range of 31.1- 31.35 and temperature range of 2.25-3.0 ^{o}C. The T/S properties of this plume reveal that it is restricted to the northern region of Mass Bay as was evident in the plots for T, S, and density.

The third water type on the T-S plot corresponds to the cold fresh water plume in southern Cape Cod Bay, which extends east and west from Barnstable Harbor. This water had the coldest temperature (< 2 ^{o}C) and lowest salinity (< 31.5) and appears as the red 'finger' in lower left portion of the T-S plot (Fig. 5B). This water-type is here termed Barnstable Cold Plume Water (BCPW) and extends from the Cape Cod Canal entrance to the region south of Billingsgate Shoal.

From the T-S plot, it is evident that a line of mixing occurs from the BCPW to the MBBW (from red to blue). Most of the water in Cape Cod Bay falls on this line, intermediate between the MBBW and BCPW indicating it is a mixture of the two types. Further study of heating and wind forcing are required to support this hypothesis.

4.2.5 Down-welling Light

The down-welling light patterns are shown (Fig.6) to provide spatial reference for the day/night sampling periods. As can be seen, the survey covered four daylight periods including the February 24 and 26-28. The sampling positions during daylight hours are displayed on the plots as red bands along the surface of the ribbon plot. The total range of down-welling light values observed during the survey was 0-104 W/m^2. (note: An erroneous subsurface band of weak light is seen in the middle of the plot due to some bad data points from the sensor. The purpose of this plot however is simply to identify the day/night periods of the survey and show the marked attenuation of light from the surface.)

4.2.6 Fluorescence

Fluorescence was highest in the Cape Ann plume and in general higher fluorescence was present in the colder fresher water along the coast and in Cape Cod Bay, except in the BCPW where the lowest values were observed (Fig. 7A). The fluorescence in the middle portion of Massachusetts Bay tended to be lower than in Cape Cod Bay (Fig. 7A).

The high fluorescence in the Cape Ann plume is striking. The shape of the fluorescence plume is very similar to the density and salinity plumes except that the fluorescence plume extends as a continuum from Cape Ann westward to Boston Harbor and then south along the South Shore past Plymouth and and into Cape Cod Bay. The physical data show no such continuity.

Kriging results for fluorescence show these patterns very clearly with highest values appearing in the CAPW (Fig. 7B). Higher fluorescence values follow the coast down into Cape Cod Bay. The stack plots also show that the fluorescence concentrations are surface intensified with lower values appearing at depth.

The pre- and post-storm sections of fluorescence reveal similar patterns before and after the storm (Fig. 7C). Noticeably higher values occurred following the storm, possibly due to increased mixing and nutrient input into the water column, or perhaps the spring phytoplankton bloom had become more advanced. The fluorescence values in Cape Cod Bay (left) were particularly higher after the storm.

4.2.7 Attenuation

Attenuation values were high in western Cape Cod Bay and along the South Shore and were much lower in all other areas (Fig. 8A). The kriged plots show this pattern clearly (Fig. 8B). The high attenuation in this region is restricted to the upper 20 m of the water column. This region of high attenuation coincides with an area of low density water off the entrance to the Cape Cod Canal.

4.3 Distributional Patterns in Plankton Taxa

4.3.1 General Abundance Values

The abundance (number/liter) observed in the 5-s time-bins for each taxon is shown in Table 2. Maximum and mean values are given for each taxon. Diatoms clearly dominated the plankton. Copepods were the most dominant zooplankton category with a maximum value of 3.41 per liter followed by disks and ovals (probably also copepods; see methods). Pteropods were the next most abundant zooplankton group followed by polychaetes and *Pseudocalanus* with eggs. Marine snow was the most abundant non-diatom group with a value of 5.26/liter.

Table 2. Abundance (#/liter) of plankton observed during 5-s time-bins.

TAXON	Max	Mean
Diatom, rod-shaped	35.00	5.872
Diatom, *Chaetoceros* chains	28.44	4.009
Diatom, *Chaetoceros socials* colonies	43.41	6.525
Copepods	3.41	0.296
Disk, unidentified	2.99	0.140
Nauplii, unidentified	1.99	0.083
Oval, unidentified	2.35	0.094
Pseudocalanus w/ eggs	1.50	0.059
Pteropod	2.34	0.125
Polychaete	1.98	0.083
Marine snow	5.26	0.246

4.3.2 Rod-Shaped Diatoms

A subset of the training images for rod-shaped diatoms is shown in Fig. 9A. Highest abundance observed for these organisms was 35 per liter (Table 2). As stated in the methods, these abundance estimates are very low however since orientation of the rods relative to the strobe-camera axis caused only those rods in a specific orientation to be captured (Figs. 9A). Moreover, in bloom conditions with other diatoms, multiple

organisms were observed in each ROI, but each ROI is counted as one organism, so this serves as maximal cutoff on the abundance of these organisms. Most images however had only a single in-focus object. Also, the extremely high abundance in bloom conditions with *Chaetoceros socialis* overloaded the image processing system causing some in-focus diatom-rods to be missed. In non-bloom conditions, the relative abundance patterns are expected to be reasonable estimates since orientation is in all likelihood random and in most locations the VPR images did not contain multiple in-focus objects.

The rod-shaped diatoms could have been *Thalassiosira rotula* or perhaps *Rhizosolenia alata*. It was not possible for us to identify the genus of this group from the video.

Highest abundance of these diatoms occurred in the offshore region of northern Mass Bay and off Barnstable Harbor (Fig. 9B). These diatoms also were abundant in the surface waters of central and southern Mass Bay away from the coast. The distributions of rod-shaped diatoms appeared to match that of salinity with higher abundance occurring in the offshore water and low abundance in the fresh water near the coast, with the exception of the high abundance in the low salinity water off Barnstable. Log_{10}-transformed abundance of these diatoms (Fig. 9C) reveal this pattern even more clearly, with lowest abundance occurring off Cape Ann, in western Cape Cod Bay, and in the bottom water of southern Mass Bay.

Kriging plots for rod-shaped diatoms (Fig. 9D) reveal the offshore tendency for this group, with their abundance pattern appearing to follow the Gulf of Maine intrusion from the offshore location in northern Mass Bay southwestward through central Mass Bay and into the northern part of Cape Cod Bay. Much lower abundance was observed along the coastal areas of the Bays except for the very high concentrations near Barnstable. Their high abundance offshore in northern Mass Bay extends from the surface all the way to the bottom. This surface distribution of diatoms is strikingly similar to the AVHRR images for SST, which indicates an offshore intrusion of warmer Gulf of Maine water into the non-coastal waters of Mass and Cape Cod bays (Fig. 2C).

4.3.3 Temperature-Salinity-Plankton Relationships

The association of a given taxon to a particular water type is revealed in the temperature-salinity-plankton (T-S-P) diagrams (Figs. 10A, B, C). Before discussing the relationships of individual taxa to T-S properties, it is instructive to examine the T-S-P diagrams for fluorescence and beam attenuation.

The T-S-P diagrams show clearly that the highest fluorescence values are associated with the “finger” of Cape Ann Plume Water (CAPW) (Fig. 10A). High fluorescence values are also seen in the central region of the T-S-P plot. These latter values map to two different areas: the coastal regions south of Boston and the area near Provincetown in eastern Cape Cod Bay. The water in these regions fall on two different mixing lines: MBBW-CAPW and MBBW-BCPW.

The T-S-P plot for beam attenuation (Fig. 10A) is very different from that for fluorescence. High attenuation is clearly contained within the BCPW in the lower left finger on the T-S-P plot. Intermediate values of attenuation found toward the lower-

middle portion of the plot map to a broad area of Cape Cod Bay. These intermediate values also can be seen in the curtain plot for this variable (Fig. 8A).

The T-S-P plot for rod-shaped diatoms is quite revealing (Fig. 10A). It shows that the abundance of this organism follows closely the line connecting MBBW and BCPW and suggests that there is an offshore origin for this group in Cape Cod Bay. The high abundance of these diatoms in the lower finger of the MBBW indicates a presence offshore but not inshore (upper finger) in the MBBW. It is likely that this diatom was blooming in the offshore waters of the Gulf of Maine and was transported into northern Mass Bay and carried and mixed south through the middle of the bay into Cape Cod Bay. The very low abundance of rod-shaped diatoms in the CAPW is clear in this plot as well as the generally low abundance all along the line from the upper finger of the MBBW to the CAPW.

Other T-S-P relationships will be discussed below in the sections for each taxon.

4.3.4 Chaetoceros Chains

Another abundant phytoplankton group observed in the video were chain-forming *Chaetoceros* species (Fig. 11A). This group was readily identified since their long spines scattered light effectively giving them a feather-like appearance. Maximum abundance in a 5-s interval was 28/liter with a mean value of 4.0/liter (Table 1). As for the other diatom groups, these values greatly underestimate the abundance of these organisms and the data are used primarily to determine relative distributional patterns.

Unlike the rod-shaped diatoms, which occurred primarily in the warm intrusion protruding into Mass Bay from the northeast, *Chaetoceros* chains were most abundant in the eastern portion of the southern half of Mass Bay (Fig. 11B), an area where the rod-shaped diatoms were less abundant (Fig. 9B, C). These diatoms were more abundant near the surface.

Kriging results show these patterns clearly (Fig 11C). This group is only abundant in the southern half of Mass Bay away from the coast. Highest abundance was found in the 10-20m layer in the offshore region. In general, the abundance pattern for this group suggests that it entered the southern half of Mass Bay from offshore. This offshore area of high abundance corresponds to a low abundance area for the rod-shaped diatoms, the latter appearing to enter the northern half of Mass Bay from offshore, while *Chaetoceros* chains appear to enter the southern half of Mass Bay from offshore.

T-S-P diagrams for *Chaetoceros* chains reveal little association with the MBBW that was primary association for rod-shaped diatoms (Fig. 10A). While the lower finger of the MBBW includes high concentrations of the rod-shaped diatoms, low concentrations of *Chaetoceros* chains were found in this portion of the plot. The highest concentrations of *Chaetoceros* chains were found in the middle region of the T-S-P plot, corresponding to the water in the southern half of Mass Bay. Few *Chaetoceros* chains are seen in either the CAPW or the BCPW.

4.3.4 *Chaetoceros socialis* colonies

Chaetoceros socialis colonies (Fig. 12A) were the most abundant taxon observed during this cruise. They have a characteristic texture and globular shape that is readily identified by the automatic identification system. The maximum concentration in a 5-s interval as determined from the VPR's automated system was 43 colonies/liter. This value is probably low by a factor of 10-100, since individual video fields sometimes contained as many as 5 in-focus colonies. Given that the volume imaged in a single video field was 0.5 ml for the high-magnification camera, 5 in-focus colonies in a field corresponds to a concentration of 10 colonies per ml which is over 100 fold greater than the maximum average abundance determined by the automated system. The settings used for the automated system did not capture every in-focus organism and did not count more than one colony per field. Nonetheless, the data do provide important information on the relative abundance patterns for this group.

The abundance pattern for *Chaetoceros socialis* colonies (Fig. 12B) was similar to that for rod-shaped diatoms except that these colonies were less abundant in the offshore region that had high abundance of *Chaetoceros* chains (cf. Fig. 11B). The abundance pattern of *Chaetoceros socialis* colonies appears to have a hole in this region. In general, the distributional pattern for this species follows the same trend as rod-shaped diatoms with the high offshore abundance in northern Mass Bay penetrating to the south through the middle of the southern Mass Bay and into eastern Cape Cod Bay.

The kriging plot for *Chaetoceros socialis* colonies shows this pattern quite clearly (Fig. 12C). The area of high abundance in the offshore region of northern Mass Bay is seen to penetrate southward through the middle of southern Mass Bay and into Cape Cod Bay. The region of low abundance in the area of high-*Chaetoceros* chain abundance also can be seen clearly.

From the T-S-P plot for *Chaetoceros socialis* colonies it can easily be seen that this species has the same water-mass affinities as rod-shaped diatoms (Fig. 10A). High abundance is seen to extend from the lower finger of the MBBW along the bottom portion of the data and into the BCPW. A cluster of high values occurs at the fork between the fingers for CAPW and MBBW. This area maps to the region off Provincetown in eastern Cape Cod Bay (e.g. off Herring Cove).

The plot for total diatoms represents the integral of the three diatom taxa. Total diatom abundance is highest along the line running from the offshore MBBW and into southern Cape Cod Bay in the BCPW.

4.3.5 Copepods

Copepods (Fig. 13A) were grouped together because they could not be automatically identified owing to the small size of the images from the low magnification camera. This group likely comprised a mixture of the dominant copepods *Calanus* and *Pseudocalanus*. Copepods smaller than Pseudocalanus adults were too small to be captured by the image processing system for the low magnification camera, so that the very abundant genus *Oithona* was not quantified. Fortunately, *Pseudocalanus* and *Calanus* are the principal prey species for the endangered right whale and are therefore target species of this investigation.

The copepods were oriented in various directions with no obvious preferred direction. Copepods were most abundant taxon, having a maximum abundance of 3.4 /liter and a mean abundance over the whole survey of 0.30 per liter (Table 2).

Copepods were found to be most abundant in the bottom half of the water column in Mass Bay, especially in the Nearfield region (Fig. 13B). The third and fourth E-W transects south of Gloucester had the highest copepod abundance. Few copepods were found along other regions of the coast including Cape Ann and Cape Cod Bay. Few copepods were found in the right whale feeding ground in eastern Cape Cod Bay near Provincetown. This cruise, being a month earlier in the year than previous spring VPR cruises, appears to have preceded the spring population growth of the copepods.

The kriging plots for copepods (Fig. 13C) clearly shows the distributional patterns. Highest concentrations were found in the bottom two layers > 30m and the abundance in these layers was widespread throughout Mass Bay. Concentrations near the coast fell off sharply at depths < 30 m. No obvious source water for the copepods could be seen in these plots.

The T-S-P plots for copepods (Fig. 10B) reveal that most of the copepods were associated with the upper finger of the MBBW indicating higher abundance in the inshore region of northern Mass Bay. Intermediate abundance was seen in the lower finger of the MBBW indicating the presence of these animals in the offshore region of the MBBW. A localized high spot of copepods also was seen in the BCPW. The area of relatively high abundance of copepods in the middle portion of the T-P-S plot maps to a region covering the lower portion of the water column in southern Mass Bay. It appears from the T-S-P plot that the water-mass affinity of copepods is very different from that of diatoms (cf. Fig. 10B, top two panels). Likewise, the copepods and fluorescence appeared to be located in different water masses (cf. Fig. 10A, B, top right panels). The lack of spatial overlap in the distribution of copepods with either the large phytoplankton taxa or high fluorescence is interesting. This disparity could be due to grazing by the copepods on the phytoplankton, or more likely due to different transport pathways for copepods and phytoplankton.

4.3.7 Unidentified Disks and Ovals

Unidentified disks (round objects) and ovals (Fig. 14A; 15A) were most likely to be unidentified copepods. Since copepod antennules and urosomes could not be readily seen from the smaller low magnification images, it was often not possible to identify them as

copepods. We have found, after working with millions of images, that bright round and oval objects in the low magnification camera are usually copepods. Since definitive identification could not be made on these objects, they are classified into these two categories.

The distributional patterns for disks and ovals follows that for copepods but their mean abundance is lower (Table 2). In general, the distributions of ovals and disks were highest in the lower half of the water column in Mass Bay (Figs.14B; 15B). Concentrations in Cape Cod Bay were lower. As was the case for copepods, highest concentrations were observed in the Nearfield region.

The kriging plots (14C; 15C) show that the surface distributions of these groups were restricted to the middle of the Bay away from the coast. Abundance increased markedly with depth, and the deep populations were most abundant near shore.

The T-S-P (Fig. 10B) plots for these groups were grossly similar to that for copepods. Highest abundance was observed in the middle of the plot in an area corresponding to the Nearfield region.

4.3.8 Nauplii

This group was characterized by a round or oval body with small appendages and were judged to be nauplii based on prior experience identifying them from both high and low magnification images (Fig. 16A). Due to the low magnification of the camera, these nauplii were large, near 1.0mm in length, and thus were almost certainly barnacle nauplii.

These nauplii were distributed throughout the central regions of Mass and Cape Cod Bays and also had particularly high abundance in the Nearfield region (Fig. 16B). Abundance of nauplii was highest in northern Mass Bay and central Cape Cod Bay with lower surface abundance in the region between the northern and southern halves of Mass Bay.

This gap in the surface distribution of nauplii can be seen more clearly in the kriging plot (Fig. 16C). This plot reveals the higher surface abundance in northern Mass Bay and northern Cape Cod Bay. A very high local abundance off Barnstable is also seen. Abundance was highest in the 30-40 m depth layer where relatively dense concentrations were found offshore north of Plymouth as well as at the Gulf of Maine boundary in northern Mass Bay.

The T-S-P plot for nauplii (Fig. 10B) is very similar to that for copepods implying similar affinities for these groups at this time. The nauplii were present in both fingers of the MBBW and their abundance also was high in the BCPW. Low abundance was observed in the CAPW.

4.3.9 Pseudocalanus with eggs

These copepods could be readily distinguished despite their small size, owing to the fact that they carry a large sac containing eggs (Fig. 17A). Maximum and mean abundance for *Pseudocalanus* with eggs were 1.5 and 0.059 per liter, respectively. The average

abundance (59/m^3) is low for adult female Pseudocalanus, but these were only those females carrying eggs. Other *Pseudocalanus* could not be distinguished from other copepods.

The curtain plot for *Pseudocalanus* with eggs indicates that the spatial distribution for this group is similar to that for the other copepods (Fig. 17B). High abundance was found in the nearfield region near the bottom. Intermediate abundance was found at mid and lower depths throughout Mass Bays. Low abundance was found in the surface waters off Cape Ann and in eastern Cape Cod Bay off Provincetown, the historical right whale feeding ground for this prey species.

Kriging plots for *Pseudocalanus* with eggs reveal several interesting patterns (Fig. 17C). The general abundance increases with depth in all areas. In the upper 10 m, patches of intermediate relative abundance are scattered throughout the Bays. In the second two layers (10-20 and 20-30 m) a relatively dense patch is seen in the middle of southern Mass Bay. At the two lowest layers (30-40 and >40 m), two areas of high concentration were found, one in the Nearfield region and one in northern Cape Cod Bay. Thus, although abundance of Pseudocalanus w/eggs was relatively low in the surface waters of Cape Cod Bay, the concentrations increased markedly near the bottom.

These distributional patterns for Pseudocalanus with eggs are reflected in the T-S-P plots (Fig. 10B). The relatively high abundance of Pseudocalanus near bottom in the Nearfield region is seen in the higher values in the upper finger of MBBW. This relatively high abundance extends into the middle of the T-S plot as it did for copepods. For Pseudocalanus however, the pattern extends further along this line (cf. 2nd and last panels in Fig. 10B). This extension corresponds to the relatively higher abundance of Pseudocalanus with eggs in the bottom water of northern Cape Cod Bay.

4.3.10 Polychaetes

These organisms were identified by their squat rod-like shape, and in certain cases body segmentation could also be seen (Fig. 18A). We routinely identify pelagic Tomopterid worms in our Georges Banks studies and are familiar with their appearance in the video images from both high and low magnification cameras.

Polychaetes abundance was typically low throughout the region with a mean value of 0.083 /liter (Table 2). Abundance was spread over the whole area but was relatively higher in the deeper water of northern Mass Bay (Figs. 18B, C). The kriging plots show relatively high abundance near bottom next to shore south of Gloucester. Small areas of localized abundance were observed in southern Mass Bay and Cape Cod Bay.

4.3.11 Pteropods

Pteropods were identified by their bright round edge together with a dark central body region (Fig. 19A).. This characteristic body form of pteropods allowed them to be readily distinguished

The curtain plot for pteropods indicates that they were relatively more abundant in the bottom water of northern Mass Bay (Fig. 19B). As was seen for copepods, the abundance was highest in the bottom in the vicinity of the Nearfield region. The kriged data reveal that the relatively high abundance pattern at the bottom extends south from the Nearfield region into southern Mass Bay and Cape Cod Bay (Fig. 19C).

The T-S-P plot for pteropods is very similar to that for copepods (Fig. 10C) suggesting a common origin. Unlike copepods, however, no pteropods were found in the BCPW.

4.3.12 Marine Snow

Marine snow was easily identified by the dull matted appearance with dark spots inside Fig. 20A. These particles were the most abundant non-diatom object seen in the video (Table 2).

Marine snow was most abundant in the central region of northern Cape Cod Bay and southern Mass Bay (Fig. 20B, C). Abundance was higher deeper in the water column. An area of highest abundance was observed next to the entrance to the Cape Cod Canal (Fig. 20C). The latter high spot coincided with the area of high beam attenuation at the surface. The relationship if any between strong beam attenuation at the surface and marine snow near bottom is not known but may be due to sinking and aggregation of small particles from the surface layer.

The T-S-P plot for total zooplankton (the sum of all zooplankton taxa plus marine snow) is distinct from that for total phytoplankton (cf. Fig. 10B, C). Highest zooplankton ran along the line from the inshore MBBW through the middle portion of the T-S-P plot but not along the lower half of the curve as was seen in the phytoplankton.

4.4 Correlation Length Scales

The variograms computed for kriging the different depth layers for each variable were used to determine the corresponding correlograms. In this section, the correlograms are described for each variable at each of the five depths corresponding to the kriging plots.

4.4.1 Physical Variables

The correlograms for temperature varied as a function of depth (Fig. 21A). In the top three layers (0-10 m, 10-20m, 20-30m) the covariance fell off nearly linearly with the lagged distance. Negative correlations were found at length scales of 30-60 km. The covariance crossed the zero line between 25-40 km for these three surface layers. In contrast, the covariance function in the deeper layers decreased more abruptly with distance, with the covariance at a lag of 20 km having a value close to zero. Thus, in the upper layers, temperature was positively correlated over longer scales than it was in the deeper layers. In the lowest layer temperature values were uncorrelated at the longest length scales (~40 km), while in the upper layers a strong negative correlation was found at these scales.

The covariance in salinity values in the upper 20 m fell off more quickly than that for temperature (Fig. 21B). The upper layers quickly became negatively correlated at longer scales and the bottom layer became uncorrelated.

An explanation for these patterns can be found by considering the underlying source of the variability. Temperature is forced over large spatial scales through surface heating. Salinity on the other hand is influenced by local discharge and runoff, so this forcing is operates over shorter spatial scales than does the forcing of temperature. The larger correlation length scales for temperature than for salinity in the surface layers then is likely due to the larger scale over which the temperature forcing operates. Correlograms for temperature and salinity are more similar to each other in the deeper layers, since surface heating has less influence at these depths.

4.4.2 Fluorescence and Attenuation

Covariance in fluorescence (Fig. 21C) falls off much more sharply with distance, reaching zero at 20 km and staying there. The fluorescence also had a small "dip" at about 15-20 km with a negative correlation at this scale and zero correlation on either side. Rapid fall in the covariance to zero at scales larger than 10 km indicates substantial random patchiness at these scales.

The correlograms for attenuation (Fig. 21D) were more similar to those for salinity than for fluorescence. It is possible that the higher attenuation is associated with turbid local freshwater runoff.

4.4.3 Planktonic Taxa

Correlograms for the planktonic taxa are presented in Figure 22A-K.

4.4.3.1 Diatoms

The correlograms for rod-shaped diatoms and *Chaetoceros socialis* colonies were similar to each other but differed from that for *Chaetoceros* chains (Fig. 22A, B, C). In the upper 10 m, the normalized covariance function fell off more quickly with length scale for both rod-shaped diatoms and *Chaetoceros socialis* colonies reaching a value of zero at 15 km, while zero correlation was reached at 25 km for *Chaetoceros* chains.

It is interesting to note that the rod-shaped diatoms and *Chaetoceros socialis* colonies appeared to be contained in the same water masses and had similar T-S-P plots. These latter two groups appeared to enter northern Mass Bay from the Gulf of Maine, while *Chaetoceros* chains entered southern Mass Bay from the Gulf of Maine. The connection between correlation length scales and water type affinity is not immediately clear and requires further in-depth analysis.

The correlogram for *Chaetoceros socialis* colonies shows a pronounced "dip" into negative values at a distance of 25 km in the 10-30 m layers. This may have been due to

the apparent exclusion from the region of high abundance of *Chaetoceros* chains (cf. Fig. 11C and 12C).

For all diatom groups the correlation length scale at depths > 20 m was much shorter than in the upper layers. A sharp drop-off within the first 2 km was found in the deeper layers. In the bottom layer (>40 m), rod-shaped diatoms and *Chaetoceros socialis* colonies had a sharp drop to negative correlation within the first 2 km but the covariance quickly became positive again at 4 km, reaching a small peak near 10 km and then decreasing to zero at 15 km. By contrast, in this bottom layer, covariance in *Chaetoceros* chains fell to zero by 6 km and remained there at all larger length scales.

In the surface layer, the correlograms for rod-shaped diatoms and *Chaetoceros socialis* colonies are similar to that for fluorescence in that the covariance falls to zero at about 15 km. A strong negative correlation at the largest scale (~60 km) was found for fluorescence but only weak negative correlations were found for these two diatom groups at this longest scale. The pronounced negative "dip" in the covariance function at 15 km for fluorescence (10-40 m layers) was not observed for the diatoms.

The correlograms for all the diatoms were also very different from those for the physical variables (cf. Fig. 21A, B and Fig. 22A, B, C). Both temperature and salinity had positive normalized covariance values over much greater length scales than the diatoms did. Also, diatoms were generally uncorrelated at length scales greater than about 15 km, whereas temperature and salinity had large negative covariance at scales greater than 30-40 km. The lack of correlation at large scales, despite strong negative covariance in the physical properties, appears to imply that these diatoms, like the fluorescence in general, are not affected by the large scale gradients in temperature and salinity. This lack of relationship is in marked contrast to the apparently strong affinity that the diatoms have with the T-S properties of the water masses. The reason for this discrepancy is not clear at present and will require further investigation.

4.4.3.2 Zooplankton and Marine Snow

The correlograms for all zooplankton taxa fell off to zero much more rapidly than those for three diatom species (Fig. 22A-J). Typically, zooplankton covariance functions (Fig. . 22D, E, F, G, H, I, J) reached a zero value at length scales ≤ 10 km, rather than the 15 km scale observed for the diatoms (Fig. 22A, B, C). The shorter correlation length scale for zooplankton may be indicative of smaller scale patchiness due to swimming behavior interacting with local flows such as convergences.

This rapid loss in covariance was found for all the zooplankton taxa but not for marine snow (Fig. 22K). Covariance in marine snow fell off a little more gradually and reached zero at ~12-15 km. In the bottom layer, correlograms for all zooplankton taxa except copepods fell to zero within the first 2 km and stayed there at all larger length scales. Copepod covariance in the bottom layer remained positive until 10 km. By contrast, covariance in marine snow in the bottom two layers (>30 m) remained positive until about 20 km, beyond which the covariance was zero. So marine snow in the bottom layers appear to be positively correlated over relatively longer length scales (~20 km), whereas zooplankton taxa have zero covariance at scales > 10 km.

In the upper three layers (< 30 m), zooplankton taxa generally had positive covariance values at distances < 10 km. For copepods, covariance values were clearly positive at distances up to 10 km at all depths (Fig. 22D). At distances > 10 km, covariance in all the zooplankton taxa was zero (Fig. 22D, E, F, G, H, I, J).

In short, the zooplankton taxa in the upper 30 m had positive covariance values at distances < 10 km but lacked correlation at larger scales. In the bottom layer, covariance fell to zero within 2 km for all taxa but copepods, which had positive values at up to 10 km. Marine snow at depths > 30 m had positive covariance values at scales up to 20 km, whereas at depths <20 m covariance in marine snow fell to zero within 10 km.

In general, zooplankton taxa had shorter correlation length scales than diatoms or marine snow. This short length scale may be indicative of small-scale patchiness in zooplankton due to interaction of swimming behavior and small scale flows. The lack of correlation at larger scales, indicates that the observed zooplankton patterns were unrelated to the observed gradients in phytoplankton, temperature, or salinity.

4.5 HOM-VPR Data Comparison

The VPR survey on the OSV *Peter W. Anderson* (2/23-28/1999) coincided with the second HOM water column survey cruise of the year (2/23-28/1999). During the latter survey, CTD casts (with bottles) and zooplankton net tows were made at the standard HOM survey stations. In this section of the report, data from this HOM survey on salinity, temperature, fluorescence, and phytoplankton and zooplankton abundances are compared with similar data from the VPR survey. The high-resolution VPR data covering the entire region provides a broad context within which to view the sparser HOM station data, while the HOM species level data provides taxonomically more refined data on plankton species abundances.

4.5.1 Temperature-salinity comparisons

HOM data used in the comparison were chosen based on geographic overlap with the VPR data, as well as data quality. No valid salinity readings are available for stations F01, F02, F32 in Cape Cod Bay because of freezing of the conductivity probe during the CTD casts. These data were excluded from the T-S comparisons. Locations of HOM stations as well as the VPR survey track used in the comparisons are shown in Figure 23A. Most of HOM stations were located in the Nearfield region and South Shore area. One station was located in Cape Cod Bay (station 33) and one at the Boundary region off Cape Ann (Fig. 23A). The HOM T-S data is contained within the range of the VPR data (Fig. 23B) and in general there is very good agreement between the data sets. A portion of the HOM data extends into the lower blue finger of the VPR data (Fig. 23B, upper right corner), and these HOM data were collected in the subsurface waters at the boundary station F27 (offshore Massachusetts Bay Bottom Water). The line of HOM T-S data points at the base of the upper blue finger of VPR data (near salinity of 32.0 and temperature >3.5^{o}C) represents data collected in the bottom waters of the Nearfield region

(near-shore MBBW). No Cape Ann Plume Water or Barnstable Cold Plume Water was seen in the HOM data since the stations were not located in these regions. The T-S properties at the one HOM station in Cape Cod (off Provincetown) fell within the values obtained by the VPR survey for Cape Cod Bay as a whole.

4.5.2 Comparison of Temperature-Salinity-Phytoplankton relationships.

The relationships between temperature, salinity, and phytoplankton taxa in the HOM data could be determined, since the phytoplankton were collected at known depth intervals using Nisken bottles on a CTD rosette. Zooplankton data, however, were collected by vertically integrated net hauls, and therefore the T-S properties were not precisely known, and the data were much sparser (single net hauls versus multiple bottles per station). Thus, T-S-P plots could not be made for the HOM zooplankton data. Cape Cod Bay was not included in the T-S-P analysis owing to lack of T-S data from stations F01, F02, and F32 and lack of phytoplankton data from stations F32 and F33. To make the comparison between the HOM and VPR phytoplankton data as valid as possible, we grouped the HOM species identified microscopically in the laboratory into the groupings observed in situ by the VPR system. These groupings are shown in Table 3, and the HOM data used in the T-S-P plots are given in Table 4.

Table 3. Phytoplanton species identified in the HOM samples and grouped for comarison with the VPR data.

	VPR TAXA		
HOM TAXA	Diatom, rod-shaped	Diatom, *Chaetoceros* chains	Diatom, *Chaetoceros socialis* colonies
Chaetoceros debilis		✓	
Chaetoceros socialis			✓
Eucampia zoodiacus	✓		
Pseudonitzschia pungens	✓		
Rhizosolenia hebetata	✓		
Stephanopyxis turris	✓		
Thalassiosira rotula	✓		
Thalassiothrix longissima	✓		

(*note: "Diatom, rod-shaped" is the term used to describe diatom chains that lacked observable spines in the VPR images, so that the chains appear as rods (see Fig. 9A). The constituent cells in the chains were not necessarily rod shaped).

Table 4. HOM data used in the T-S-P plots.

HOM Station Number	Station Latitude	Station Longitude	Sample Depth (m)	Temperature (°C)	Salinity	Fluorescence (µg Chl a/liter)	Diatom, rod-shaped (cells/ml)	Diatom, *Chaetoceros* chains (cells/ml)	Diatom, *Chaetoceros socialis* (cells/ml)
F06	42.17142	-70.5767	2.10	3.30	32.029	1.45	37.73	7.55	172.79
F06	42.17142	-70.5767	15.62	3.28	32.043	1.87	64.96	3.02	352.02
F13	42.26909	-70.7362	1.91	2.36	31.343	0.46	29.15	0	449.45
F13	42.26909	-70.7362	12.08	2.68	31.553	7.13	48.79	0	362.94
F27	42.54935	-70.4469	2.75	2.78	31.536	2.26	20.62	8.84	580.22
F27	42.54935	-70.4469	57.69	3.73	32.367	0.14	81.00	10.31	265.07
N04	42.44431	-70.7368	2.37	2.96	31.780	1.64	51.63	11.16	507.99
N04	42.44431	-70.7368	23.83	2.95	31.779	6.61	57.21	19.57	597.71
N16	42.39519	-70.7541	2.28	3.08	31.764	10.20	63.27	12.34	541.63
N16	42.39519	-70.7541	19.35	3.21	31.891	7.91	63.86	30.48	589.21
N18	42.36781	-70.7781	2.13	2.90	31.779	0.51	42.15	10.54	471.24
N18	42.36781	-70.7781	15.17	2.89	31.779	6.78	46.36	15.94	576.60

4.5.2.1 T – S – Fluorescence

The T-S-P plots for the HOM fluorescence were similar to those seen for the VPR data (cf. Fig. 23C and Fig. 10A). The peak HOM fluorescence values (~10 µg Chl a /liter, Fig. 23C) were four times lower than the peak VPR values (~40 µg Chl a /liter, Fig. 10A) due to the HOM survey occupying no stations in the Cape Ann Plume Water (CAPW). The highest HOM values were found in the lower central portion of the T-S plot, where values of similar magnitude were observed in the VPR data (cf. Fig. 23C and Fig. 10A). These values fall along the two lines of the mixing curve, namely MBBW-CAPW and MBBW-BCPW. The latter data are from the coastal stations south of Boston, while the former are from the station off Provincetown in Cape Cod Bay.

4.5.2.2 T – S – Phytoplankton taxa

Plots for HOM phytoplankton groups were also relatively similar to those seen for the VPR data (cf. Fig. 23C and Fig. 10A). Note, however, that the diatom abundances are not comparable in an absolute sense between HOM and VPR data sets, because HOM diatom abundance was measured as cells/ml rather than as colonies (or chains) per liter in the VPR data. The colonies and chains could not be measured in the HOM data since they were broken in the collection and sieving process. Likewise, the resolution of the VPR images is not sufficient to identify and enumerate individual cells in these phytoplankton colonies (or chains). In addition, as noted above, the absolute number of colonies (or chains) was underestimated by the VPR in regions where colony (chain) densities were higher than 2 per ml. Nonetheless, we can expect that the relative distributional patterns of these groups should be similar between HOM and VPR data sets.

In both data sets, the T-S-P plots for rod-shaped diatoms indicate highest concentration in the offshore MBBW (cf. Fig. 23C and Fig. 10A). (Recall that the MBBW is represented by the bottom blue finger in the color-coded T-S plot, Fig. 5B). Higher abundance of rod-shaped diatoms also is seen in the middle portion of the T-S-P diagrams for both HOM and VPR data, while lowest concentrations were observed toward the lower left portion of the plots toward the BCPW (e.g. temperature ~2.2 ^{o}C and salinity ~31.25). In general, the relative T-S-P patterns are very similar between the two data sets for the rod-shaped diatoms. Although the comparable HOM data are very sparse, they agree with VPR data, indicating an offshore origin of this taxon.

The HOM T-S-P plot for *Chaetoceros* chains is also in general agreement with the VPR T-S-P plot for this taxon (cf. Fig. 23C and Fig. 10A). Highest abundance of this taxon in the HOM data is seen to occur in the middle of the T-S-P plot toward the bottom, which is the same region where highest abundance occurred in the VPR plot. Likewise, in both plots, lower abundance was found in the offshore MBBW and in the lower left portion of the diagram toward the BCPW. These data support the VPR data, which showed highest abundance in southern Massachusetts Bay and a likely offshore origin in this area.

Chaetoceros socialis abundance was found to be highest in the lower middle portion of the T-S-P diagram. High abundance was not observed at the offshore station indicating lower abundance in the MBBW. This observation is in contrast with the VPR data which showed relatively high abundance of *C. socialis* colonies extending along the lower finger of the MBBW (cf. Fig. 23C and Fig. 10A). This discrepancy may be due to there being only a single station in the HOM data in this region and local patchiness could have caused a lack of observation of this group. High abundance was found in the lower half of the T-S line running from MBBW to BCPW, agreeing with the VPR data. In both the VPR and HOM data, *Chaetoceros socialis* was found to be the most abundant taxon.

4.5.3 HOM-VPR Zooplankton Data Comparison

4.5.3.1 Copepod Species Composition

The dominant zooplankton taxa found in the HOM net samples were copepods. The two copepod groups observed using the VPR (camera 2) were *Pseudocalanus* with eggs and unidentified copepods (see Table 2). The unidentified ovals and disks were also likely to be unidentified copepods, but the resolution was not high enough to observe antennules of other distinguishing characteristics in these groups. The magnification of this camera was too low to capture the usually dominant smaller copepod *Oithona*, but since our principal focus was to quantify abundance of whale prey species (primarily *Pseudocalanus* and *Calanus*), we limited our comparison of HOM and VPR data to mid-size and larger copepods. We can see from the HOM species data for copepods of this size, that *Pseudocalanus* is by far the dominant taxon (Fig. 24A). *Pseudocalanus* is dominant at all stations except the nearshore and harbor stations. Its maximum abundance reached 1752/m^3 at station F02 in Cape Cod Bay. In nearshore regions, dominant genera included

Acartia, *Centropages*, and *Tortanus*, but these groups were present in very low abundance in regions sampled by the VPR.

4.5.3.2 Comparison of Copepod Abundance

To compare the HOM and VPR data in the most meaningful way, all the HOM copepod species in the size range observed by the VPR (i.e. all the species shown in Fig. 24A) were grouped together. The HOM stations included in the analysis are also shown in this figure. Likewise, the VPR taxa that were likely to be copepods were grouped together, including unidentified copepods, *Pseudocalanus* with eggs, ovals, and disks. The VPR data then were averaged for each towyo to approximate a double oblique plankton tow.

The HOM and VPR data were found to agree in absolute magnitude with each other (Fig. 24B). In Massachusetts Bay the HOM abundances (red circles) match closely those of the VPR (blue circles). In Cape Cod Bay, copepod abundance in the vicinity of the HOM stations was higher in the HOM data than in the VPR data. By contrast, high abundances of copepods were found in the VPR data in the BCWP water off Barnstable Harbor and in northern central Cape Cod Bay, but not in the vicinity of the HOM stations. It is probable that this difference between VPR and HOM data in the location of high copepod abundance is due to physical advection of water due to the tides or strong winds since the sites of high abundance in the respective data sets are in close proximity to each other.

4.5.3.3 Correlogram for VPR "Simulated Plankton Tows"

As discussed above, these VPR data were obtained by treating the VPR towyos as "simulated plankton tows", thus providing the equivalent of 1294 double-oblique plankton tows throughout the Mass/Cape Cod Bays. Hypothesis testing with the HOM zooplankton data assumes that the stations are independent samples of the region.

Correlation length scales were found for all the VPR data presented in Fig. 24B by plotting the normalized covariance function versus lagged distance (Fig. 25). We can see that there is a strong positive correlation at scales less than 10 km, but that this correlation is near zero at length scales of 20-50 km (~12 nautical miles) and then becomes negative at the bay-wide scales (>50 km) (Fig. 25).

Since the station separation in Cape Cod Bay for F01 and F02 is >20 km, the assumption that these stations are independent of each other appears to be a reasonable one. Stations spaced closer than 20 km (e.g. those near Boston Harbor and in the Nearfield region) are likely to be correlated to a certain extent and this correlation should be accounted for in the statistical analyses used to test for significant post-discharge effects.

LITERATURE CITED

Angel, M. V. and M. J. R. Fasham. 1983. Eddies and biological processes. pp. 492-524. in A. R. Robinson, ed., Eddies in marine science. Springer, Berlin.

Benfield, M. C., C. S. Davis, P. H. Wiebe, S. M. Gallager, R. G. Lough, and N. J. Copley. 1996. Comparative distributions of calanoid copepods, pteropods, and larvaceans estimated from concurrent Video Plankton Recorder and MOCNESS tows in the stratified region of Georges Bank. Deep Sea Res. II, 43, 1925-1946.

Bigelow, H. B. 1926. Plankton of the offshore waters of the Gulf of Maine. Bull. U. S. Bur. Fish., 40, 1-509.

Bridges, W. L., R. D. Anderson, J. D. Davis, and D. Merriman.1984. A brief survey of Pilgrim Nuclear Power Plant effects upon the marine aquatic environment. Observations on the Ecology and Biology of Western Cape Cod Bay, Massachusetts., Lect. Notes Coast. Estuar. Stud., 11, 263-271

Cassie, R. M. 1959a. An experimental study of factors inducing aggregation in marine plankton. N.Z. J. Sci., 2, 339-365.

Cassie, R. M. 1959b. Some correlations in replicate plankton samples. N.Z. J. Sci., 2, 473-484.

Cassie, R. M. 1960. Factors influencing the distribution pattern of plankton in the mixing zone between oceanic and harbor waters. N.Z. J. Sci., 3, 26-50.

Cibik, S. J., K. B. Lemieux, C. S. Davis, D. M. Anderson. 1998. Massachusetts Bay plankton communities: characterization and discussion of issues relative to MWRA's outfall relocation. Boston: Massachusetts Water Resources Authority. Report ENQUAD 98-08. 140 p.

Cushing, D. H. 1975. Marine Ecology and Fisheries. Cambridge University Press, Oxford.

Davis, C. S., G. R. Flierl, P. J. Franks and P. H. Wiebe. 1991. Micropatchiness, turbulence, and recruitment in plankton. J. Mar. Res., 49, 109-151.

Davis, C. S., S. M. Gallager, M. S. Berman, L. R. Haury, and J. R. Strickler. 1992a. The Video Plankton Recorder (VPR): Design and initial results. Arch. Hydrobiol. Beih., 36, 67-81.

Davis, C. S., S. M. Gallager, and A. R. Solow. 1992b. Microaggregations of oceanic plankton observed by towed video microscopy. Science 257, 230-232.

Davis, C. S., S. M. Gallager, M. Marra, and W. K. Stewart. 1996. Rapid visualization of plankton abundance and taxonomic composition using the Video Plankton Recorder. Deep Sea Res. II, 43, 1947-1970.

Davis, C. S. and S. M. Gallager. 1998a. Cruise Report for OSV *Peter W. Anderson* cruise 9803, March, 11-14, 1998. MWRA Report, 4/1998.

Davis, C. S. and S. M. Gallager. 1998b. Data Report for Video Plankton Recorder Cruise OSV *Peter W. Anderson*, March, 12-14, 1998. Boston: Massachusetts Water Resources Authority. Report ENQUAD 98-22. 118 p.

Davis, C. S. and S. M. Gallager. 1999. Cruise Report for OSV *Peter W. Anderson* cruise 9902, February 23-38, 1999. MWRA Report, 7/1999.

Davis, C. S. and S. M. Gallager. 2000. Report of data collected during Video Plankton Recorder studies in Massachusetts and Cape Cod Bays in March 1996, March 1997, and June, 1998. EPA Data Report, (in preparation).

Davis, C. S., S. M. Gallager, X. Tang, L. Vincent, and C. J. Ashjian. Real-time visualization of taxa-specific plankton distributions. (submitted)

Denman, K. L. 1992. Scale-determining biological-physical interactions in oceanic food webs. In: Giller, P.S., A. G. Hildrew, and D. G. Raffaelli, (eds.), Aquatic Ecology: Scale, Pattern, and Process. Blackwell Scientific, Oxford, pp. 377-402 .

Denman, K. L., and A. E. Gargett. 1995. Biological-Physical interactions in the upper ocean: the role of vertical and small scale transport processes. Ann. Rev. Fluid Mech., 27, 225-255.

Fasham, M.J.R. 1978. The statistical and mathematical analysis of plankton patchiness. Oceanogr. Mar. Biol. Ann. Rev., 16, 43-79.

Gallager, S. M., C. S. Davis, A. W. Epstein, A. Solow, and R. C. Beardsley. 1996. High resolution observations of plankton spatial distributions correlated with hydrography in the Great South Channel, Georges Bank. Deep Sea Res. II, 43, 1627-1664. Haeckel, E. 1890 Plankton Studies. [transl. by G.W. Field]. Rep. U.S. Comm. Fish Fish. 1889-1891, p. 565-631.

Haeckel, E. 1890 Plankton Studies. [transl. By G.W. Field]. Rep. U.S. Comm. Fish Fish. 1889-1891, p. 565--631.

Hardy, A. C. 1936. Observations on the uneven distribution of the oceanic plankton. Discovery Rep., 11, 511-538.

Hardy, A. C. and E. R. Gunther. 1935. The plankton of the South Georgia whaling grounds and adjacent waters, 1926-1927. Discovery Rep., 11, 1-456.

Haury, L. R., J. A. McGowan and P. H. Wiebe. 1978. Patterns and processes in the time-space scales of plankton distributions, in Spatial Patterns in Plankton Communities, J. H. Steele, ed., Plenum Press, New York, 277-327.

Haury, L. R. P. H. Wiebe, M. H. Orr, and M. G. Briscoe. 1983. Tidally generated high-frequency internal wave packets and their effects on plankton in Massachusetts Bay. J. Mar. Res., 41, 65-112.

Horst, T., R. Lawton, R. Toner, M. Scherer, J. D. Davis, and D. Merriman. 1984. Seasonal abundance and occurrence of some planktonic and ichthyofaunal communities in Cape Cod Bay: Evidence for biogeographical transition. Observations on the Ecology and Biology of Western Cape Cod Bay, Massachusetts., Lect. Notes Coast. Estuar. Stud., 11, 241-261.

Jossi, J.W. and J.R. Goulet. 1990. Zooplankton community abundance, coherence, and stability of the northeast shelf ecosystem. ICES C.M. 1990/L:93.

Lemieux, K. B., S. J. Cibik, S. J. Kelly, J. K. Tracey, C. S. Davis, C. A. Mayo, J. W. Jossi. 1998. Massachusetts Bay zooplankton communities: a historical retrospective. Boston: Massachusetts Water Resources Authority. Report ENQUAD 98-21. 120 p.

Longhurst, A. R., ed. 1981. Analysis of marine ecosystems. Academic Press, London. 741 pp.

Mackas, D. L., K. L. Denman, and M. R. Abbott. 1985. Plankton Patchiness: Biology in the physical vernacular. Bull. Mar. Sci., 37,652-674.

Okubo, A. 1980. Diffusion and ecological problems: mathematical models. Biomathematics, 10, Springer Verlag, NY.

Owen, R. W. 1989. Micro and finescale variations of small plankton in coastal and pelagic environments. {\it J. Mar. Res.}, {\bf 47}, 197--240.

Sieracki, M. E., D. J. Gifford, S. M. Gallager, and C. S. Davis. 1998. Ecology of a *Chaetoceros socialis* Lauder patch on Georges Bank: Distribution, microbial associations, and grazing losses. Oceanography, 11, 30-35.

Toner, R.C. 1984. Zooplankton of Western Cape Cod Bay. In: Lecture notes on Coastal and Estuarine Studies 11. Observations on the Ecology and Biology of Western Cape Cod Bay, Massachusetts, J.D. Davis and D. Merriman, eds. pp. 65-76.

Turner, J.T. 1994. Planktonic Copepods of Boston Harbor, Massachusetts Bay, and Cape Cod Bay, 1992. Hydrobiologia, 292/293: 405-413.

APPENDIX

Cruise Narrative

(Dates/time given in local time, EST, with GMT in parentheses)

02/21/1999 (Sunday)

We spent the day loading the ship in Woods Hole (on south side of WHOI dock.) We installed the VPR system on the ship including winch (Dynacon) and block (NMFS orange block used), underwater sled, and data acquisition/processing system.

The winch was mounted, as on previous OSV *Anderson* cruises, on starboard side of fantail facing to port side. The winch was bolted to aluminum angles welded to the main deck. As before, the VPR was rigged for towing from the crane boom off the port side of the ship. A forward stay was affixed to the end of the crane boom and to the stantion supporting the winch control house. An after stay was rigged by running a line from the end of the boom to the port side of the A-frame. Another line was attached from the side of the block to the starboard side of the A-frame to control the angle of the block relative to the tow cable.

The tow cable was the same as on prior cruises: a 3-fiber, 3-conductor, triple-armor, 0.68 inch diameter cable. The tow cable was terminated on the VPR towfish (4' V-fin) and a tapered strain-relief "boot" was made by wrapping rubber tape around the end of the termination and the cable. The fiber optic receivers were mounted in the winch drum and the video and data as well as power to the underwater unit ran through the coaxial/copper slip-rings. A deck cable ran from winch to the main lab through the long stuffing tube in the breezeway overhead.

Our surveillance cameras were mounted to monitor winch and deck operations. The fixed-focus camera was mounted adjacent to the winch to monitor cable winding while the pan-tilt-zoom camera was mounted on the 01 deck to monitor deck operations, the cable/block, and the VPR at the water surface. Cables from these cameras also entered the main lab through the stuffing tube and were connected to rack-mounted monitors and the joy-stick control unit.

VPR data entered the acquisition system in the ususal way via coaxial and copper conductor cables. Incoming video was time-stamped with GMT using the Horita GPS time-code generator that was jam-synched to GMT via serial input from GPS. The environmental data (CTD, fluorescence, attenuation, light) from the VPR entered the data logging PC via a serial line using our standard C acquisition/logging program (running under DOS). The data logging PC wrote data to a zip disk as well as via NFS mount to a Toshiba notebook PC (Tecra 8000 266Mhz Pentium II) running windows NT.

Because of a fundamental limitation of Microsoft operating systems, the logging file could not be read from while it was being written to. To plot the data (at 2 minute intervals), we had to stop the logging program, copy the file to a temporary file, and then start logging again. The temporary file then was read into the parsing/plotting program. This method caused interruptions in data acquisition, and on subsequent cruises we have switched from NT to Linux as the operating system on the notebook.

Video from the high magnification camera (named camera 4) was sent to the image processing PC where in-focus organisms were extracted as tiff files to the local disk. Image features from these files were extracted in real time and saved as companion .dat files using the Tang/Vincent routines ported to the NT from the unix workstations by Bob Eastwood. Manual sorting of images for training the neural network classifier could not be done since the NT machine was too slow to allow the image sorting program (ThumbsPlus) to be used. We extracted tiff images and their features for nearly all of the high magnification video collected during the cruise. Training and classification is being done in the laboratory.

02/22/1999 (Monday)

Winds were gale force all day and prevented us from leaving the dock. We conducted some dockside test deployments of the VPR and found all systems working well.

02/23/1999 (Tuesday)

We left the WHOI dock at 0700 (1200 GMT), underway for the Cape Cod Canal. We passed through Quick's Hole channel at 0750 (1250) and were clear of the east end of the Cape Cod Canal by 1015. Winds were 16 knots with seas 5-7'.

At 1105 (1605), we reached the Barnstable Harbor Sea Buoy and deployed the VPR for flight stability/trim adjustments. Several deployments were needed to get the proper trim. Trim was adjusted by cutting away portions of the plastic trim tab on the starboard side of the tail fin.

The VPR data was intermittent at regular intervals as the winch rotated. A loose fiber connector was found in the winch drum and the connector was cleaned and reseated, which solved the problem.

The VPR was occasionally giving intermittent data at tow speeds above 6 knots, and the reason for this problem was not clear. We decided to conduct the survey at 5 knots rather than spend time chasing down the intermittent problem.

We began towyoing along the Barnstable/Gloucester transect line at 1536 (2036 GMT). A right whale was sighted 600 m off the port beam at 1620. By this time, winds had diminished to 6 knots with seas only 2 feet. A line was cleared from fish at 1940 (0040), causing a brief loss of data. It was noticed that the zip disk ejected at 2037 (0137), causing another brief (<2 min) loss of data. To prevent further occurrences, a protective plate was placed over the eject button.

We noticed that the V-fin was rolling too much, so we re-deployed it several times after readjusting the trim tab size. We found that we had to cut away a significant section of starboard trim tab. We then found that Girard had reduced the angle of the trim tab mounts which may have accounted for need to remove a larger area of the trim tab to achieve the desired roll angle.

The VPR was redeployed with the proper trim adjustment at 2339 (0439), and a new NFS logging file was started. We resumed towyoing at 5 knots (speed over ground). The haul-back speed through water was 6-7 knots according to the VPR flow-meter.

02/24/1999 (Wednesday)

We cleared a line from the sled at 0149 (0649) and again at 0248 (0748). The Barnstable-Gloucester transect was completed at 0330 (0830), and we changed course to the northeast to begin the radiator survey pattern. A fouled line was removed at 0452 (0952).

A new NFS data logging file was opened at 0536 (1036). It was taking about 6-8 seconds for the logging file (~10MB) to be copied to the temporary file for plotting, so we decided to open new NFS logging files more frequently. Another line was cleared from the VPR tow cable at 0930 (1430).

The fish was held at the surface and ship speed was slowed to 1.5 knots to exchange EPA personnel. Dave Tomey departed and Eric Nelson came aboard from a chartered vessel that came along side the *Anderson*.

During this exchange process Anne Sell collected a bucket surface sample to examine the algal colonies under a dissecting microscope (provided by ship's technician). The colonies were confirmed to be *Chaetoceros socialis* as was initially determined from the VPR video images.

We resumed towyoing the VPR at 0948 (1448). New logging files were opened at 1011 (1511). The ship's speed was increased to 6 knots.

At 1120 (1620), the video signal was lost from both cameras, but the environmental (CTD, fluor etc) data was still coming in fine. The ship was slowed to 3 knots, and the video came back on at 1130 (1630), and we resumed towyoing at 5 knots. The video signal was lost again at 1154 (1654) and returned at 1157 (1657). We decided to resume towyoing to obtain as much data as possible before the upcoming storm set in. We planned to fix the video problem in Provincetown Harbor while we were weathered out.

Towyoing was resumed at 1217 (1717). At 1228 (1728), a fouled line was cleared from the tow cable. The VPR was brought aboard at 1415 (1915) to adjust fins on the cable and was re-deployed at 1440 (1940). Towyoing was resumed at 1458 and the next 8 hours were routine towyoing operations. The ship's fathometer started giving bad data at 2241 (0341) due to increased sea state producing bubbles under hull.

By 2157 (0357) winds had increased to 20 knots and a northeaster was predicted with 50 knot winds and snow. At 2300 (0400) we were in Stellwagen Basin approaching the bank. Another fouled line was cleared at 2320 (0420). At 2340 we came across the sharp edge of the bank. Toward the end of this northeasterly leg, the ship's autopilot had difficulty steering a straight line due to the increasingly bad weather conditions (22 knot NE winds).

02/25/1999 (Thursday)

The transect was completed at 0100 (0600), and we brought the VPR on board in the snow and began steaming for Provincetown Harbor to ride out the storm. During the 7 hour ride to Provincetown, we rode the trough, and the winds increased to 28 knots. We reached the harbor at 0800 and anchored 1 mile from shore. We spent the next 24 hours at anchor. The northeaster was a serious storm with winds recorded on the ship reaching a steady 45 knots in the lee of Provincetown. Snow accumulations on Cape Cod were over 2 feet.

02/26/1999 (Friday)

Wind speeds had dropped to 20 knots by 0800 (1300), and the Captain decided it would be safe to attempt sampling again. We deployed the VPR at 0915 (1415) while the ship was still at anchor. We then weighed anchor and were underway at 0926 (1426). The plan was to towyo NW to intersect the Barnstable/Gloucester line and then towyo north toward Gloucester to resample the line after the storm. We would then towyo to where we left off before the storm.

We began towyoing on this NW line at 1031 (1531) at 5 knots. At 1115 (1615), a few glitches in camera 2 were noticed, so the connectors on the winch junction box were adjusted. The ship's fathometer was giving bad data again due to the sea state. At 1133 we turned to port, back into Cape Cod Bay, because the offshore swells from north of Race Point were too large (5-8 feet).

At this point we decided to sample in the lee of land along the coast in eastern Cape Cod Bay. We towyoed back around Wood End and NE to the 20 m bottom contour, then, at 1353 (1853) we turned southeast and followed this depth contour. Data from the light sensor was becoming intermittent, perhaps due to a leak in the connector.

We turned east into the region south of Billingsgate shoal at 1718 (2218) and turned around heading west at 1843 (2343). Once we were west of Billingsgate Shoal at 2015 (0115), we towyoed NNE toward Wood End. At this point the winds increased again to 25-35 knots from the NW, and the seas started to build (5-8 feet). Despite the poor sea state, we continued towing NNE until 2246 (0346) when we turned onto a short leg to the NW. At 2320 (0420), we turned to the SSW and sampled along a line across the middle of Cape Cod Bay toward a point west of Barnstable harbor.

02/27/1999 (Saturday)

We continued towing toward the SW until 0148 (0648) when we turned onto a short leg to the WNW. At 0222 (0722) we turned to the north again and ran a leg northward to the mouth of Cape Cod Bay. By 0300 (0800) the winds had dropped off to 20 knots but the seas were still running high (6-9 feet).

At 0430 (0930), we turned onto a short westerly leg, and then at 0508 (1008) we turned south for a long run through the western part of the bay. By 0700 (1200), the winds had dropped to 15 knots from the NW, and the sea state had improved substantially (2-4 feet). At 0737 (1237), we turned NW and then to the north at 0810 (1310), sampling the westernmost transect in Cape Cod Bay.

Along this line, the video data became intermittent for short periods and the data stream "froze" for a few minutes from 0900-0905 (1400-1405). The image in the high magnification camera became progressively worse from 0940-1110 (1450-1610). At 1110 (1610) the VPR was brought on deck, and the lens on the high magnification camera was found to have vibrated loose. It was resecured, and the VPR was relaunched at 1208 (1708). By this time the winds had increased again to 22 knots and the seas had increased to 3-6 feet.

We continued to roughly follow the 20m isobath to the NNW north of Plymouth until 1438 (1938) when we began a short leg to the NE. During this period, the winds dropped from 22 to 12 knots and the seas dropped to 2-4 feet. The plan at this point was to survey the southern half of Massachusetts Bay using a radiator pattern.

From 1500-1600 (2000-2100), the power to both cameras and the strobe became intermittent. At 1530 (2030), we turned to the SSE on the second leg of the southern Mass Bay survey. Strobe and camera power became increasingly intermittent, and at 1620 (2120) we retreived the VPR to service the control electronics. We found and repaired a loose connector (P11) and redeployed the VPR at 1830 (2330), resuming towyoing to the SSE from the location where the VPR had been retreived.

Winds by this time had shifted to the west and diminished to 8 knots; seas had subsided to 1-3 feet. Ship speed was increased to 6 knots without loss of data (previously, cable strumming at this speed was causing the loose connector to yield intermittent video). After a short leg to the east, at 1903 (0203), we turned onto a leg to the NNW toward Gloucester Harbor. We would sample this leg all the way to Glocester to obtain data from the northern half of Mass Bay after the northeast storm. In this way, we would have data along a complete transect from Barnstable to Gloucester both before and after the storm.

02/28/1999 (Sunday)

Along the line to Gloucester, the fish was held at the surface briefly on two occasions 0030 and 0137 (0530 and 0637) to remove debris. The winds remained low (3-9 knots) as well as the seas (1-2 feet). We reached the end of this line at Gloucester Harbor at 0245 (0745) and brought the VPR on board.

We steamed to the easternmost transect line in southern Mass Bay and deployed the VPR at 0437 (0937), heading SSE toward a waypoint off Provincetown. We increased the ship's speed to 6.5 knots. By 0700 (1200) winds were only 3-7 knots. The water was glassy calm and many surface slicks were observed, as well as some unidentified whales. We continued SSE along this line until we were due west of Wood End.

At this point [0823 (1323)], we turned east toward Wood End and then NW along the ledge between Wood End and Race Point. We reached Race Point at 0908 (1408) and then turned SW for a short leg before turning onto a primary leg to the NNW at 0950 (1450). The wind shifted to the SE at 12 knots and the seas were 1-3 feet.

At 1253 (1753), we turned SW for a short leg before turning SSE for the final leg in southern Mass Bay. By 1300 (1800), the wind speed had increased to 22 knots from the SE and seas were 3-4 feet. At 1335 (1835), we brought the VPR on board to excise a portion of the strain-relief boot which had been split. We re-deployed the VPR and resumed towyoing at 1352 (1852). Winds had increased to 22 knots by 1600 (2100) with seas running 2-4 feet. We ended the VPR survey operations at the end of this transect at 1614 (2114).

We then conducted high speed tow test over the next hour, towing the VPR at ship speeds up to 11 knots. The VPR flew stably at these speeds but the winch hydraulic pressure reached a maximum at 3500 psi and we were unable to haul back at 10.5 knots. Thus, the upper limit of ship speed for towyo operations using this Dynacon winch (30 hp motor) was 9-10 knots.

The VPR was brought on board at 1712 (2212). Winds at this point had reached 30 knots and seas were running 3-5 feet and continued to increase to 35 knots and 3-8 feet during our transit home.

VIDEO TAPE INVENTORY

TAPE #S	DATE (GMT)	START TIME (GMT)
1,2	2/23/1999	2036*
3,4	2/23/1999	2149
5,6	2/23/1999	2349
7,8	2/24/1999	0149
9,10	2/24/1999	0439
11,12	2/24/1999	0641
13,14	2/24/1999	0847
15,16	2/24/1999	1049
17,18	2/24/1999	1248
19,20	2/24/1999	1449
21,22	2/24/1999	1651
23,24	2/24/1999	1854
25,26	2/24/1999	2155
27,28	2/24/1999	2356
29,30	2/25/1999	0157
31,32	2/25/1999	0357
33,34	2/26/1999	1415
35,36	2/26/1999	1615
37,38	2/26/1999	1830
39,40	2/26/1999	2030
41,42	2/26/1999	2232
43,44	2/27/1999	0035
45,46	2/27/1999	0234
47,48	2/27/1999	0433
49,50	2/27/1999	0638
51,52	2/27/1999	0839
53,54	2/27/1999	1050
55,56	2/27/1999	1251
57,58	2/27/1999	1455
59,60	2/27/1999	1708
61,62	2/27/1999	1909
63,64	2/27/1999	2337
65,66	2/28/1999	0138
67,68	2/28/1999	0339
69,70	2/28/1999	0539
71,72	2/28/1999	0830
73,74	2/28/1999	1138
75,76	2/28/1999	1339
77,78	2/28/1999	1540
79,80	2/28/1999	1740
81,82	2/28/1999	1954
83,84	2/28/1999	2155

(*survey starts 50 minutes into tape)

Watch Schedule

The scientific watch schedule was as follows:

0000-0400, 1200-1600	Andy Girard, Drew Lucas, Dave Tomey (2/23-24)) Eric Nelson (2/24-28)
0400-0800, 1600-2000	Scott Gallager, Sanjay Tiwari, Urmilla Malvadka
0800-1200, 2000-2400	Cabell Davis, Qiao Hu, and Anne Sell

Cruise Participants, Scientific Party

Cabell Davis	co-Chief Scientist	WHOI
Scott Gallager	co-Chief Scientist	WHOI
David Tomey	co-Chief Scientist	EPA
Eric Nelson	Scientist	EPA
Anne Sell	Postdoc (volunteer)	WHOI
Sanjay Tiwari	Visiting Investigator (volunteer)	WHOI/U. Wisconsin
Qiao Hu	Guest Student (volunteer)	WHOI
Urmilla Malvadka	Guest Student (volunteer)	Princeton University
Drew Lucas	Student (volunteer)	Formerly NE Aquarium
Andrew Girard	VPR Technician	WHOI

Ship's Officers/Crew

H. Holdsworth	Captain
B. Haney	1st Mate
S. Davis	2nd Mate
G. Leeds	Seaman
T. Holdsworth	Seaman (grandson of Captain)
G. Whitaker	Seaman

FIGURES

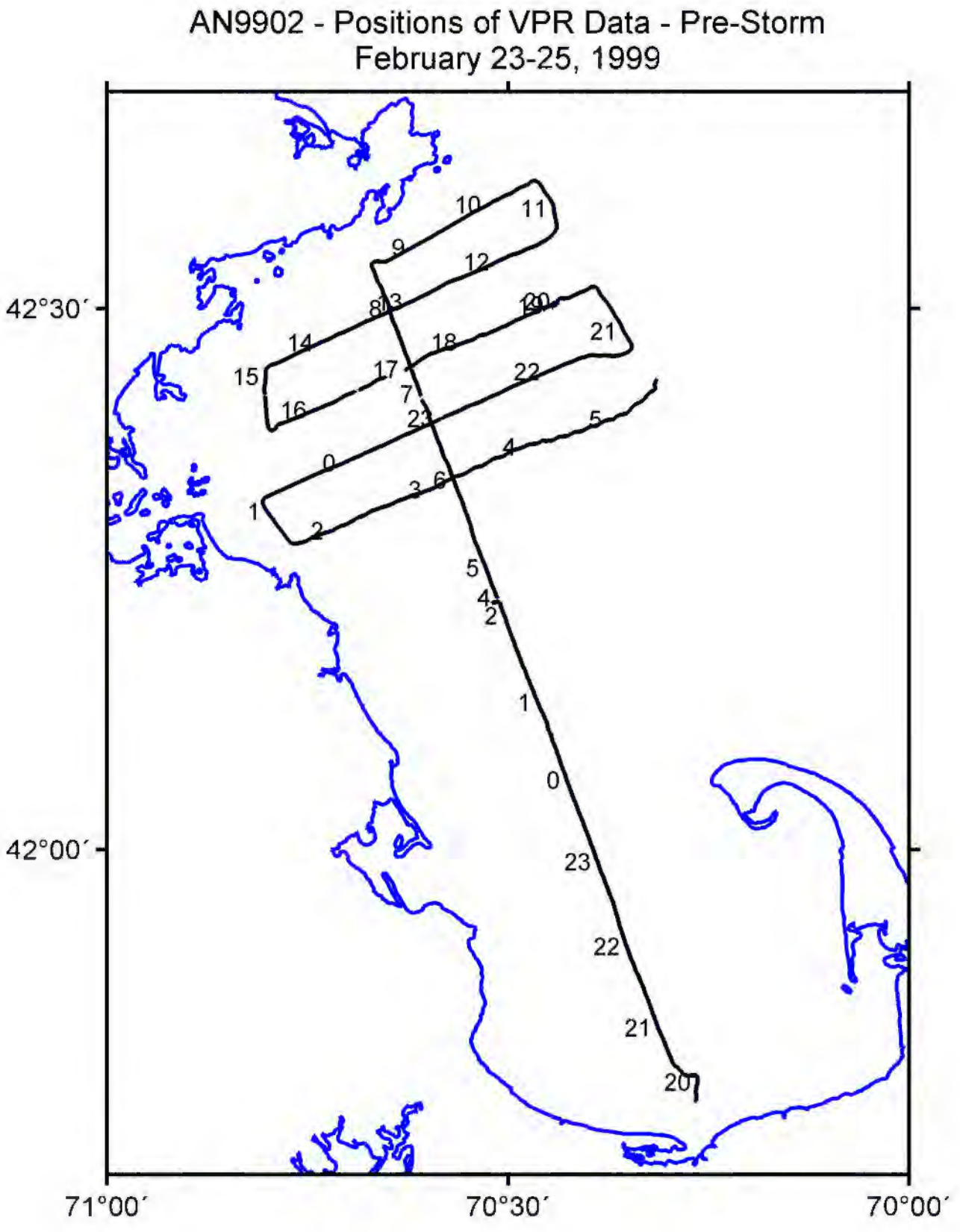
AN9902 - Positions of VPR Data - Pre-Storm
February 23-25, 1999
42°30´
42°00´
71°00´
70°30´
70°00´

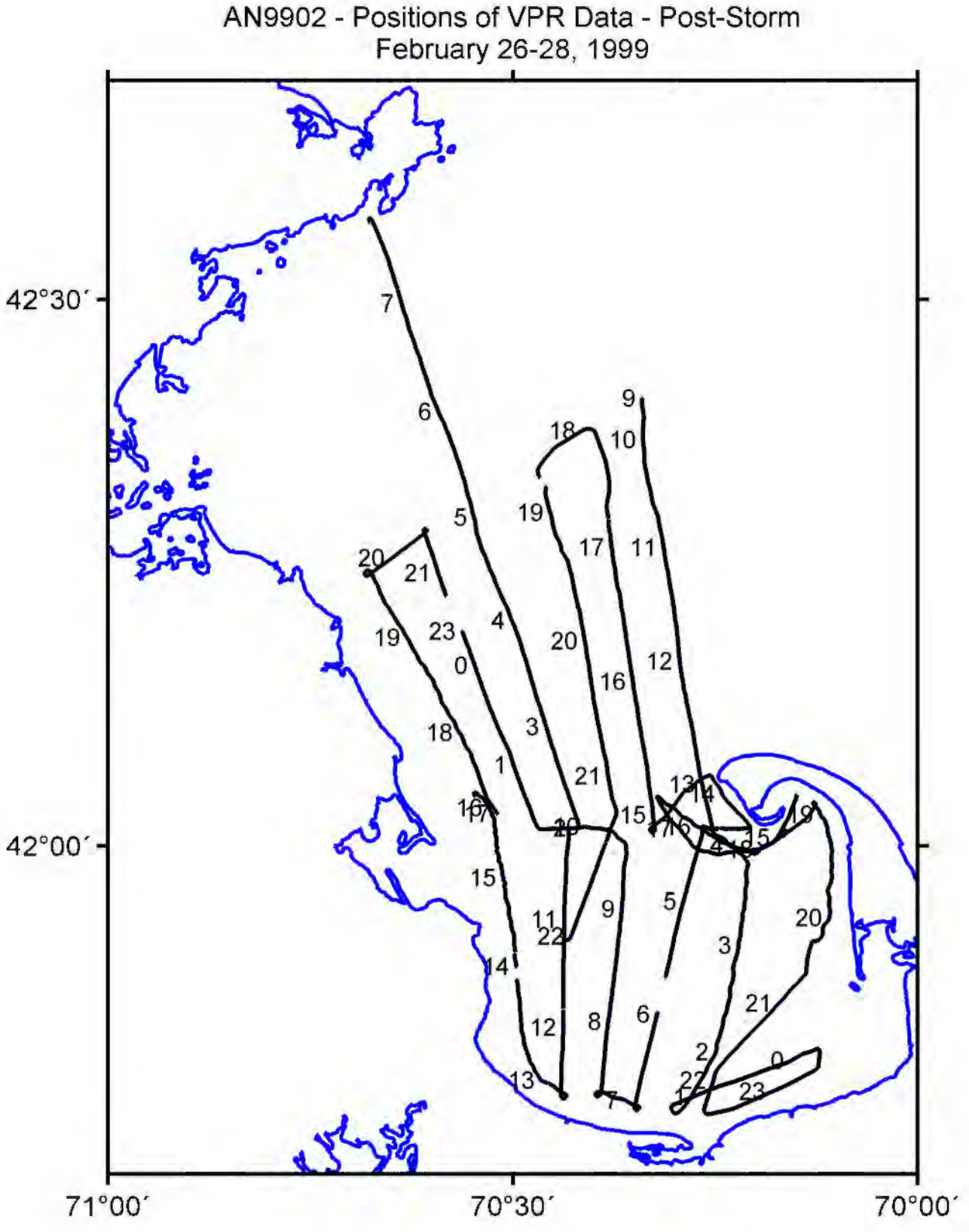
AN9902 - Positions of VPR Data - Post-Storm
February 26-28, 1999
42°30´
42°00´
71°00´
70°30´
70°00´

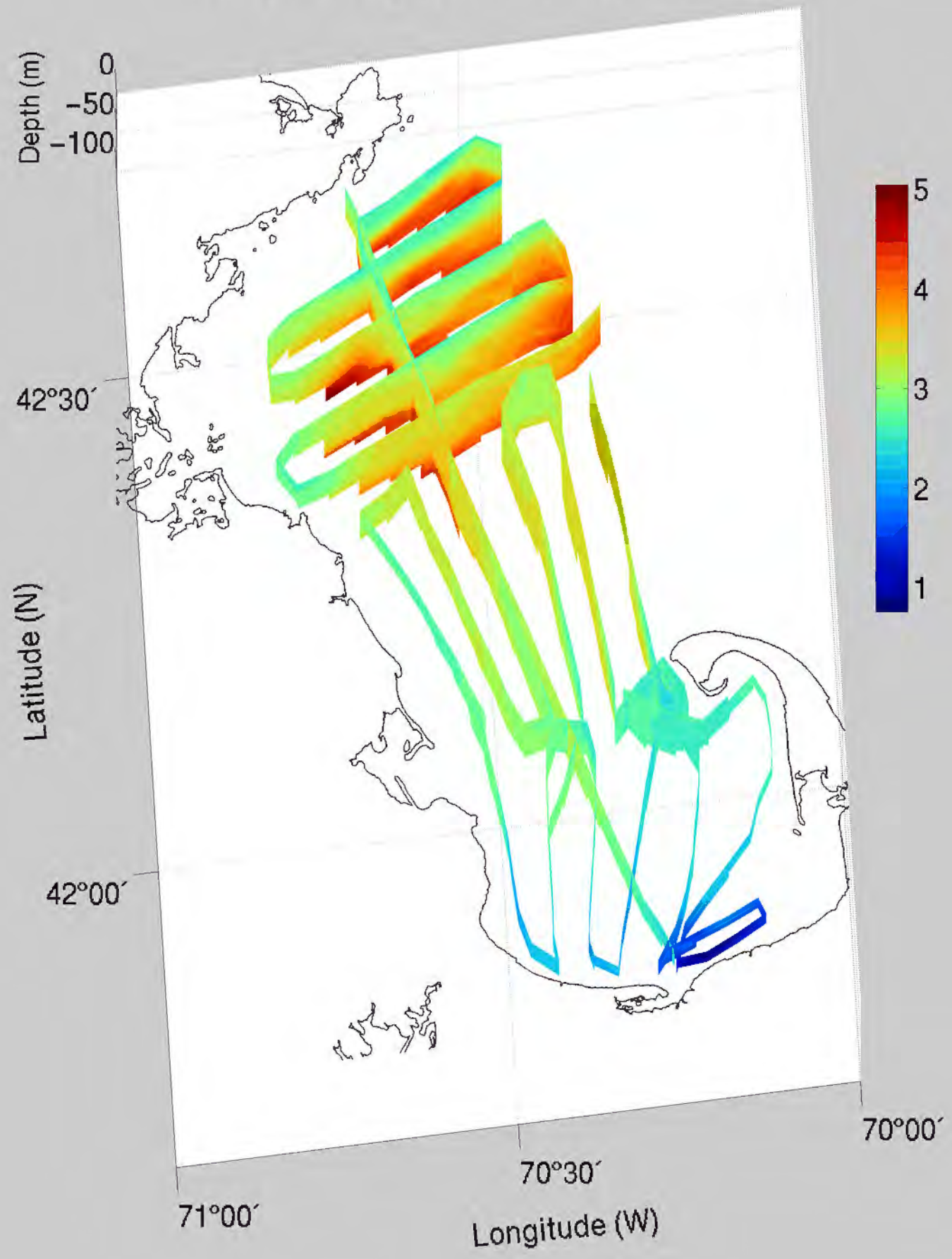
Temperature (°C) February 23–28, 1999
Depth (m)
0
−50
−100
42°30´
42°00´
Latitude (N)
71°00´
70°30´
70°00´
Longitude (W)
5
4
3
2
1

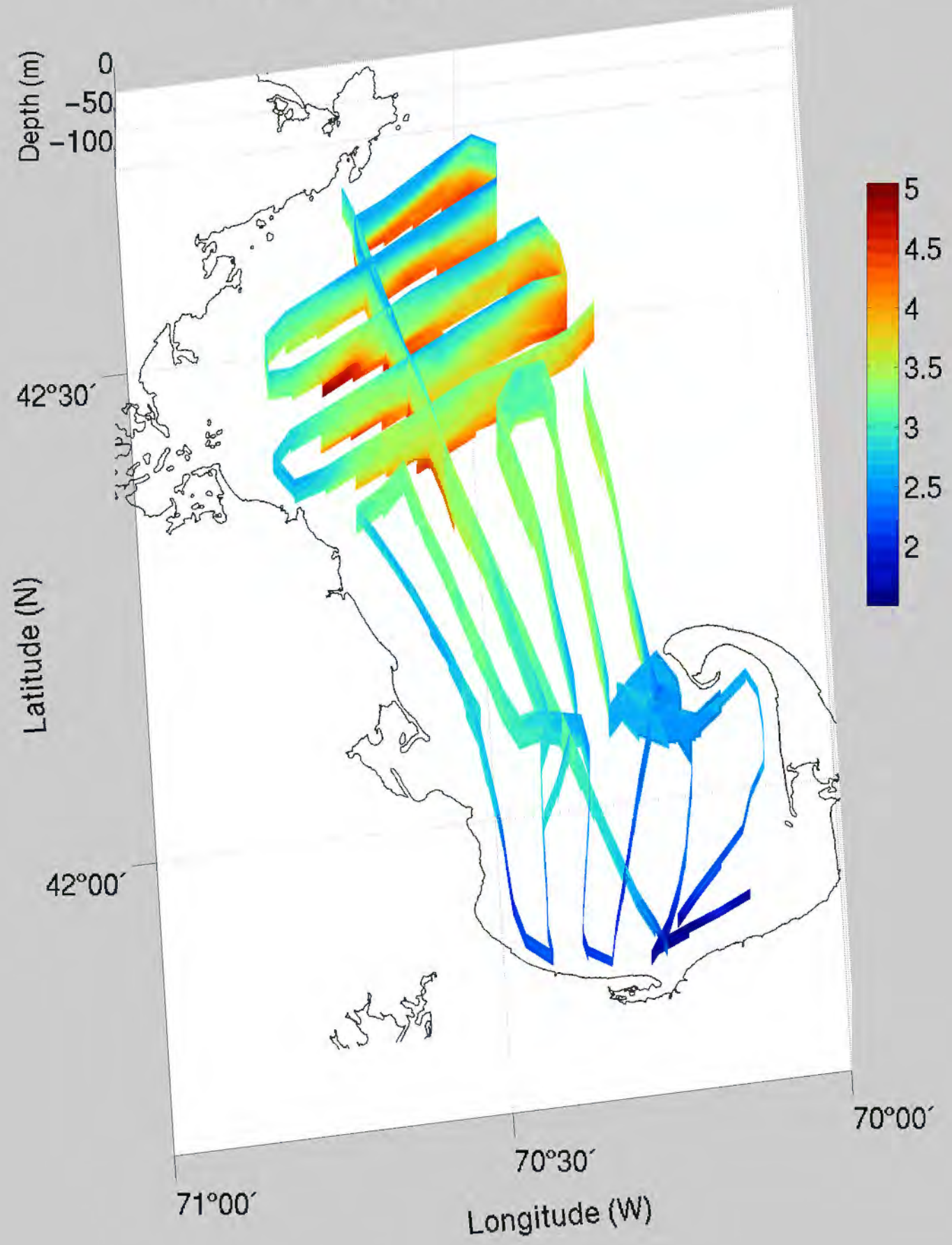
Temperature (°C) February 23–28, 1999
Depth (m)
0
−50
−100
5
4.5
4
3.5
3
2.5
2
42°30´
42°00´
Latitude (N)
71°00´
70°30´
70°00´
Longitude (W)

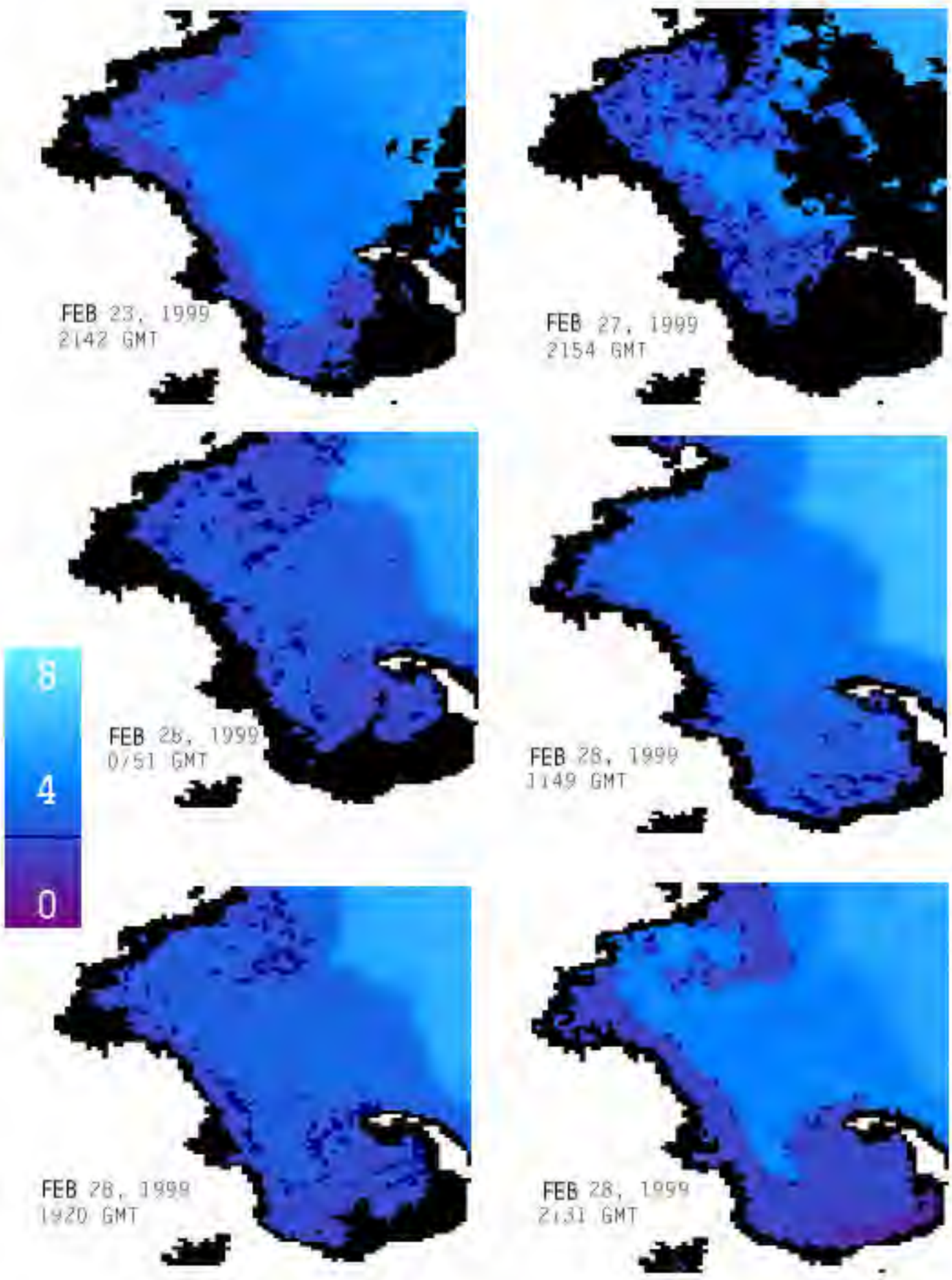
FEB 23, 1999
2142 GMT
FEB 27, 1999
2154 GMT
FEB 26, 1999
0751 GMT
FEB 28, 1999
1149 GMT
8
4
0
FEB 28, 1999
1920 GMT
FEB 28, 1999
2131 GMT

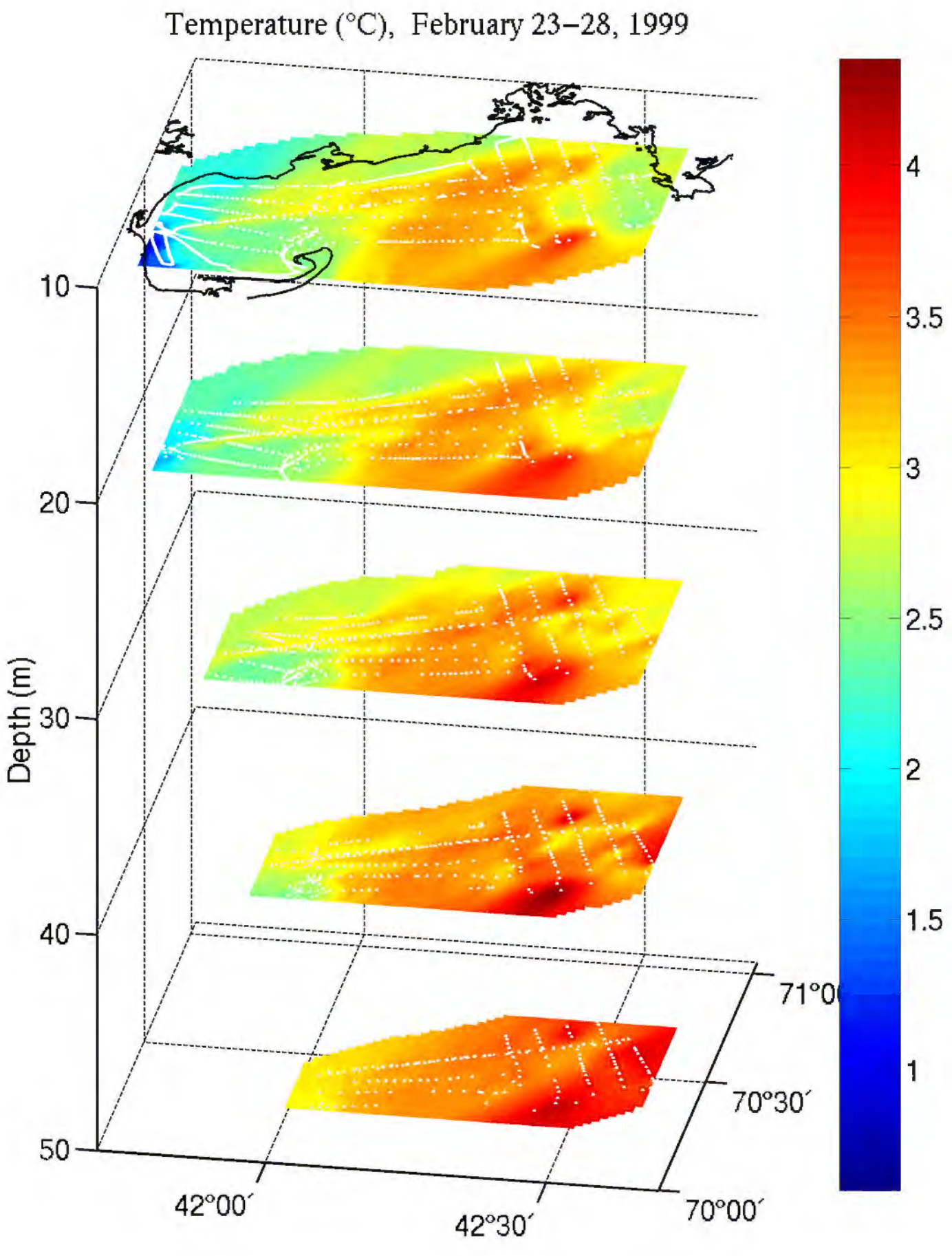
Temperature (°C), February 23–28, 1999
Depth (m)
10
20
30
40
50
42°00´
42°30´
70°00´
70°30´
71°0
4
3.5
3
2.5
2
1.5
1

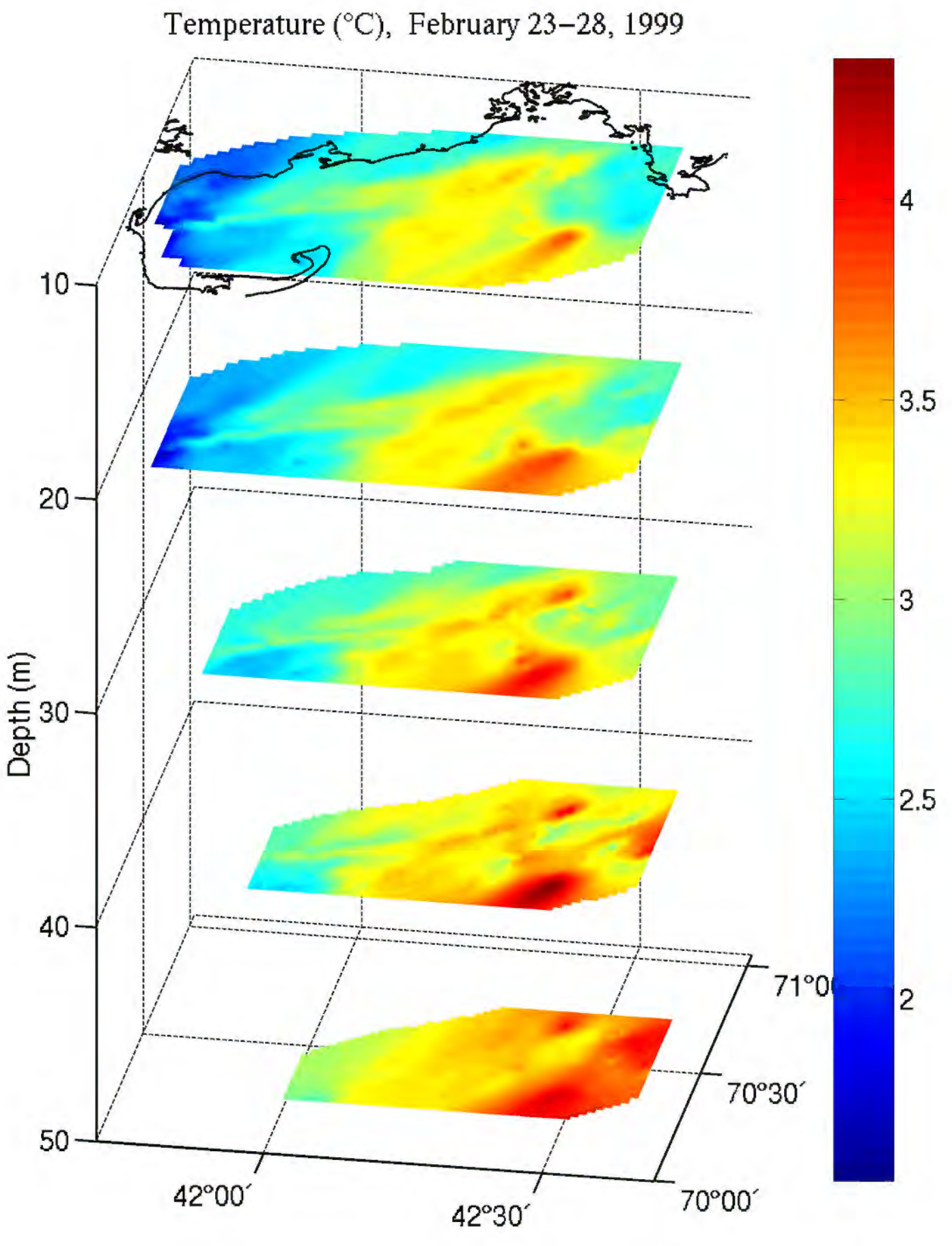
Temperature (°C), February 23–28, 1999
Depth (m)
10
20
30
40
50
42°00´
42°30´
70°30´
70°00´
4
3.5
3
2.5
2

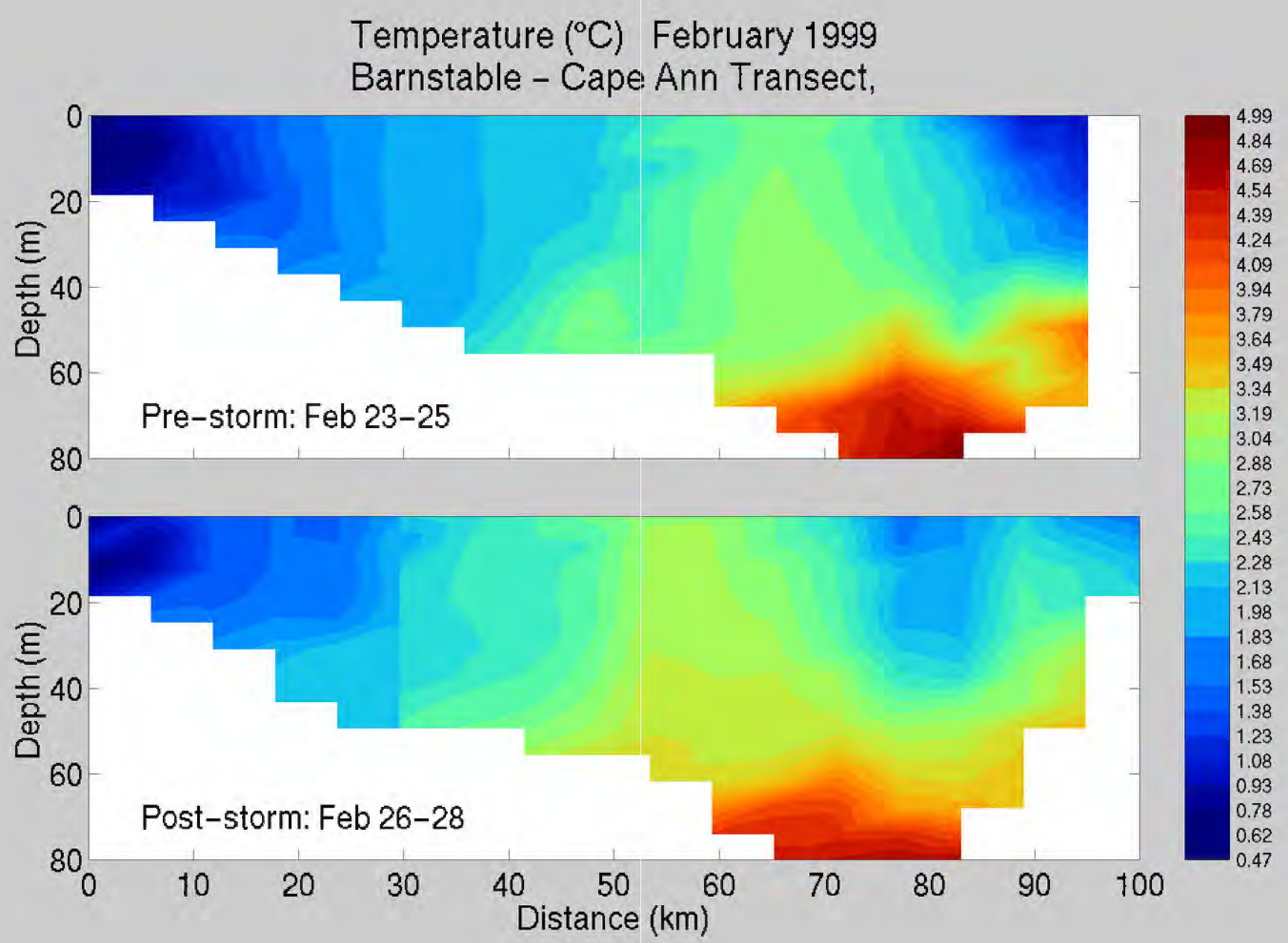
Temperature (°C) February 1999
Barnstable – Cape Ann Transect,
Depth (m)
0
20
40
60
80
Pre–storm: Feb 23–25
Post–storm: Feb 26–28
0
10
20
30
40
50
60
70
80
90
100
Distance (km)
4.99
4.84
4.69
4.54
4.39
4.24
4.09
3.94
3.79
3.64
3.49
3.34
3.19
3.04
2.88
2.73
2.58
2.43
2.28
2.13
1.98
1.83
1.68
1.53
1.38
1.23
1.08
0.93
0.78
0.62
0.47

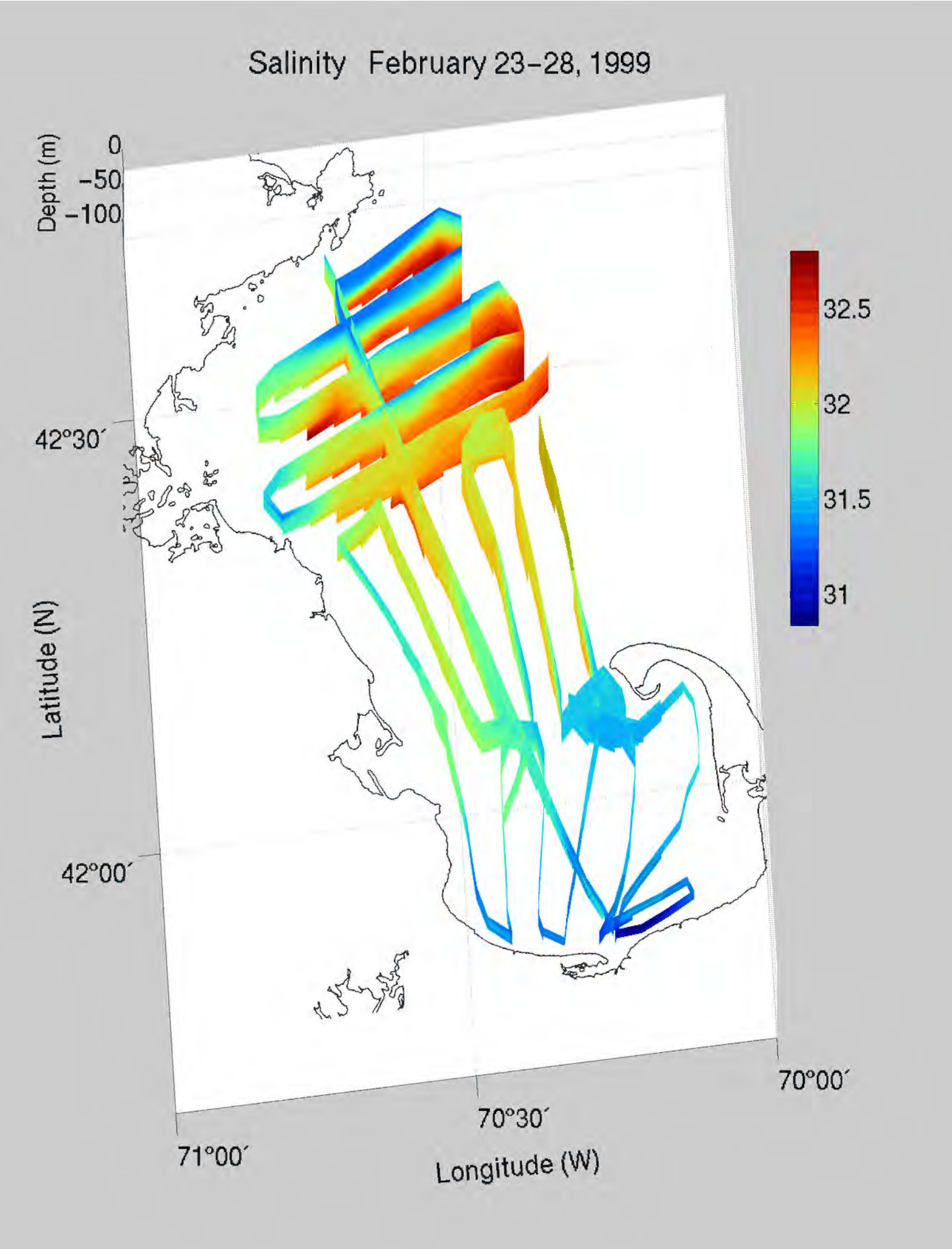
Salinity February 23–28, 1999
Depth (m)
0
−50
−100
42°30′
42°00′
Latitude (N)
71°00′
70°30′
70°00′
Longitude (W)
32.5
32
31.5
31

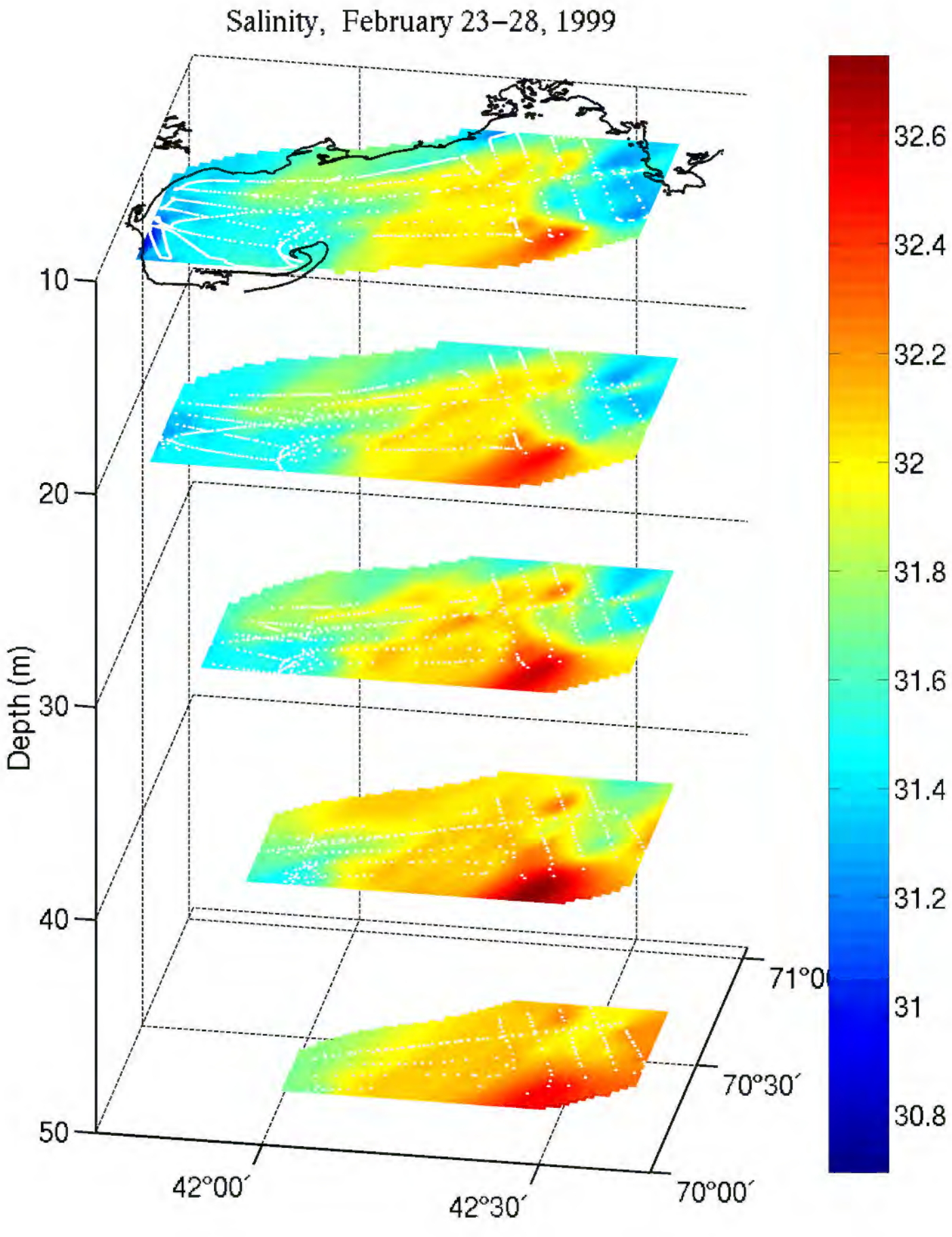
Salinity, February 23–28, 1999
Depth (m)
10
20
30
40
50
42°00´
42°30´
70°00´
70°30´
71°0
32.6
32.4
32.2
32
31.8
31.6
31.4
31.2
31
30.8

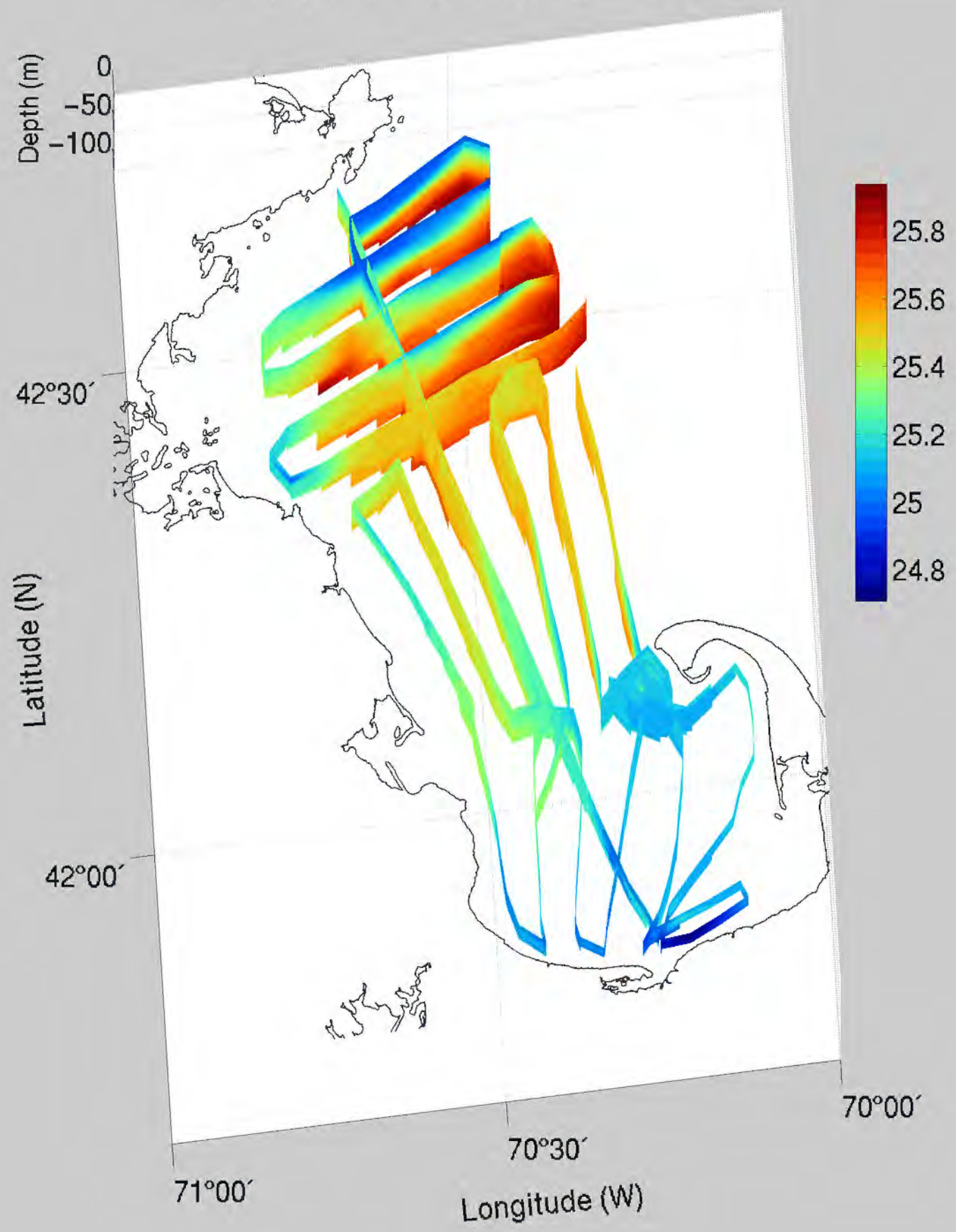
Density (sigma-t) February 23-28, 1999
Depth (m)
0
-50
-100
42°30´
42°00´
Latitude (N)
71°00´
70°30´
70°00´
Longitude (W)
25.8
25.6
25.4
25.2
25
24.8

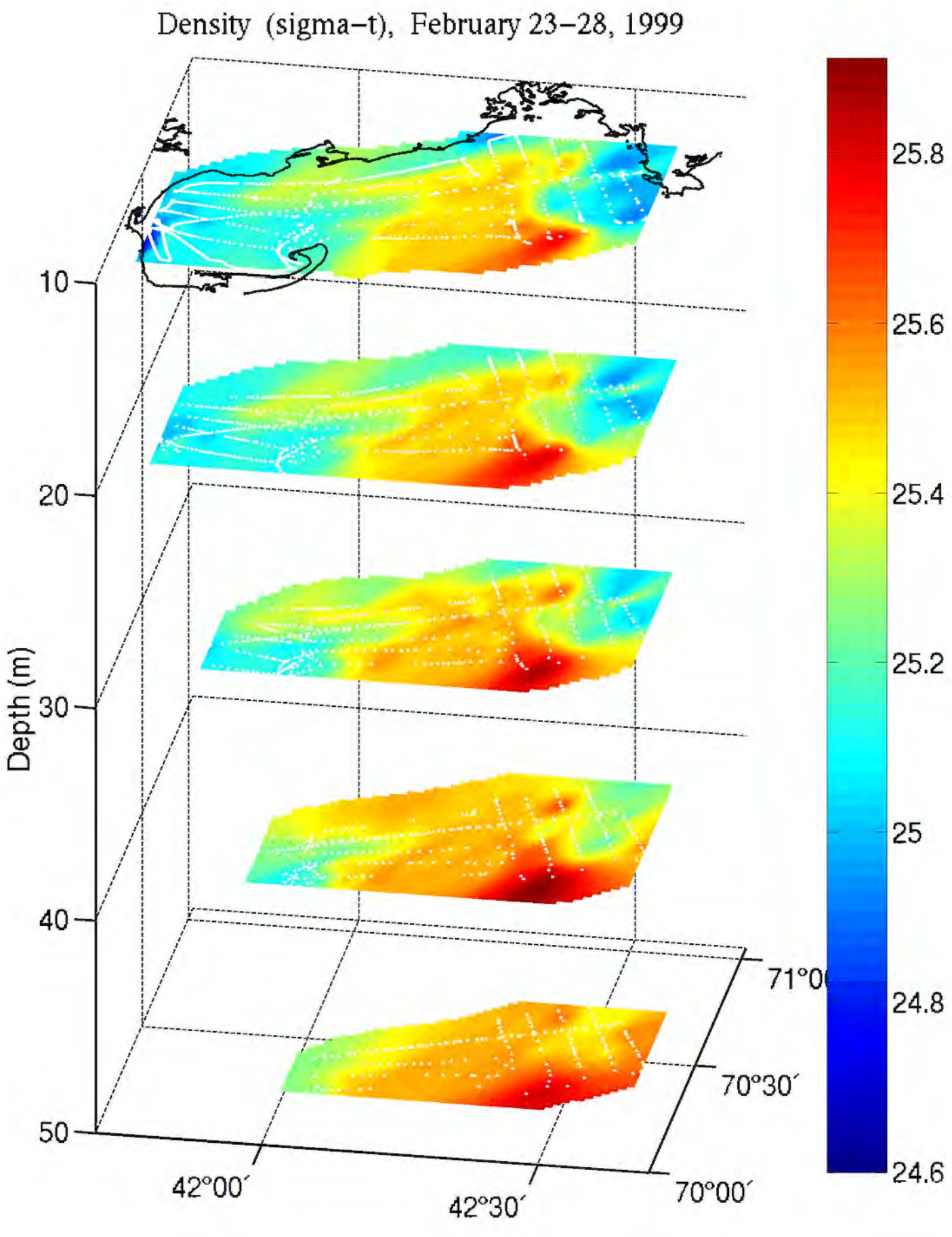
Density (sigma−t), February 23−28, 1999
Depth (m)
10
20
30
40
50
42°00´
42°30´
70°00´
70°30´
71°0
25.8
25.6
25.4
25.2
25
24.8
24.6

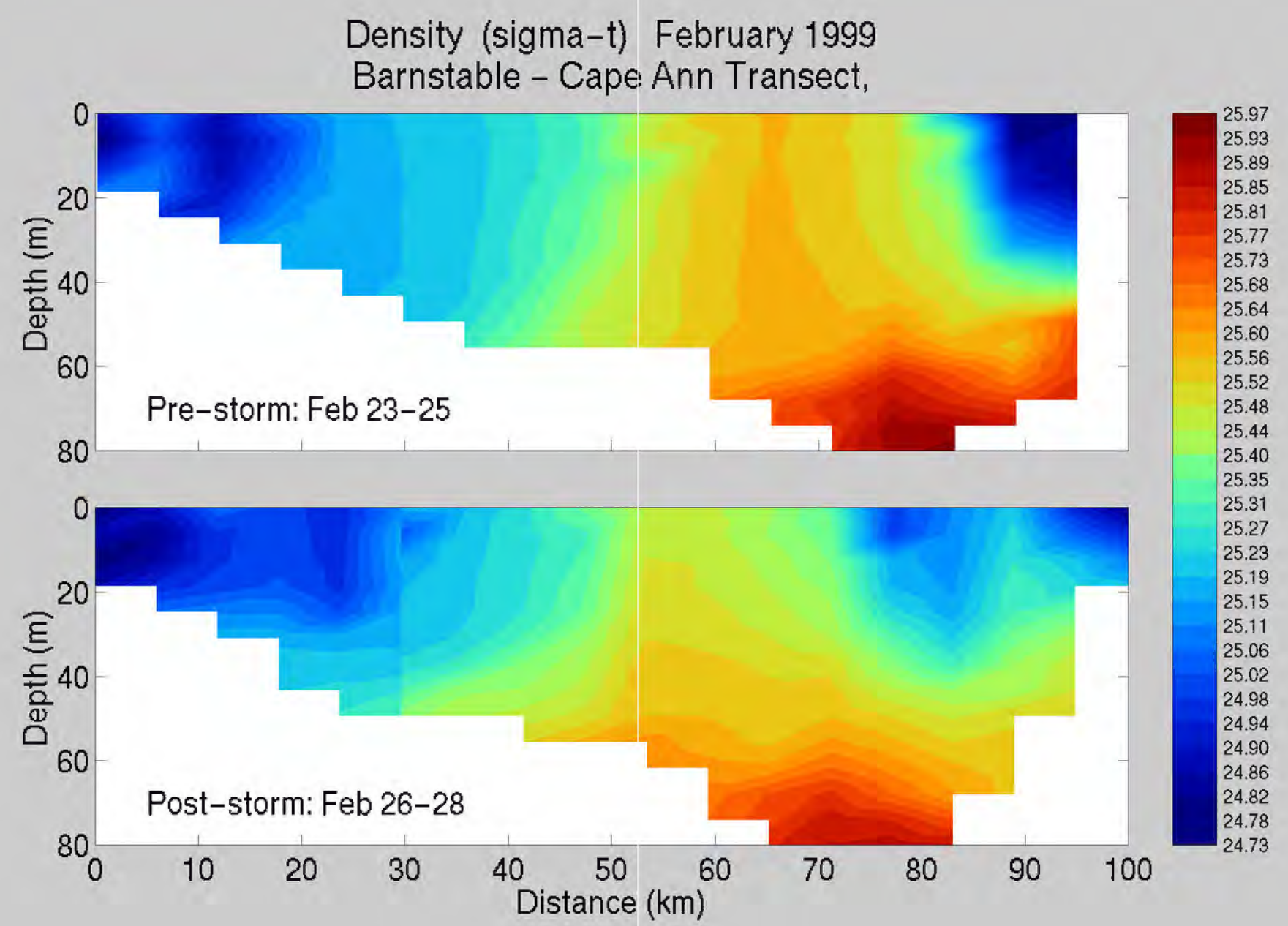
Density (sigma-t) February 1999
Barnstable - Cape Ann Transect,
Depth (m)
0
20
40
60
80
Pre-storm: Feb 23-25
Post-storm: Feb 26-28
0
10
20
30
40
50
60
70
80
90
100
Distance (km)
25.97
25.93
25.89
25.85
25.81
25.77
25.73
25.68
25.64
25.60
25.56
25.52
25.48
25.44
25.40
25.35
25.31
25.27
25.23
25.19
25.15
25.11
25.06
25.02
24.98
24.94
24.90
24.86
24.82
24.78
24.73

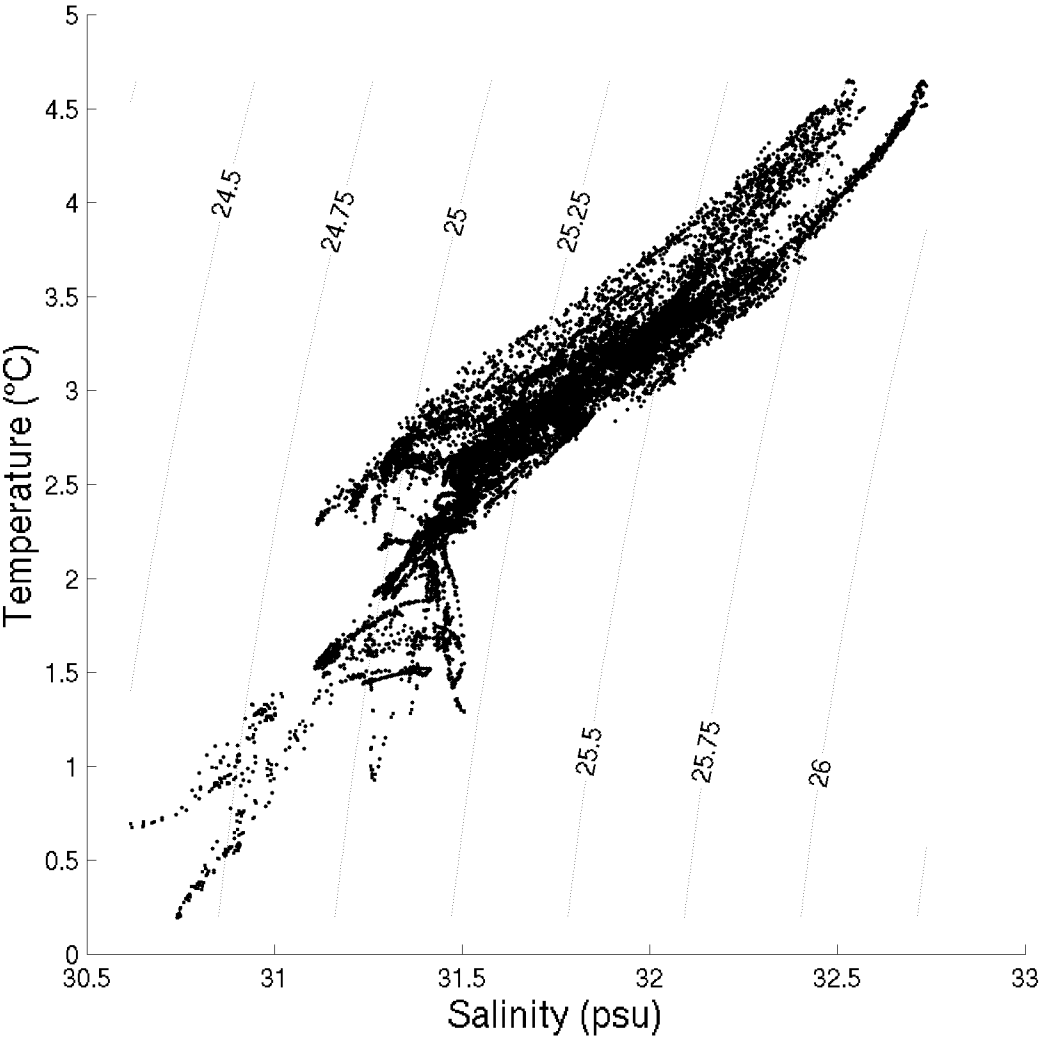
Temperature (°C)
Salinity (psu)
5
4.5
4
3.5
3
2.5
2
1.5
1
0.5
0
30.5
31
31.5
32
32.5
33
24.5
24.75
25
25.25
25.5
25.75
26

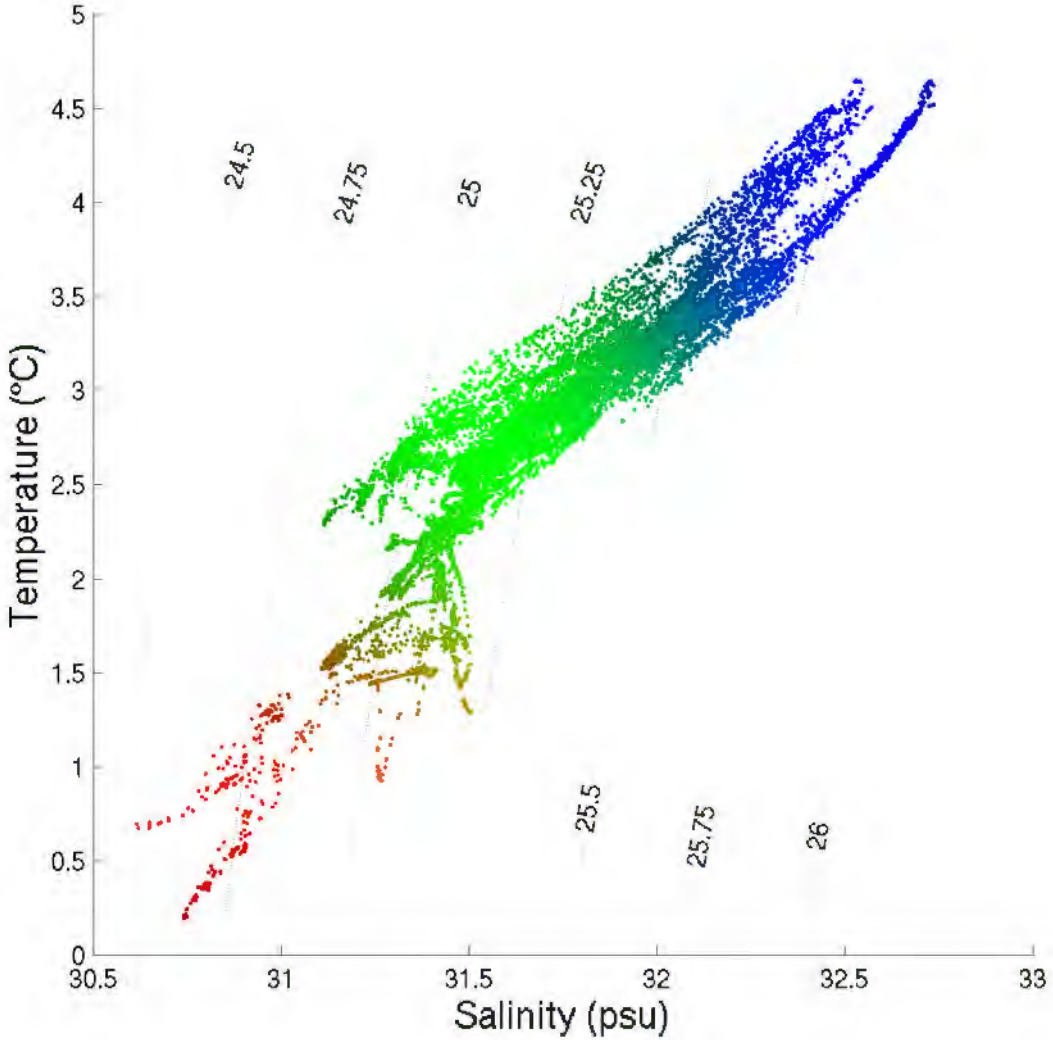
Temperature (°C)
Salinity (psu)
24.5
24.75
25
25.25
25.5
25.75
26
0
0.5
1
1.5
2
2.5
3
3.5
4
4.5
5
30.5
31
31.5
32
32.5
33

Temperature/Salinty Distribution, Febrary 23–28,1999

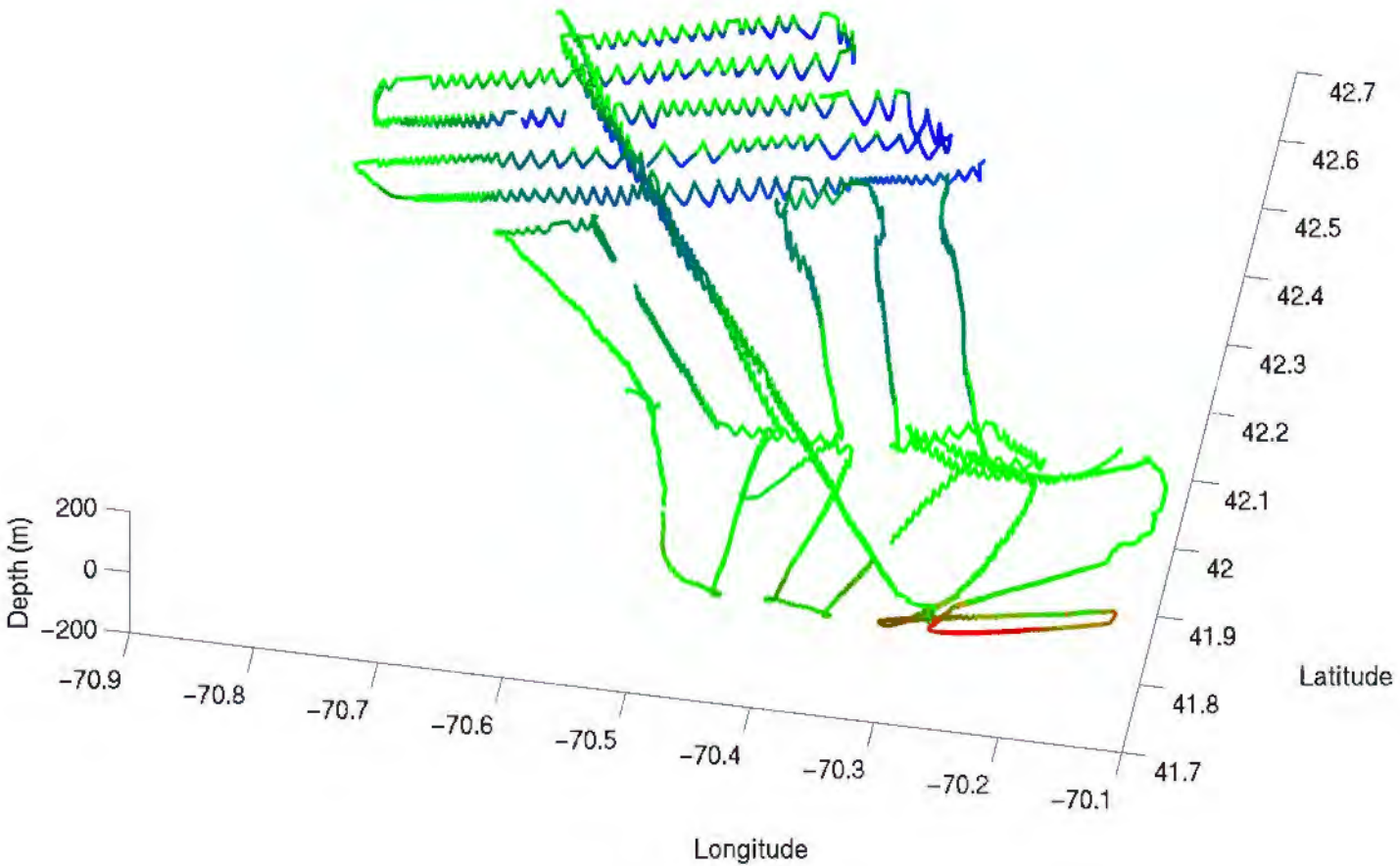

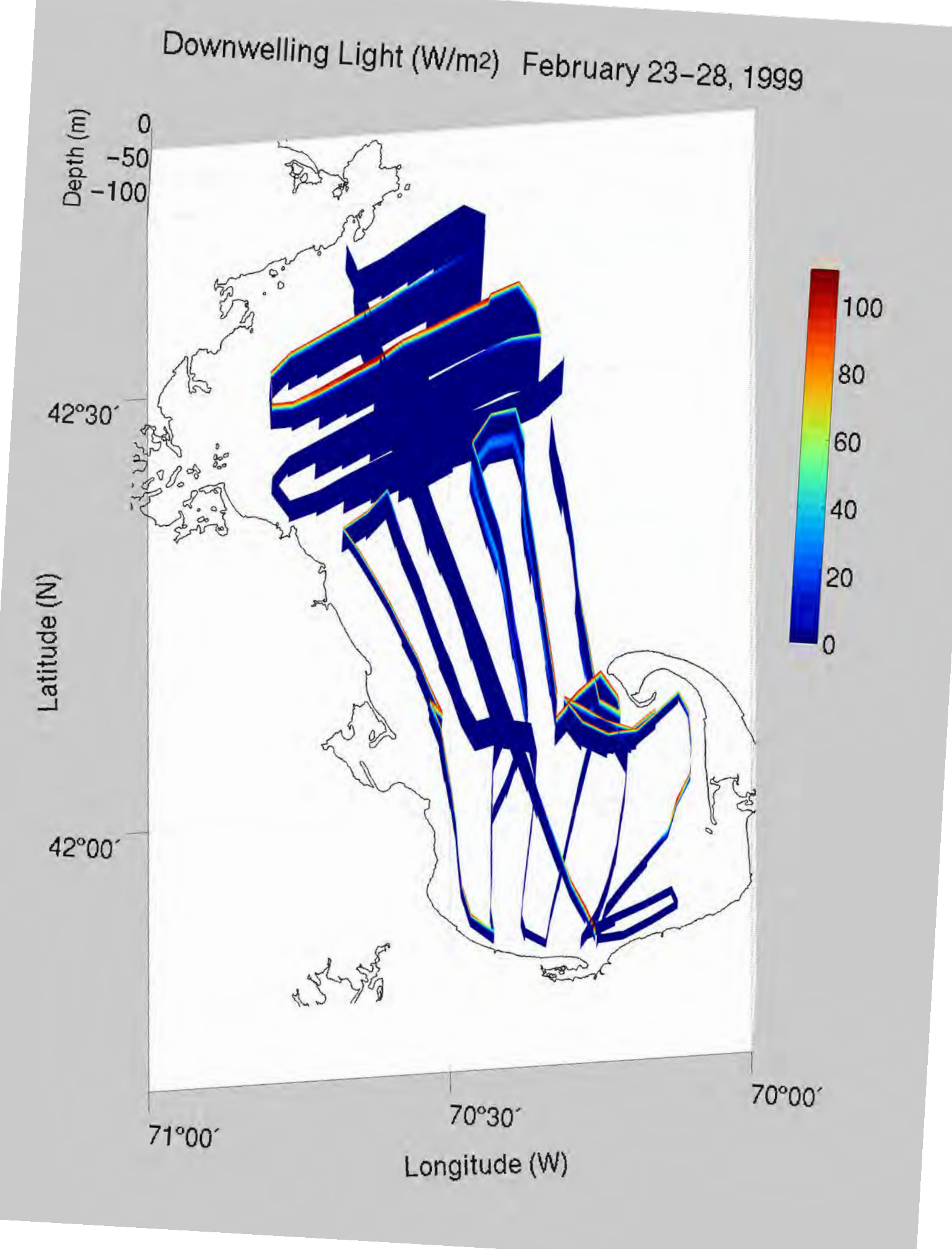
Downwelling Light (W/m2) February 23–28, 1999
Depth (m)
0
−50
−100
42°30′
42°00′
Latitude (N)
71°00′
70°30′
70°00′
Longitude (W)
100
80
60
40
20
0

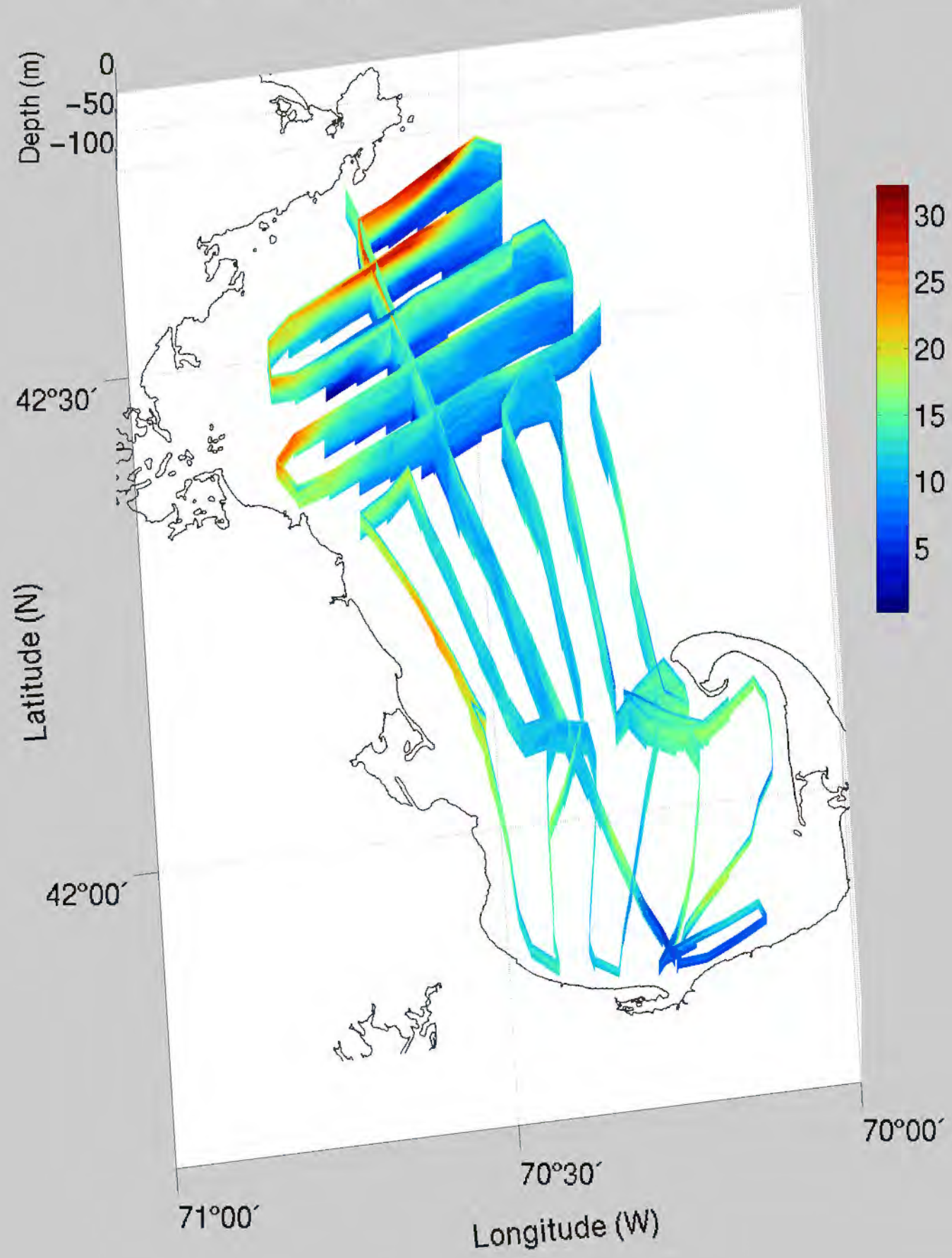
Fluorescence (µgChl/liter) February 23–28, 1999
Depth (m)
0
−50
−100
42°30´
42°00´
Latitude (N)
71°00´
70°30´
70°00´
Longitude (W)
30
25
20
15
10
5

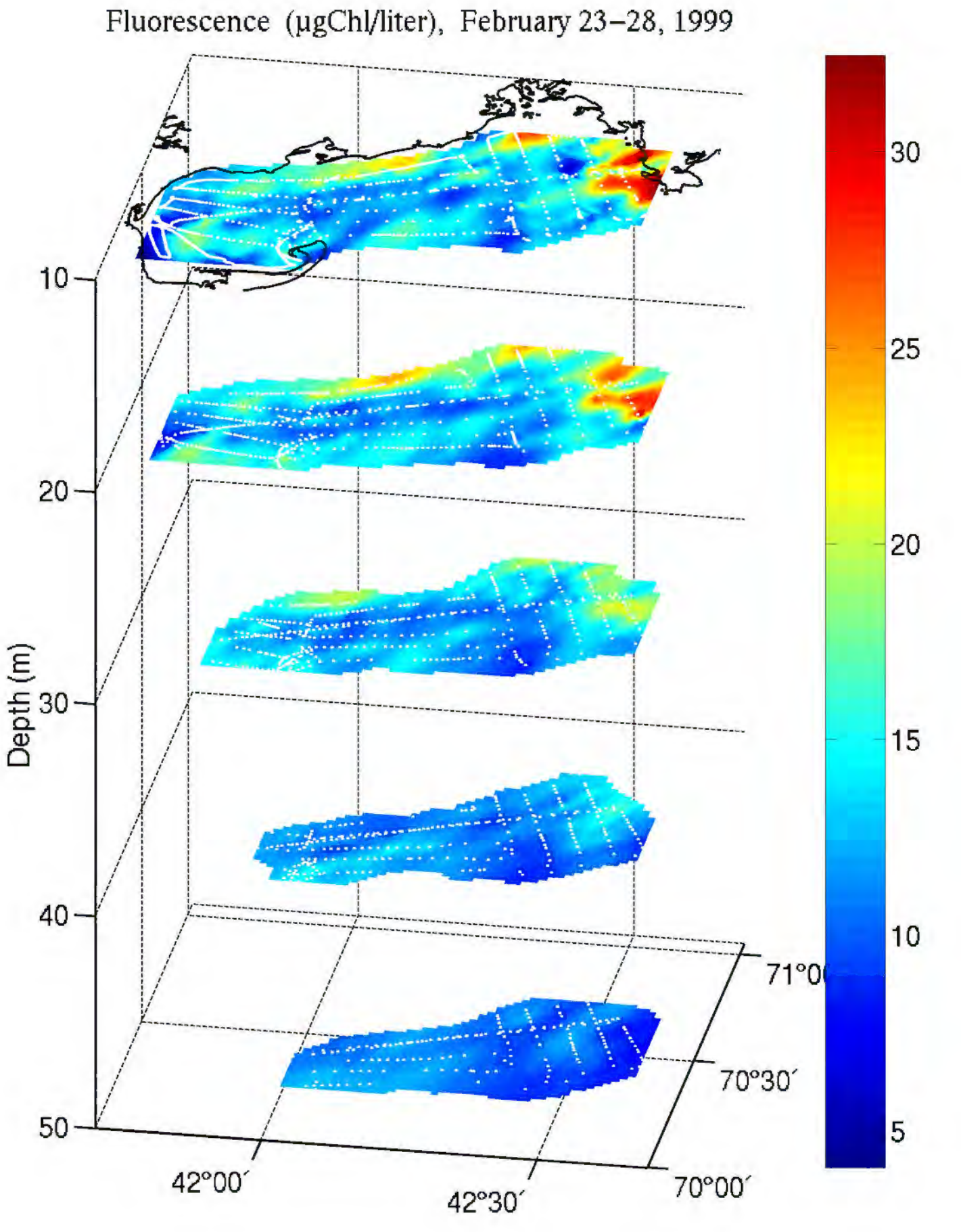
Fluorescence (µgChl/liter), February 23–28, 1999
Depth (m)
10
20
30
40
50
42°00´
42°30´
70°00´
70°30´
71°0
30
25
20
15
10
5

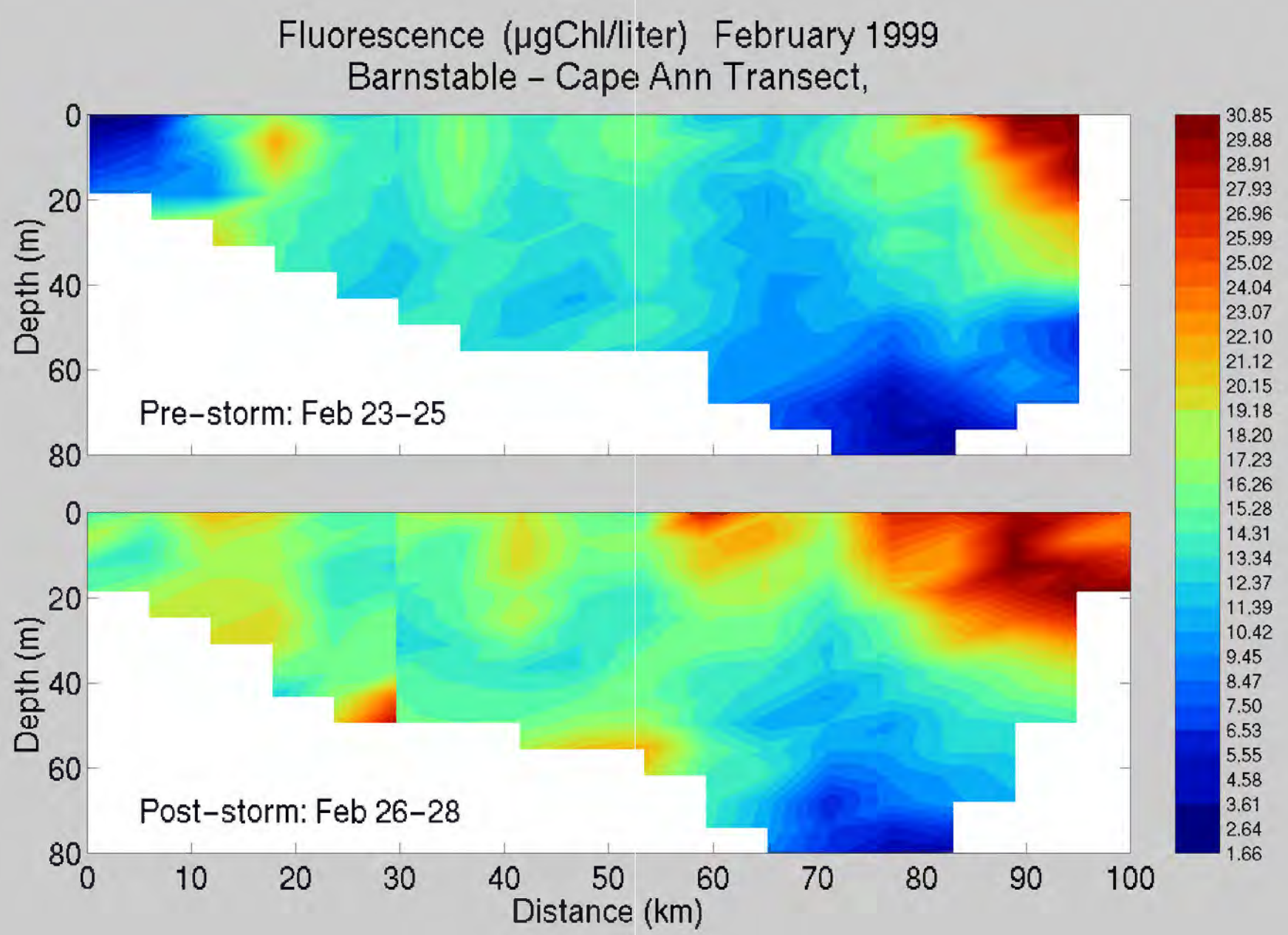
Fluorescence (µgChl/liter) February 1999
Barnstable – Cape Ann Transect,
Depth (m)
0
20
40
60
80
Pre-storm: Feb 23-25
Post-storm: Feb 26-28
0
10
20
30
40
50
60
70
80
90
100
Distance (km)
30.85
29.88
28.91
27.93
26.96
25.99
25.02
24.04
23.07
22.10
21.12
20.15
19.18
18.20
17.23
16.26
15.28
14.31
13.34
12.37
11.39
10.42
9.45
8.47
7.50
6.53
5.55
4.58
3.61
2.64
1.66

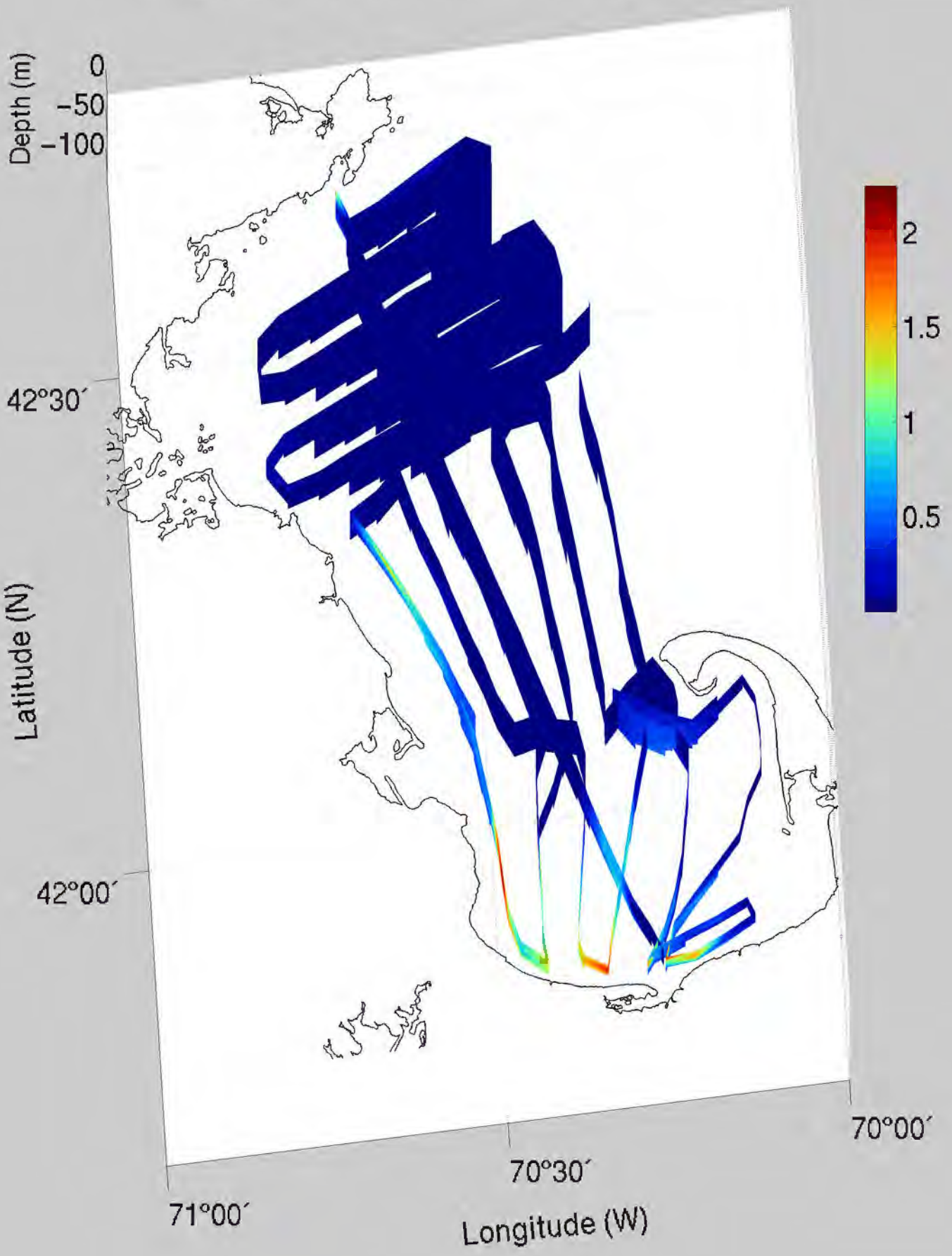
Attenuation (beam−C) February 23−28, 1999
Depth (m)
0
−50
−100
42°30′
42°00′
Latitude (N)
2
1.5
1
0.5
71°00′
70°30′
70°00′
Longitude (W)

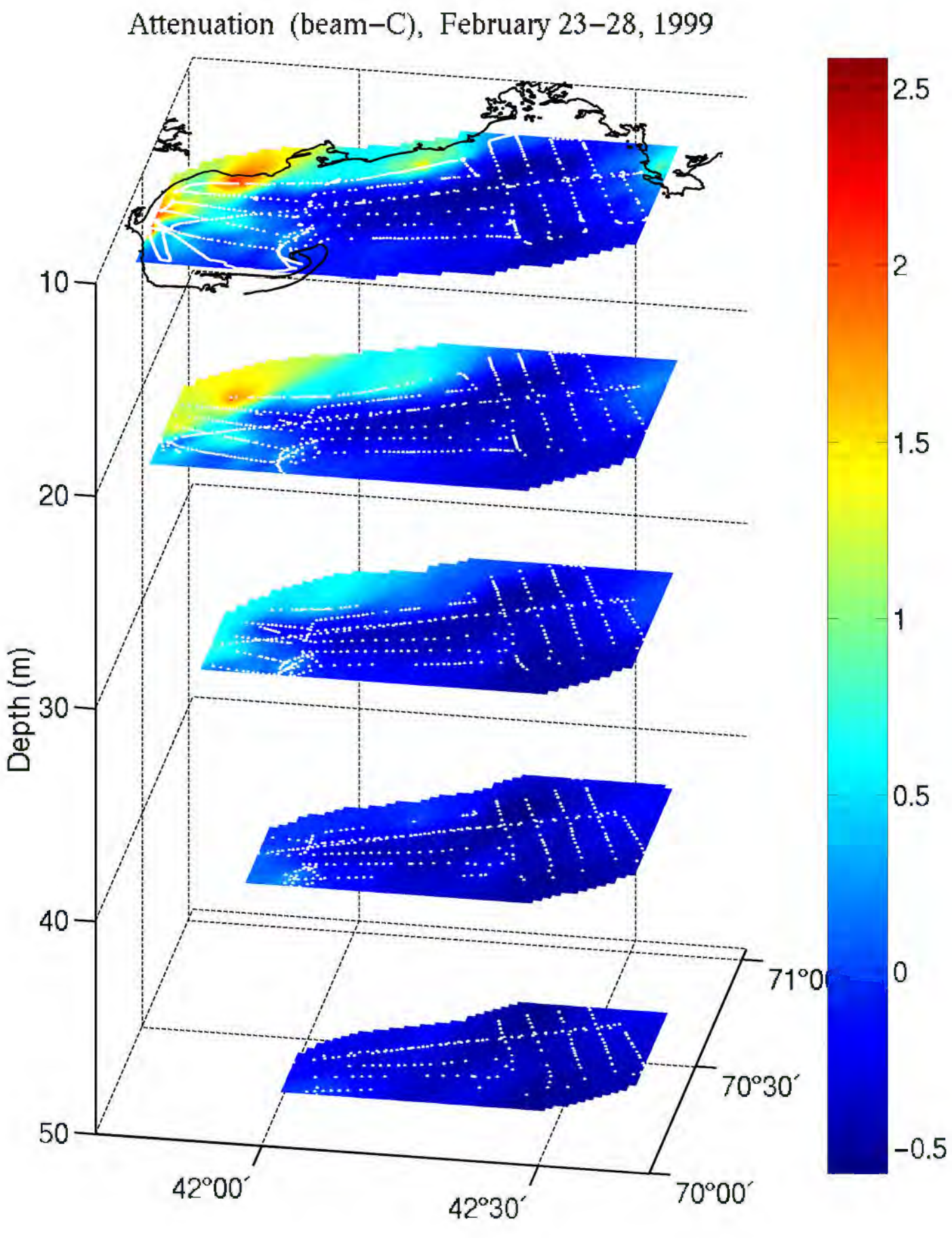
Attenuation (beam−C), February 23−28, 1999
Depth (m)
10
20
30
40
50
42°00′
42°30′
70°00′
70°30′
71°0
2.5
2
1.5
1
0.5
0
−0.5

Rod shaped
Diatoms

= 1.0 mm

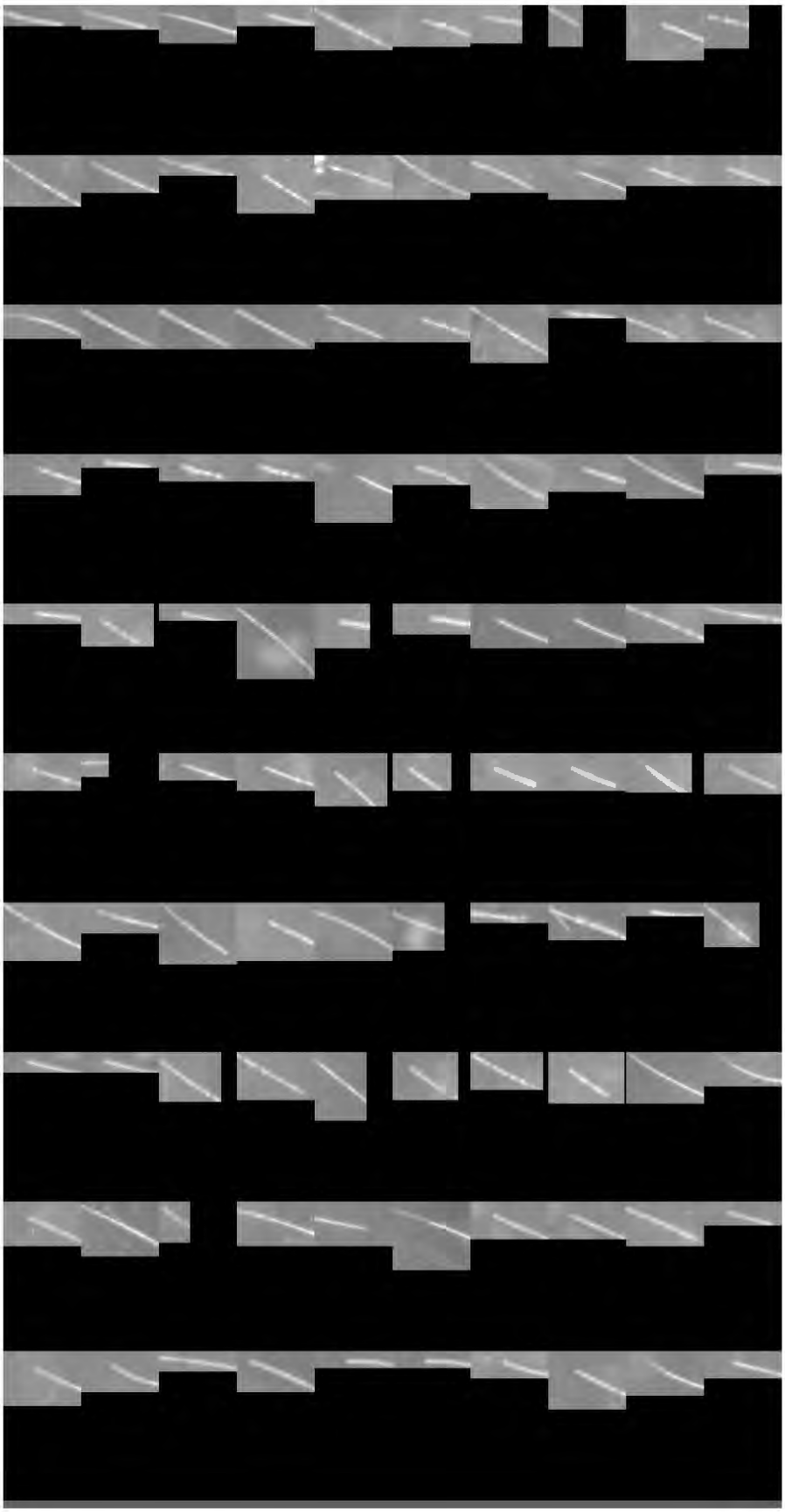

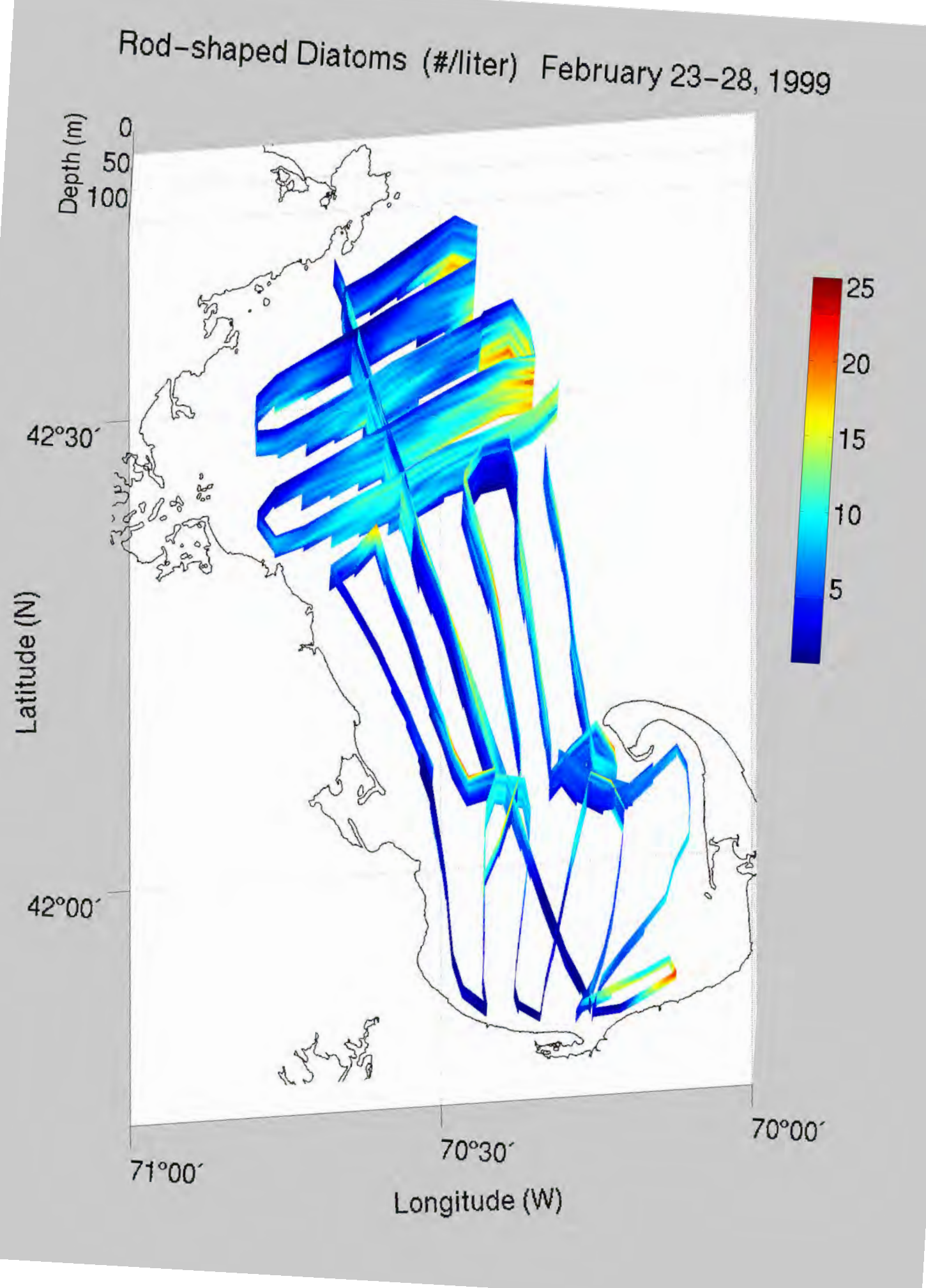
Rod-shaped Diatoms (#/liter) February 23-28, 1999
Depth (m)
0
50
100
25
20
15
10
5
42°30´
42°00´
Latitude (N)
71°00´
70°30´
70°00´
Longitude (W)

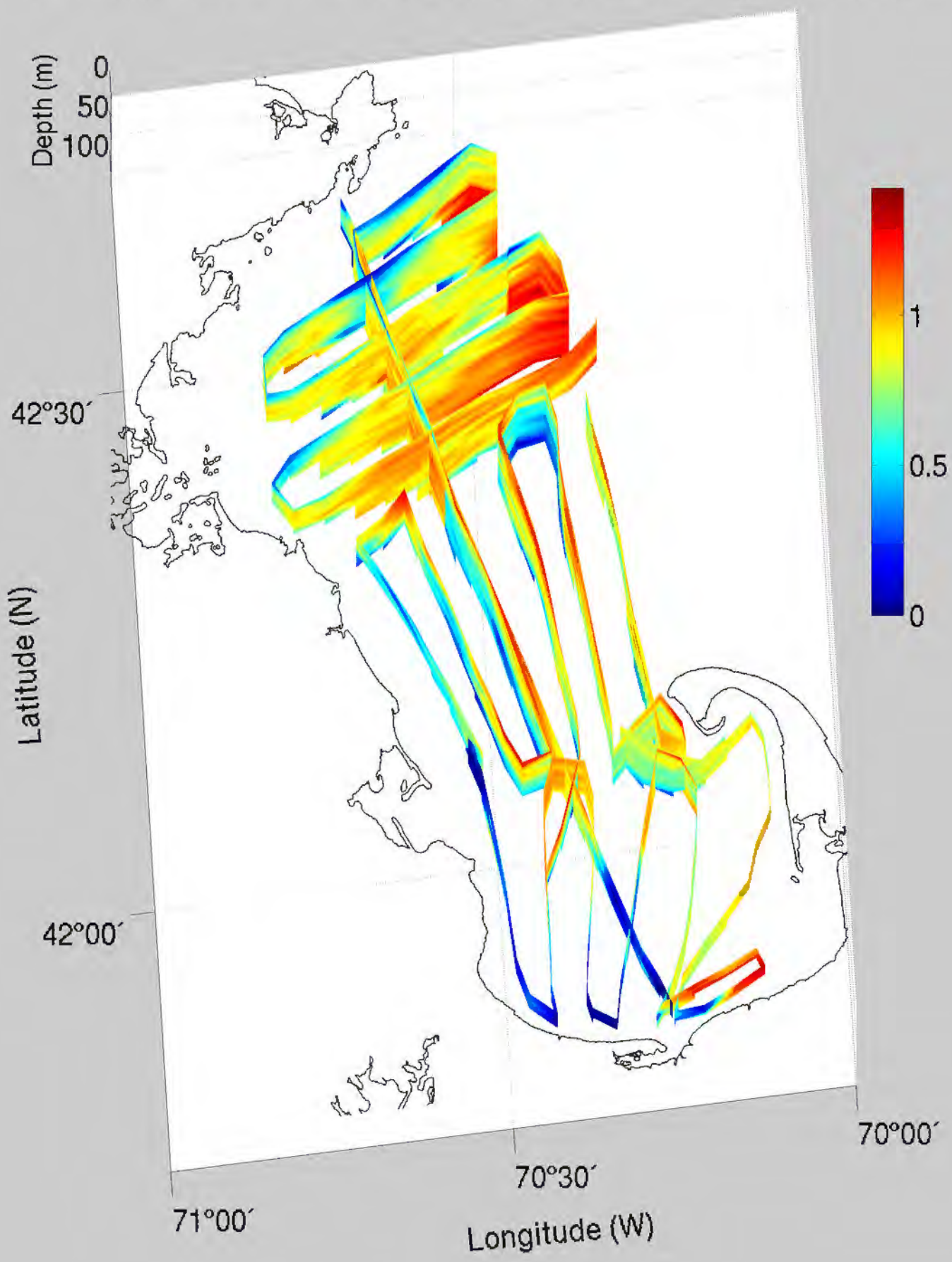
Rod−shaped Diatoms (log10(#/liter+1)) February 23−28, 1999
Depth (m)
0
50
100
42°30´
42°00´
Latitude (N)
1
0.5
0
71°00´
70°30´
70°00´
Longitude (W)

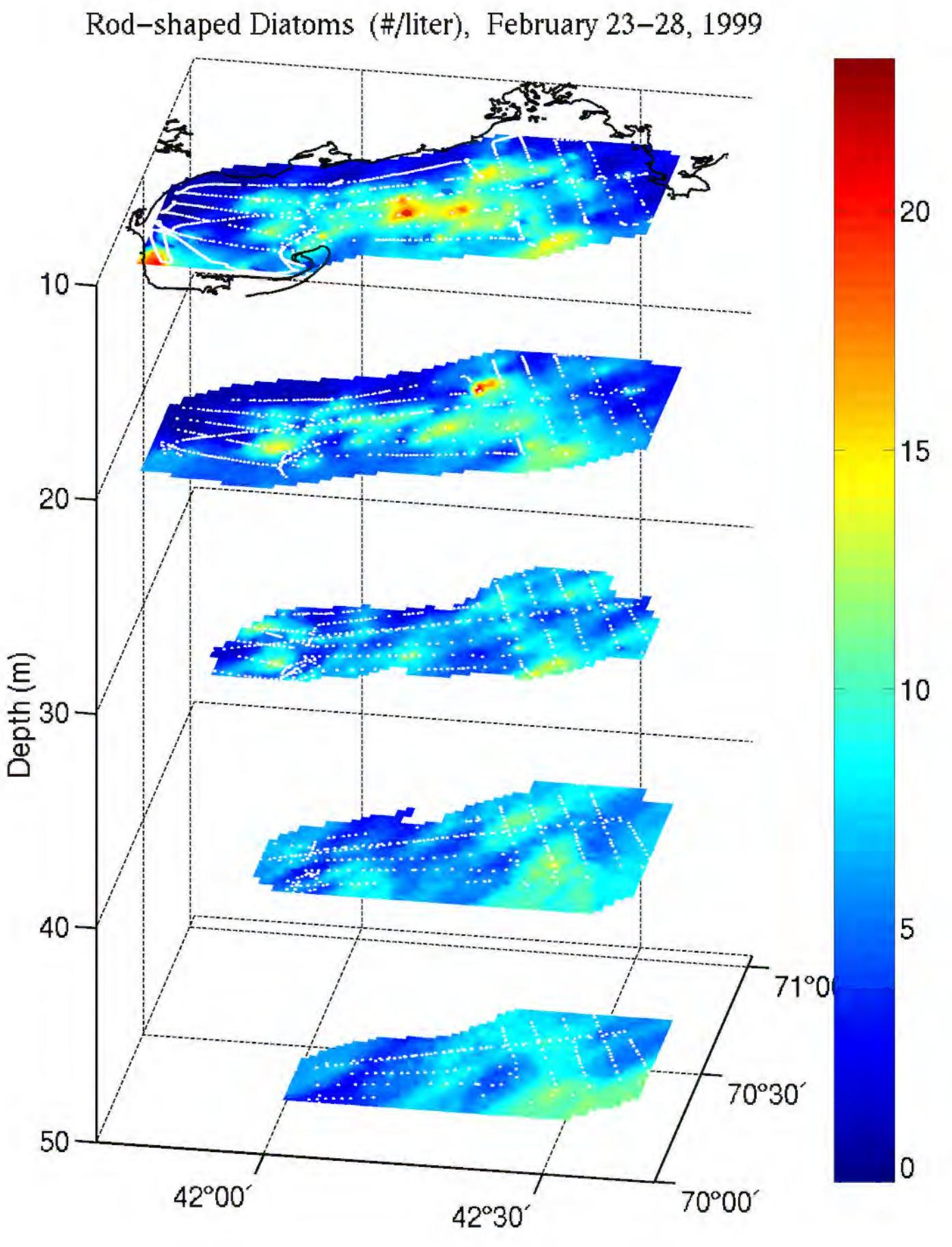
Rod−shaped Diatoms (#/liter), February 23−28, 1999
Depth (m)
10
20
30
40
50
42°00´
42°30´
70°00´
70°30´
71°0
0
5
10
15
20

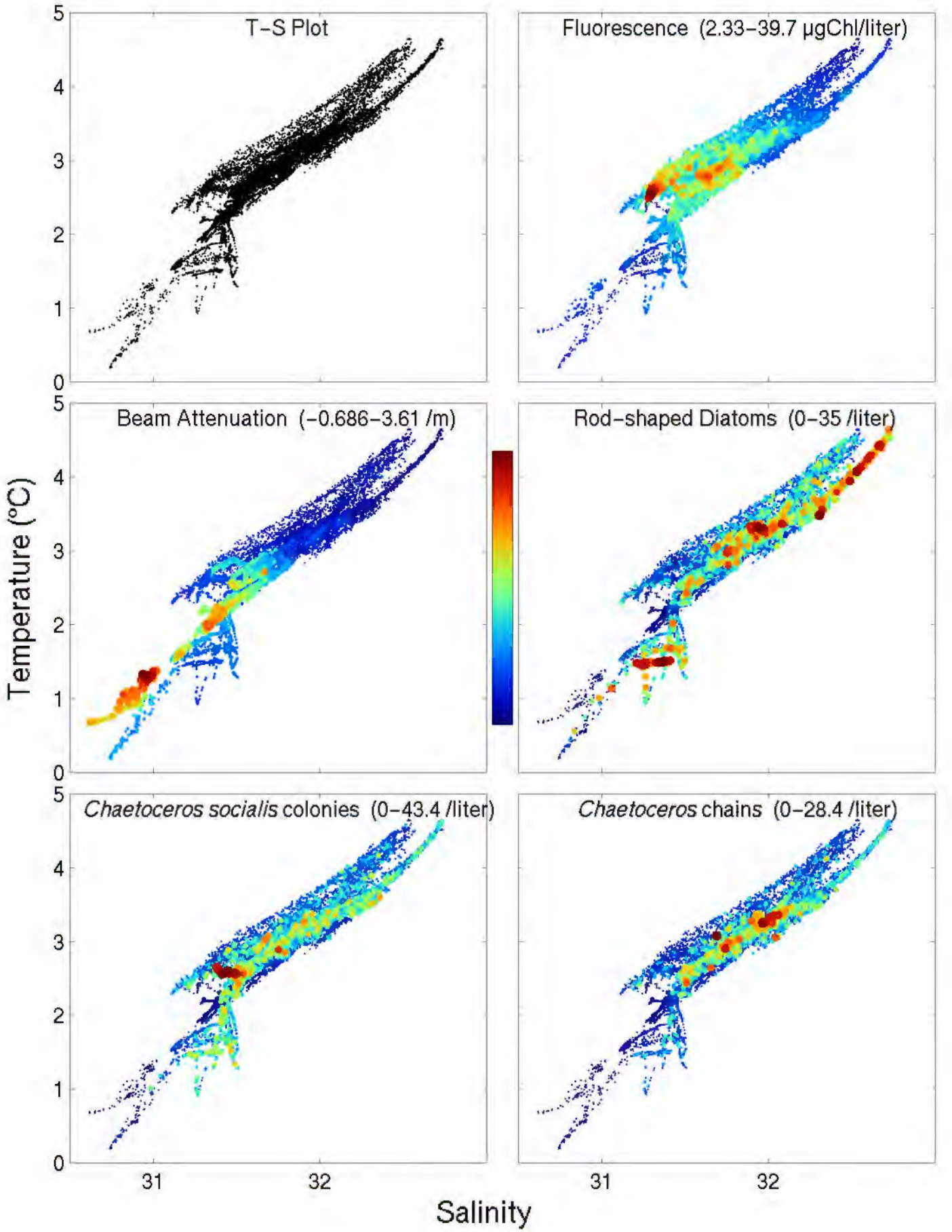
T–S Plot
Fluorescence (2.33–39.7 µgChl/liter)
Beam Attenuation (–0.686–3.61 /m)
Rod–shaped Diatoms (0–35 /liter)
Chaetoceros socialis colonies (0–43.4 /liter)
Chaetoceros chains (0–28.4 /liter)
Temperature (°C)
Salinity
0
1
2
3
4
5
31
32

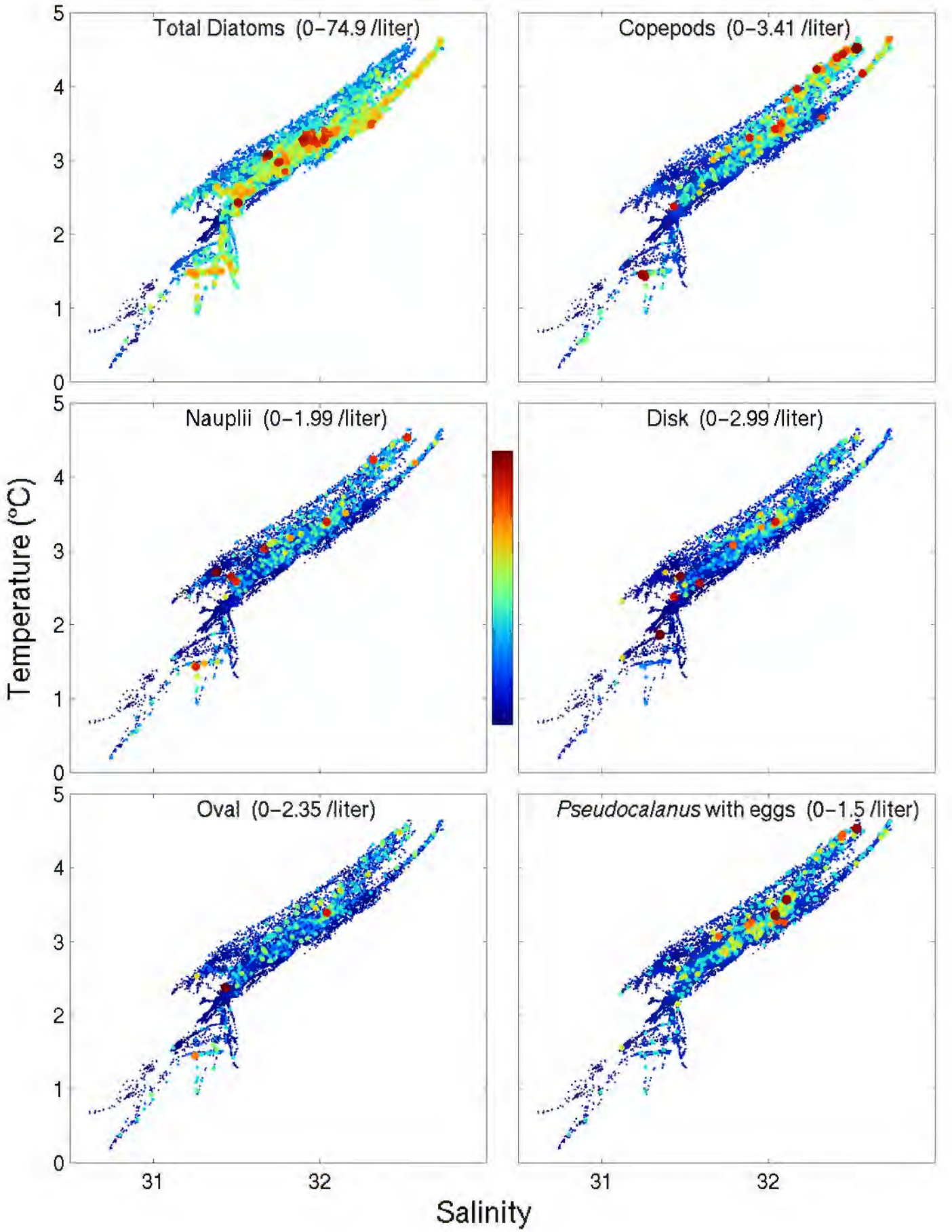
Total Diatoms (0–74.9 /liter)
Copepods (0–3.41 /liter)
Nauplii (0–1.99 /liter)
Disk (0–2.99 /liter)
Oval (0–2.35 /liter)
Pseudocalanus with eggs (0–1.5 /liter)
Temperature (°C)
Salinity
0
1
2
3
4
5
31
32

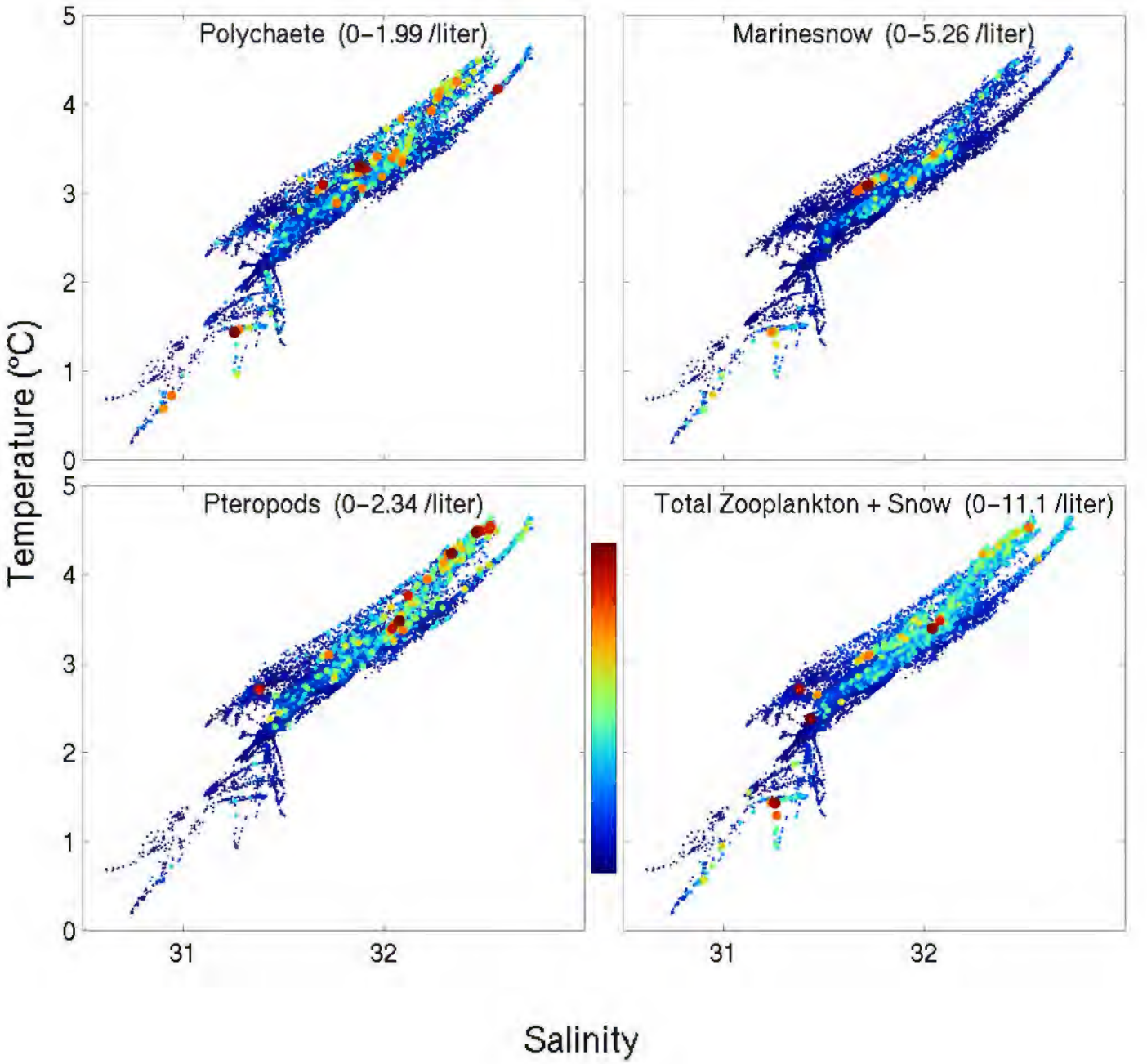
Polychaete (0–1.99 /liter)
Marinesnow (0–5.26 /liter)
Pteropods (0–2.34 /liter)
Total Zooplankton + Snow (0–11.1 /liter)
Temperature (°C)
Salinity
0
1
2
3
4
5
31
32

Chaetoceros
Chains

= 1.0 mm

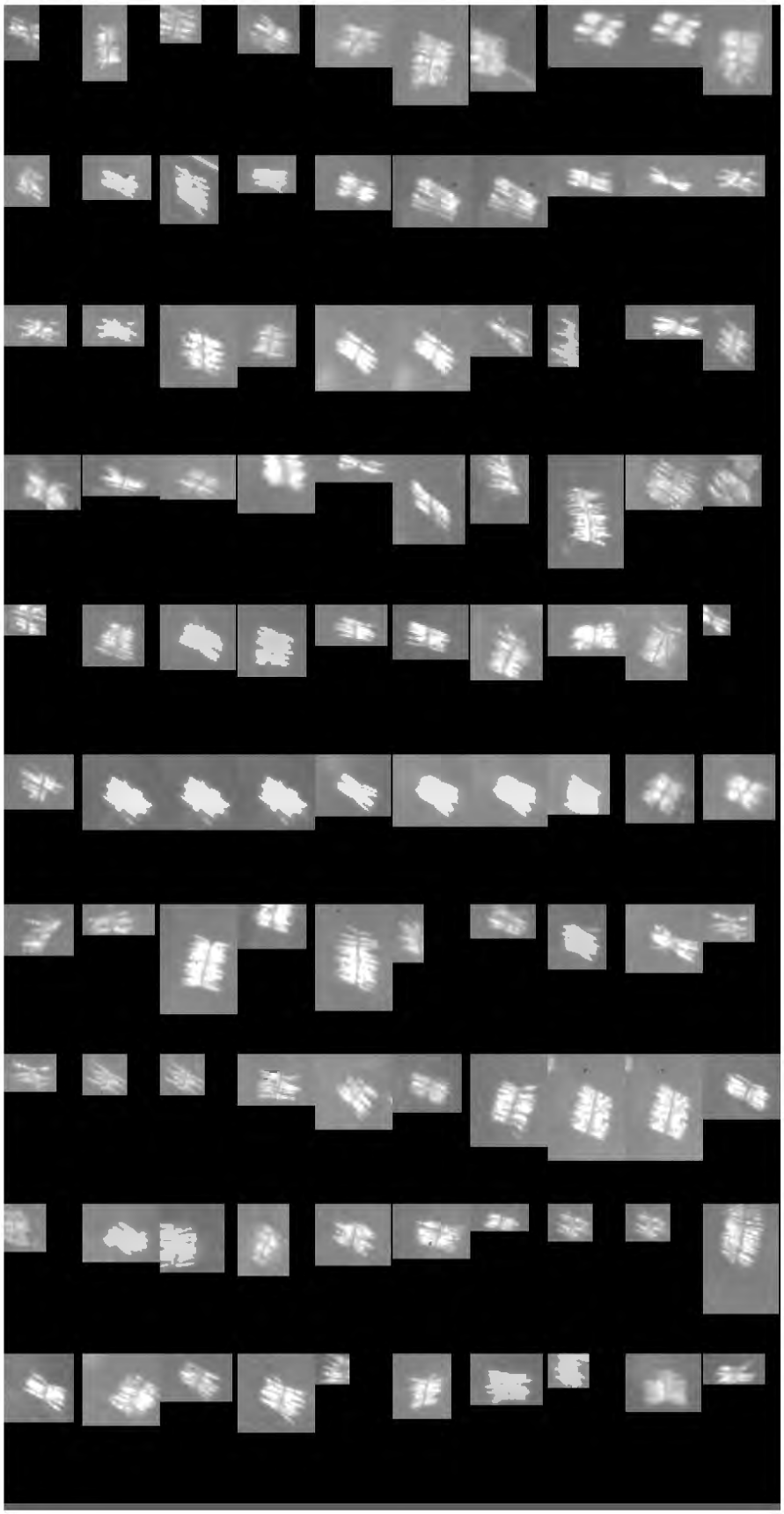

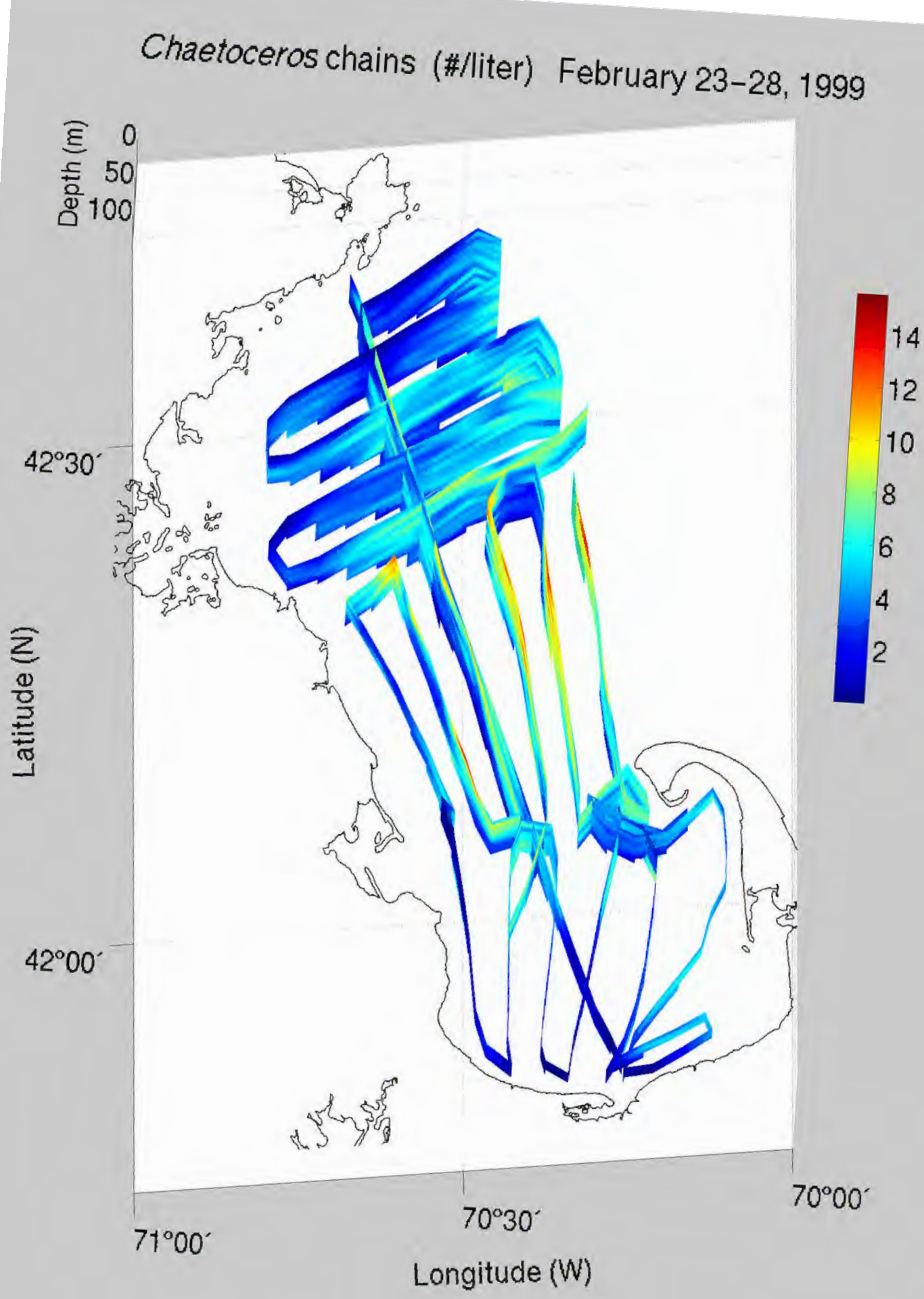
Chaetoceros chains (#/liter) February 23–28, 1999
Depth (m)
0
50
100
14
12
10
8
6
4
2
42°30´
42°00´
Latitude (N)
71°00´
70°30´
70°00´
Longitude (W)

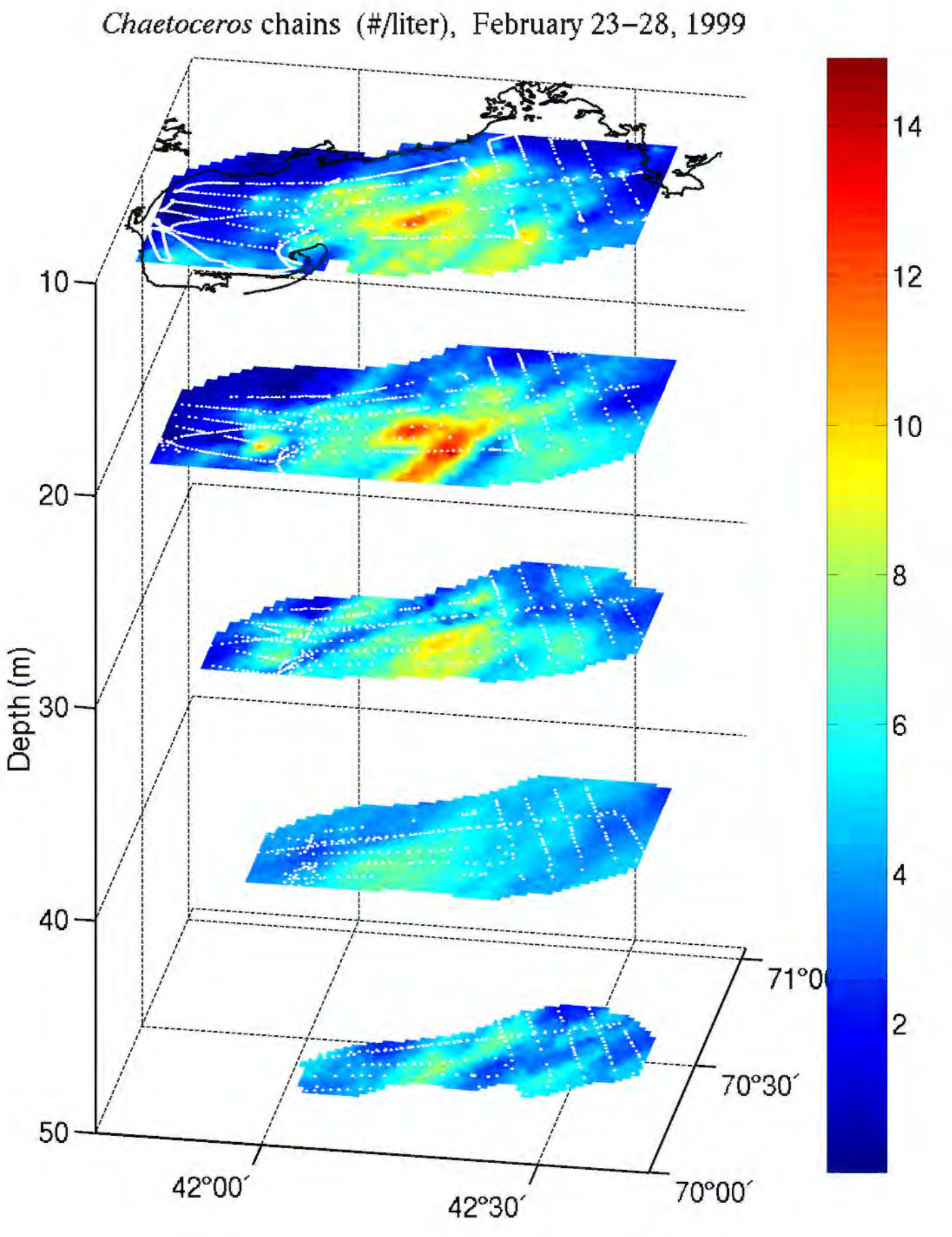
Chaetoceros chains (#/liter), February 23–28, 1999
Depth (m)
10
20
30
40
50
42°00´
42°30´
70°30´
70°00´
14
12
10
8
6
4
2

Chaetoceros socialis colonies

= 1.0 mm

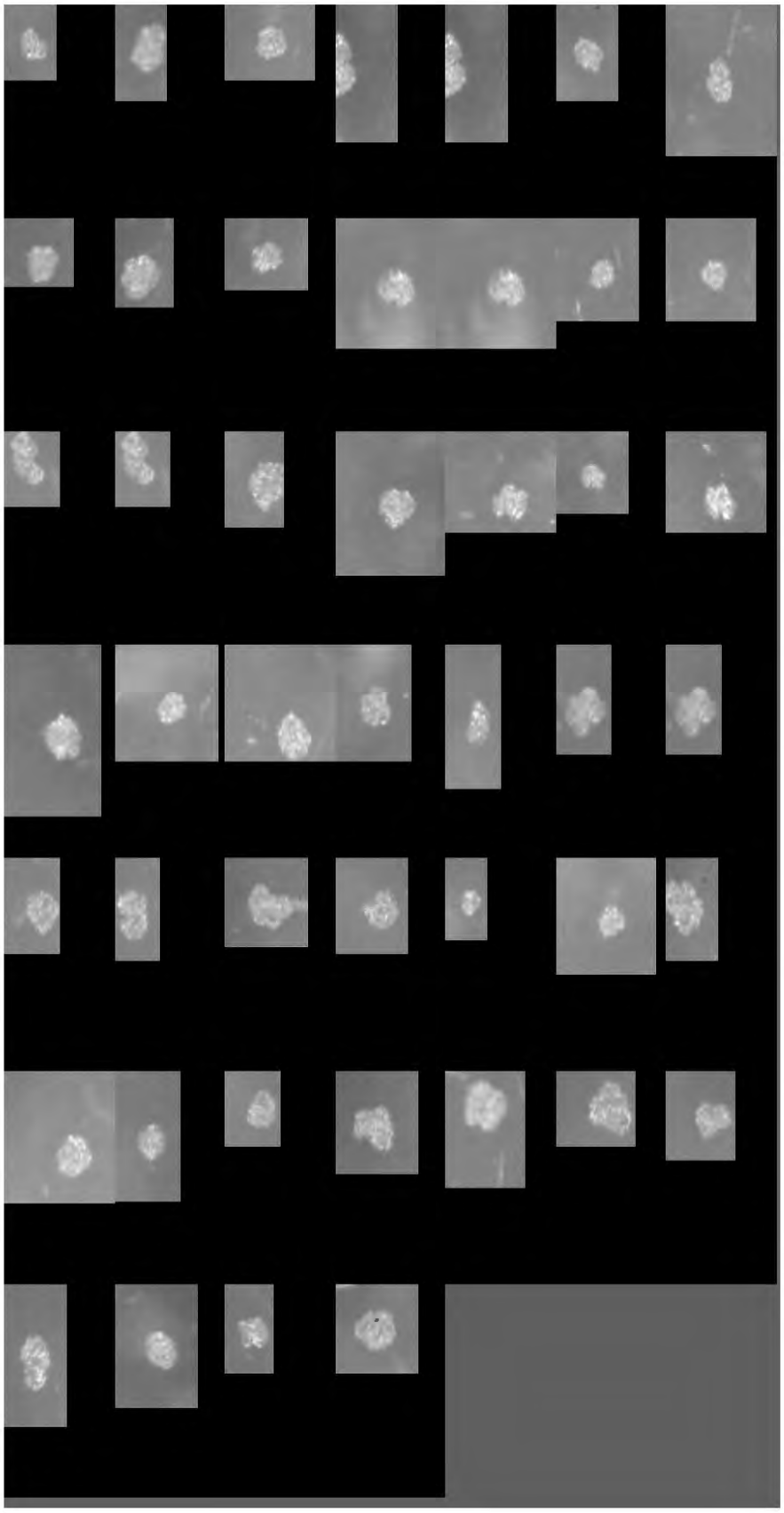

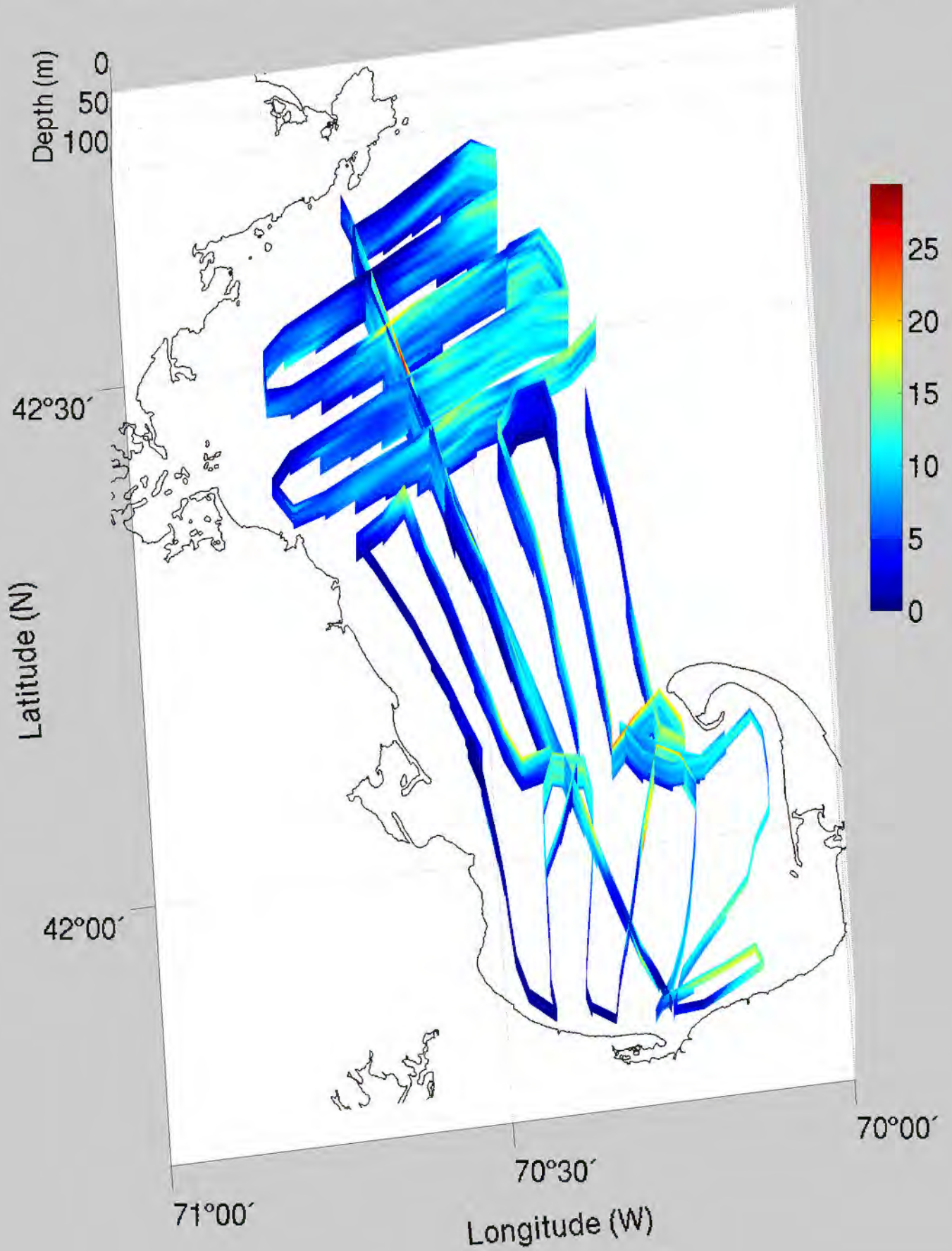
Chaetoceros socialis Colonies (#/liter) February 23–28, 1999
Depth (m)
0
50
100
42°30´
42°00´
Latitude (N)
25
20
15
10
5
0
71°00´
70°30´
70°00´
Longitude (W)

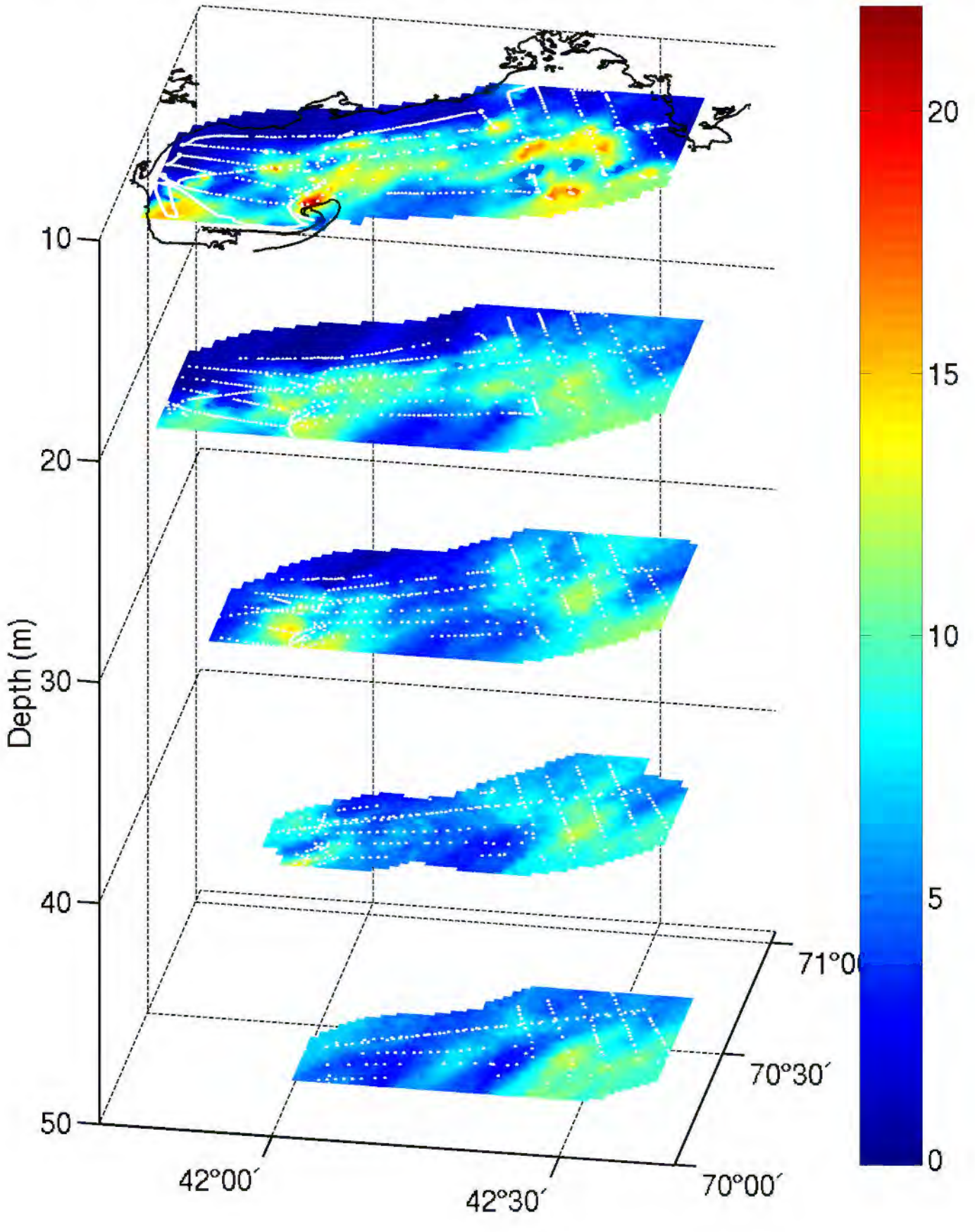
Chaetoceros socialis colonies (#/liter), February 23–28, 1999
Depth (m)
10
20
30
40
50
42°00´
42°30´
70°30´
70°00´
20
15
10
5
0

Copepods

| = 1.0 mm

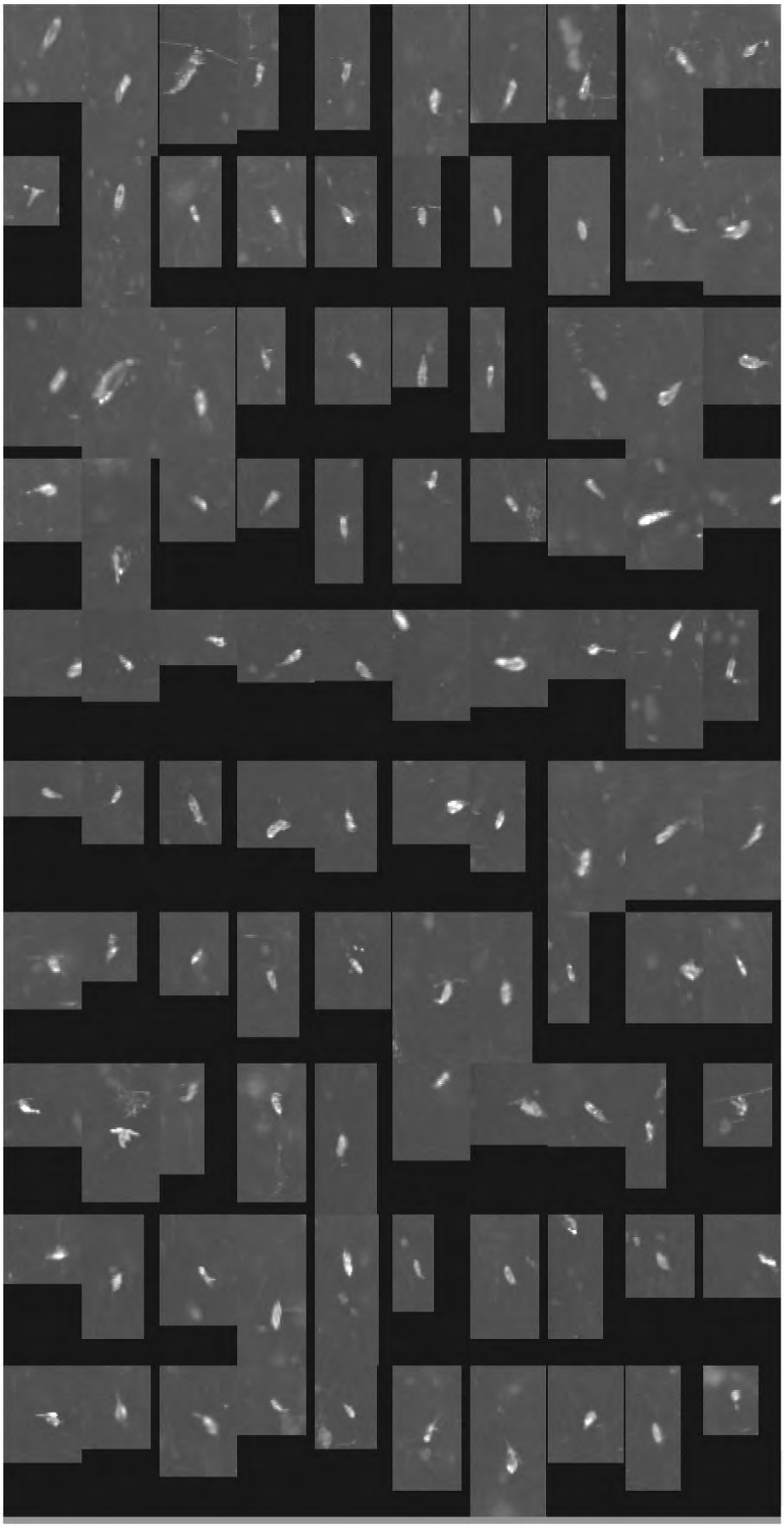

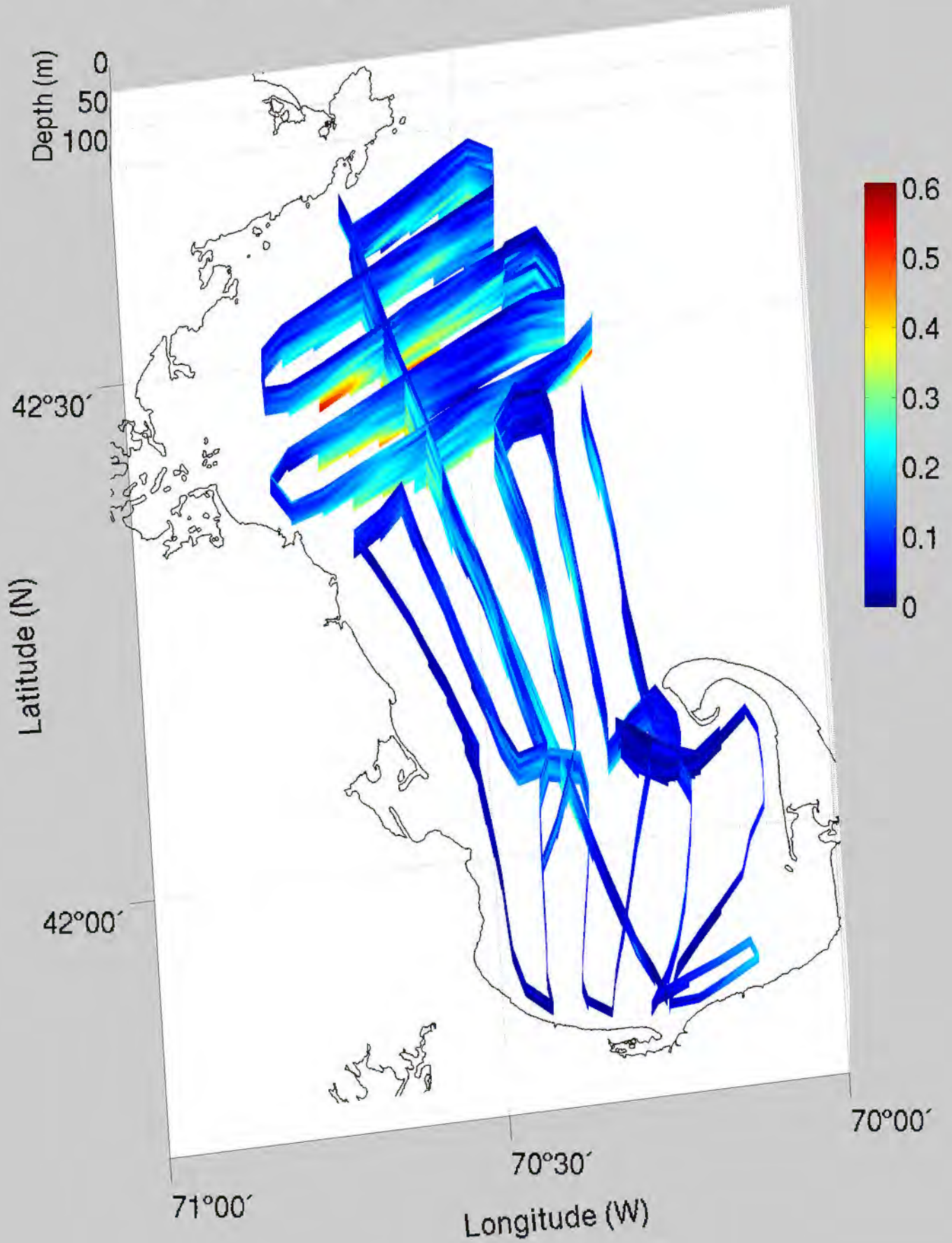
Copepods (#/liter) February 23–28, 1999
Depth (m)
0
50
100
42°30´
42°00´
Latitude (N)
71°00´
70°30´
70°00´
Longitude (W)
0.6
0.5
0.4
0.3
0.2
0.1
0

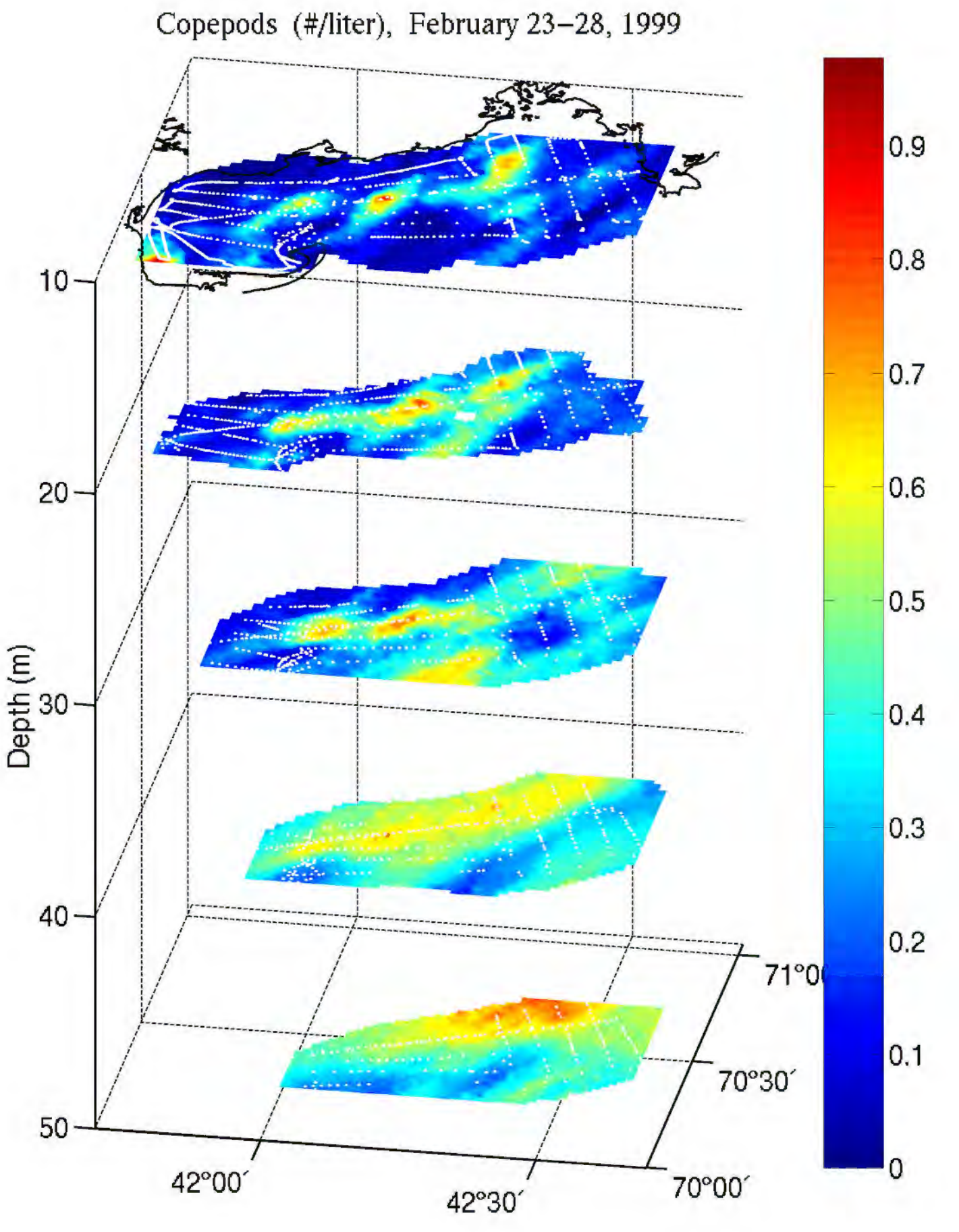
Copepods (#/liter), February 23–28, 1999
Depth (m)
10
20
30
40
50
42°00´
42°30´
70°00´
70°30´
71°0
0.9
0.8
0.7
0.6
0.5
0.4
0.3
0.2
0.1
0

Disks,
Unidentified

| = 1.0 mm

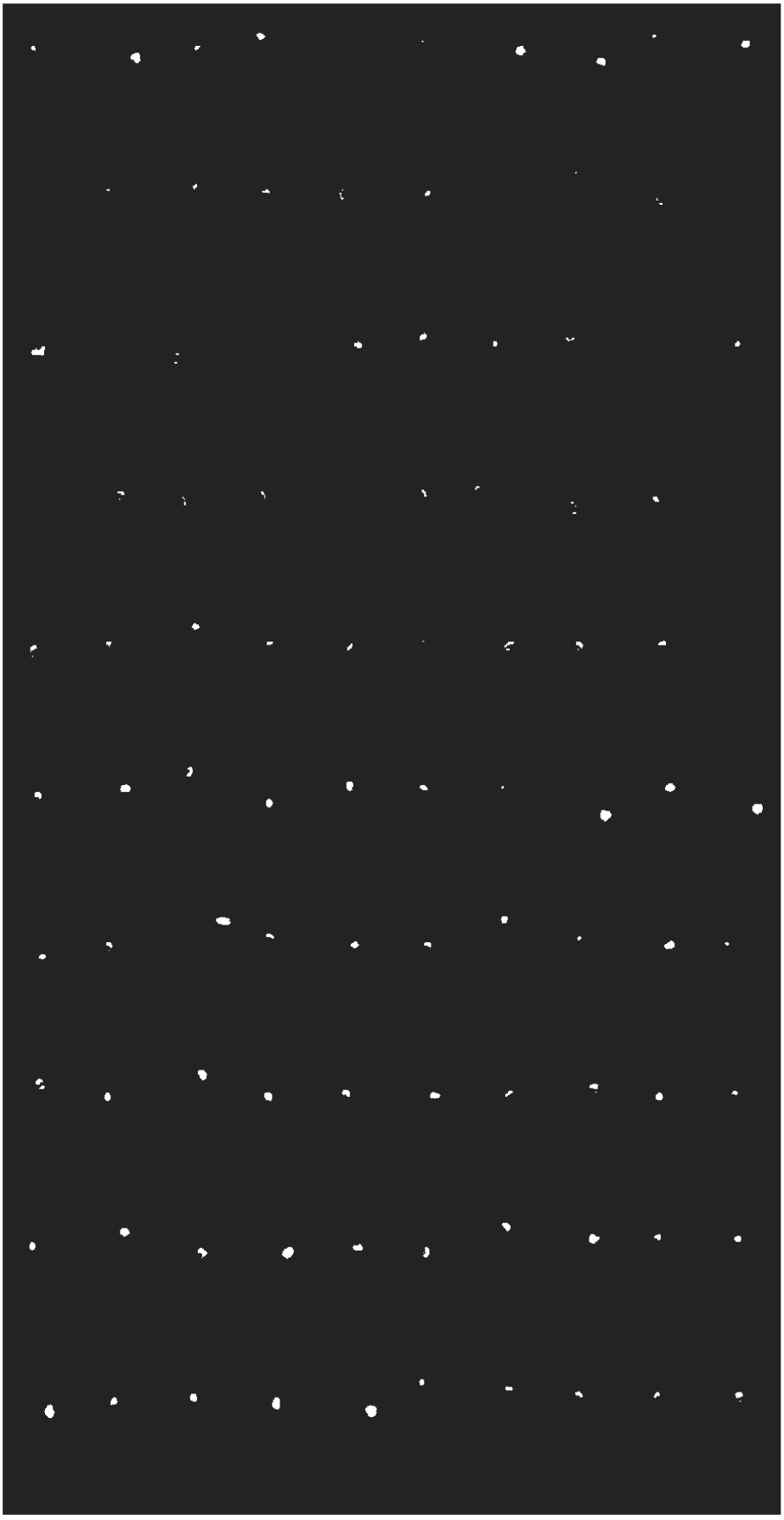

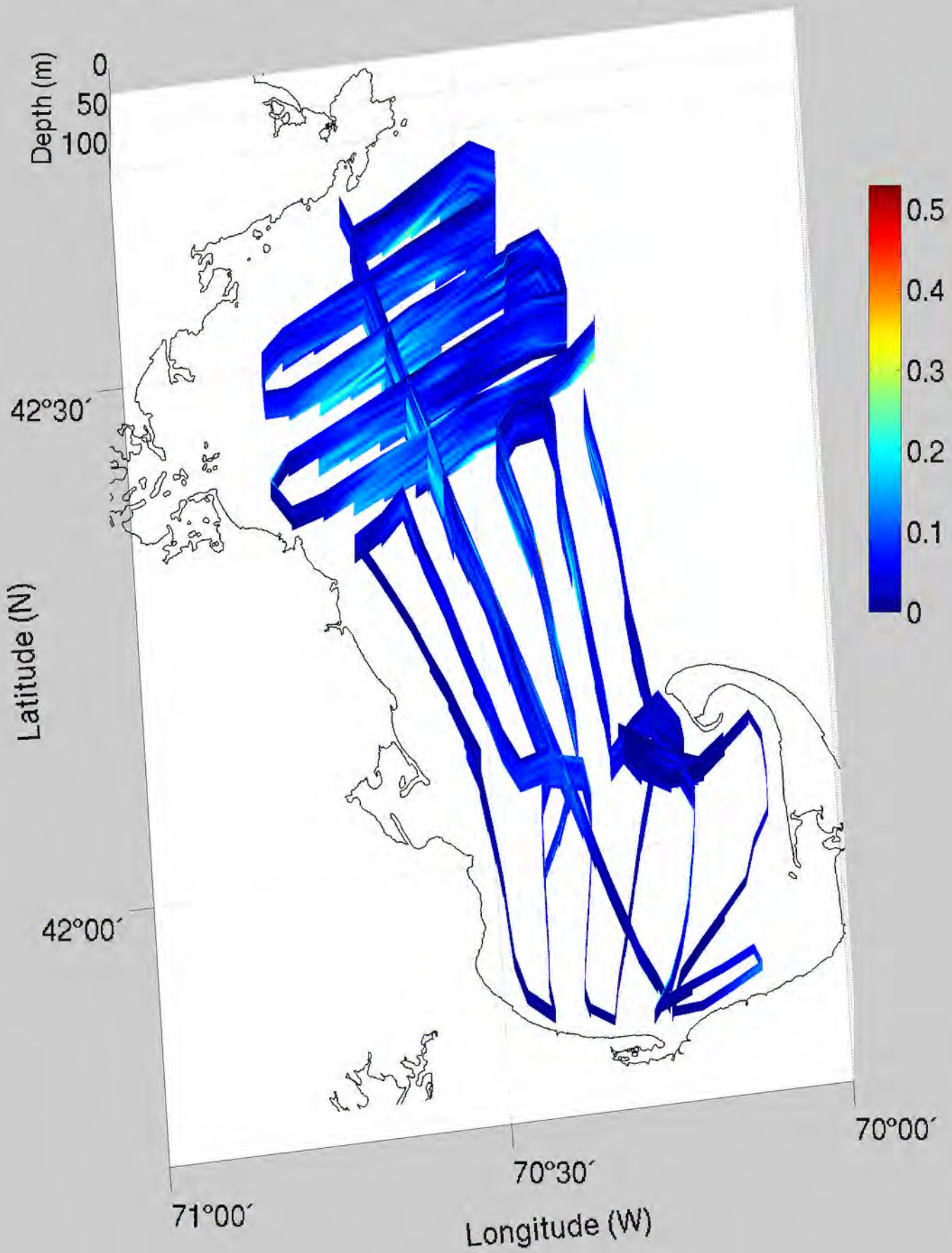
Unidentified Disk (#/liter) February 23–28, 1999
Depth (m)
0
50
100
42°30´
42°00´
Latitude (N)
71°00´
70°30´
70°00´
Longitude (W)
0.5
0.4
0.3
0.2
0.1
0

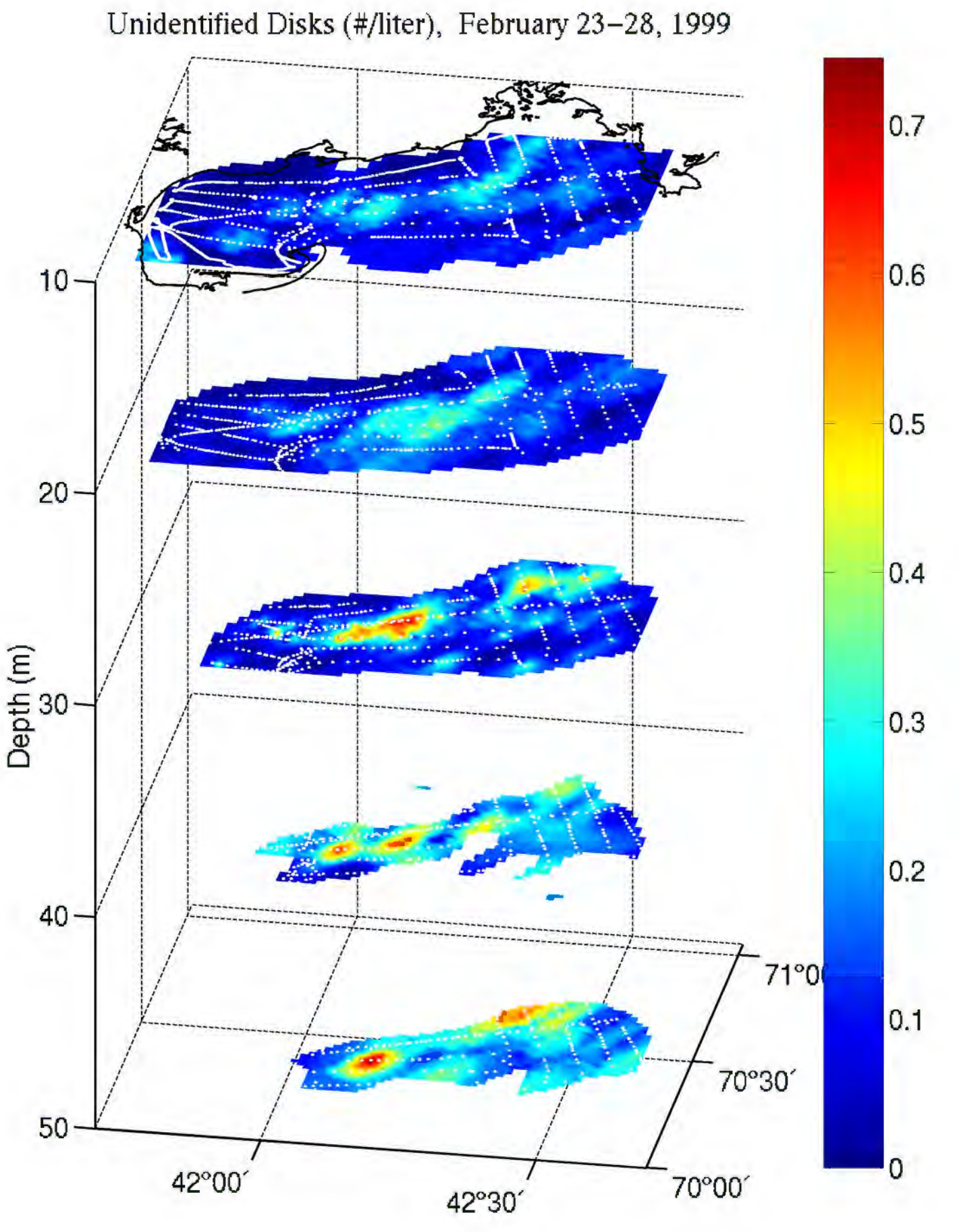
Unidentified Disks (#/liter), February 23–28, 1999
Depth (m)
10
20
30
40
50
42°00´
42°30´
70°00´
70°30´
71°0
0.7
0.6
0.5
0.4
0.3
0.2
0.1
0

Ovals,
Unidentified

| = 1.0 mm

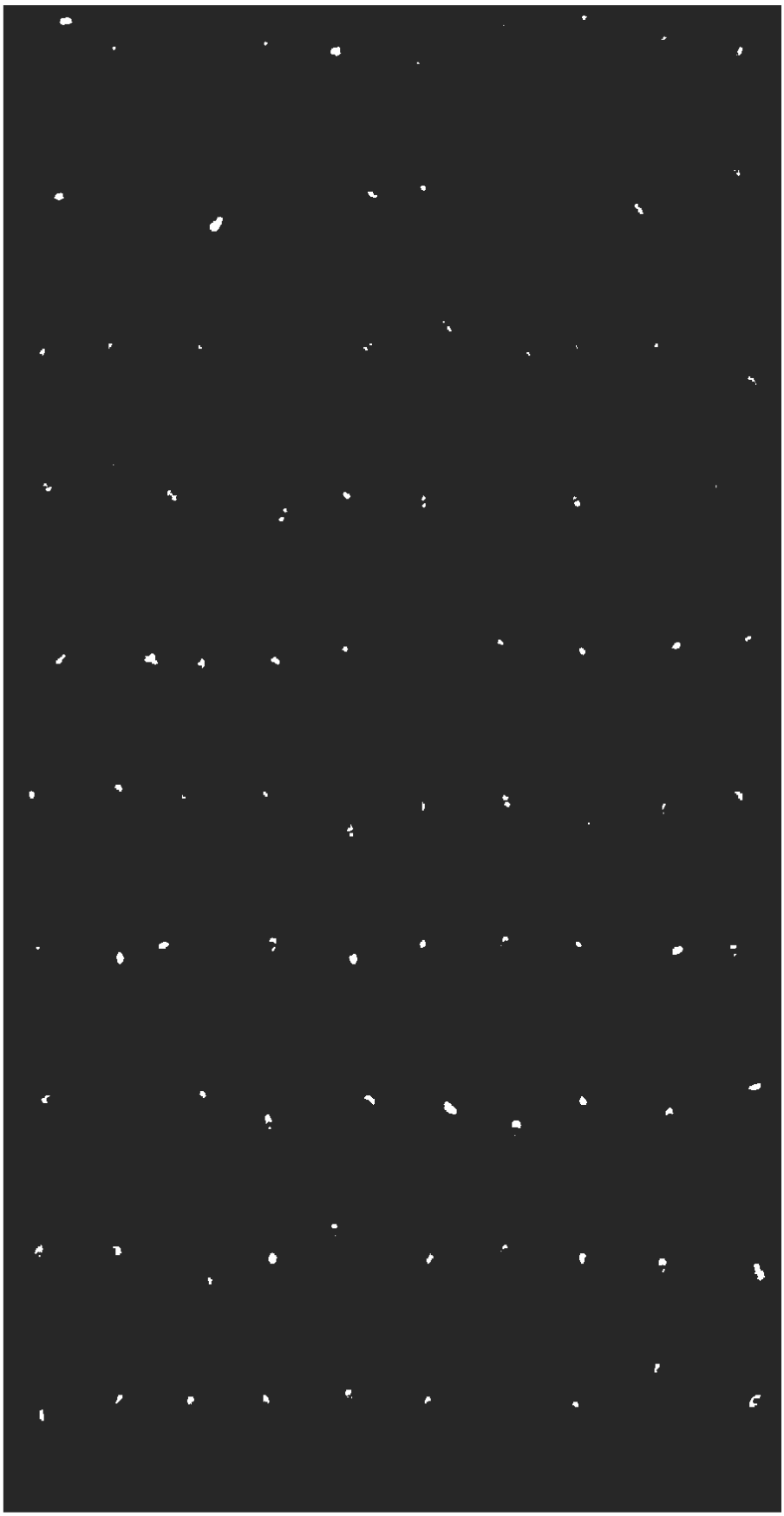

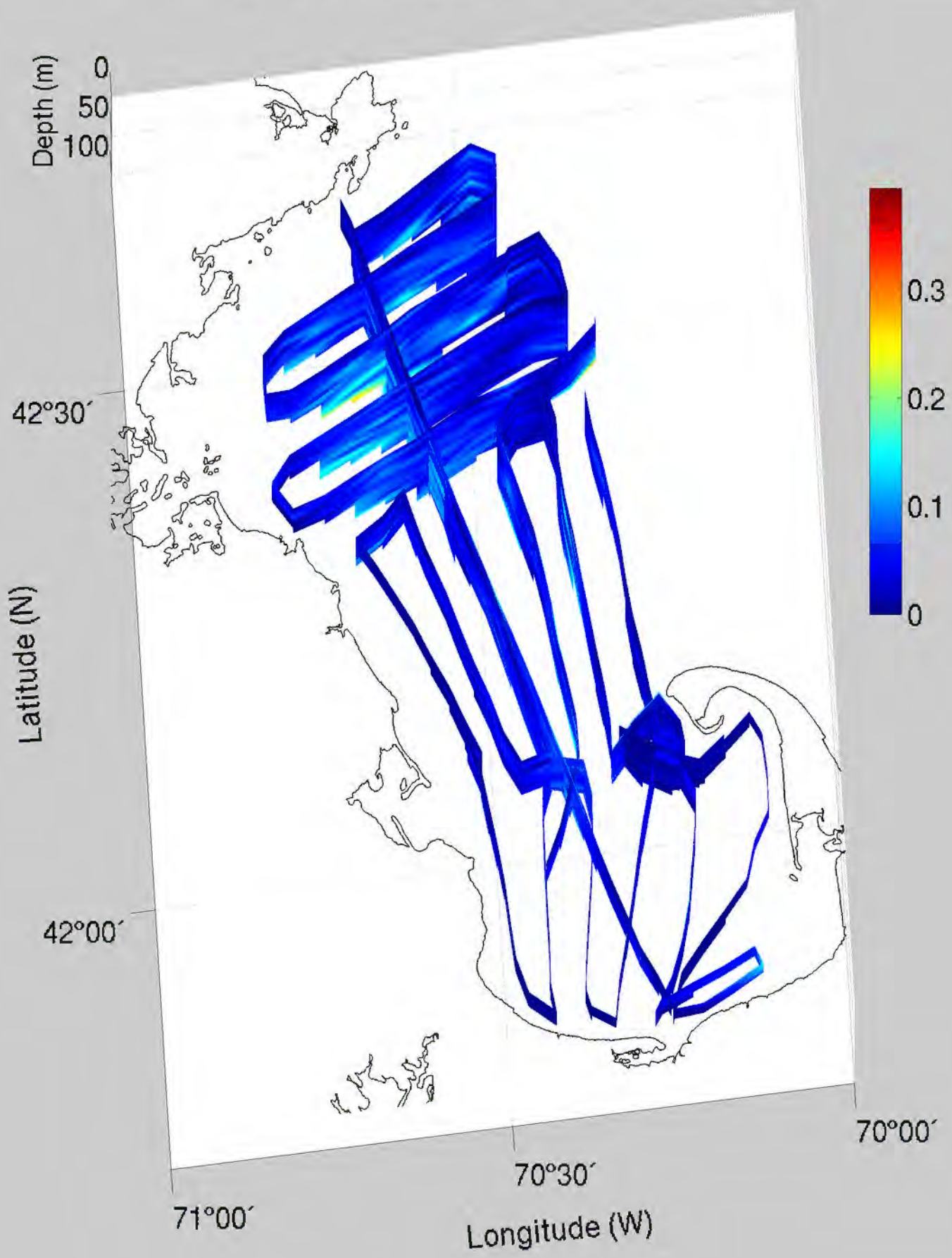
Unidentified Ovals (#/liter) February 23–28, 1999
Depth (m)
0
50
100
42°30´
42°00´
Latitude (N)
0.3
0.2
0.1
0
71°00´
70°30´
70°00´
Longitude (W)

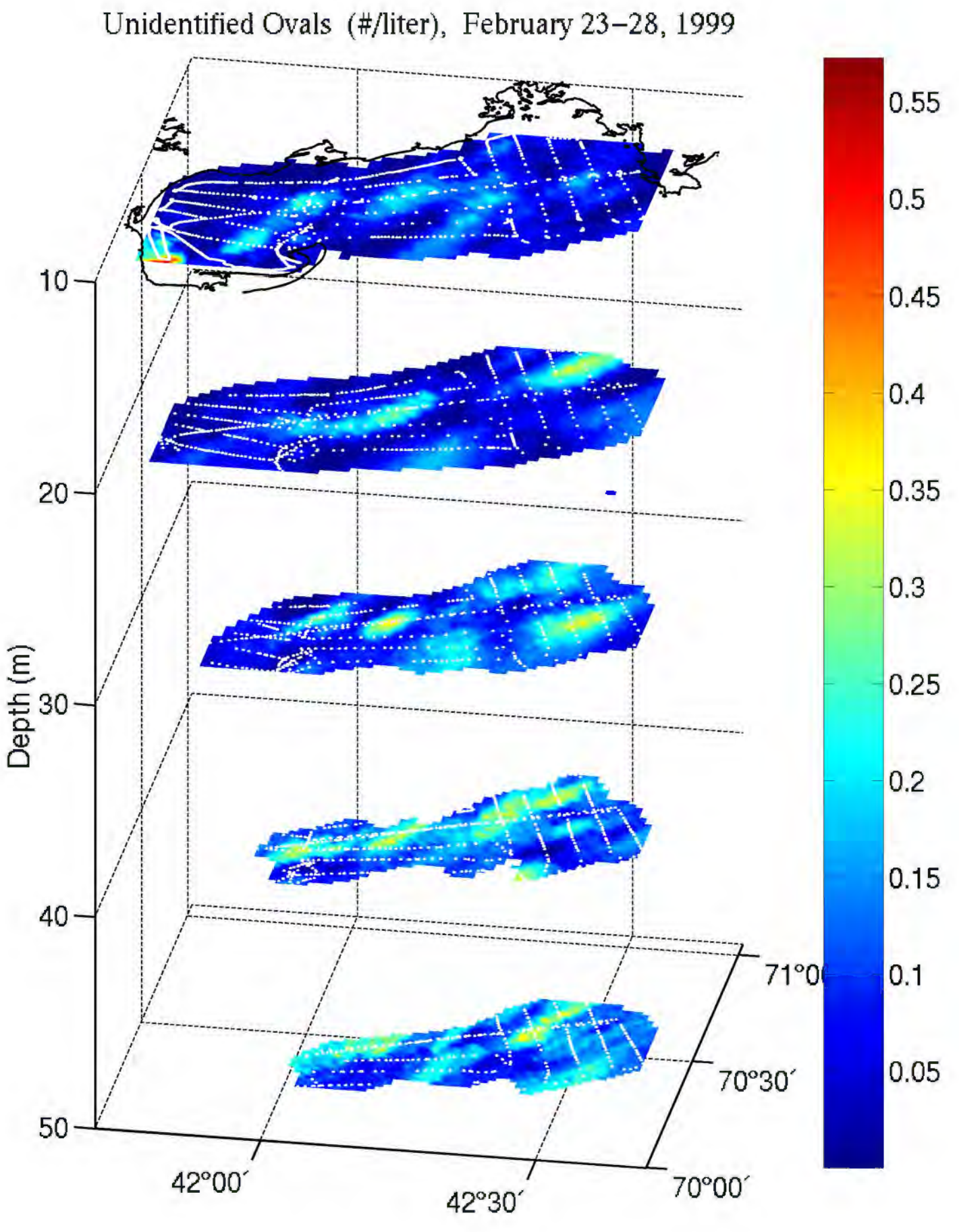
Unidentified Ovals (#/liter), February 23–28, 1999
Depth (m)
10
20
30
40
50
42°00´
42°30´
70°00´
70°30´
71°0
0.55
0.5
0.45
0.4
0.35
0.3
0.25
0.2
0.15
0.1
0.05

Nauplii

| = 1.0 mm

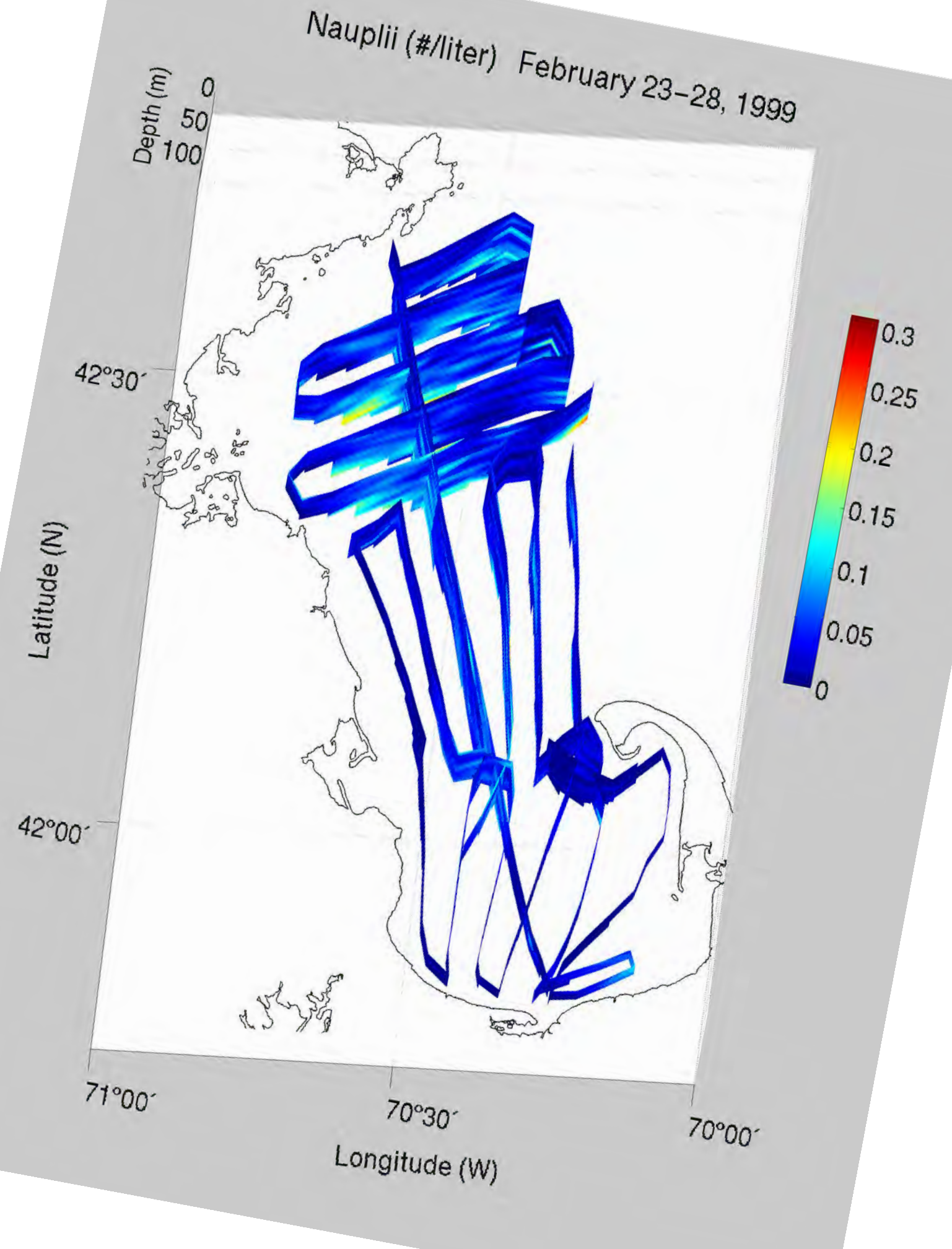
Nauplii (#/liter) February 23–28, 1999
Depth (m)
0
50
100
42°30´
42°00´
Latitude (N)
71°00´
70°30´
70°00´
Longitude (W)
0.3
0.25
0.2
0.15
0.1
0.05
0

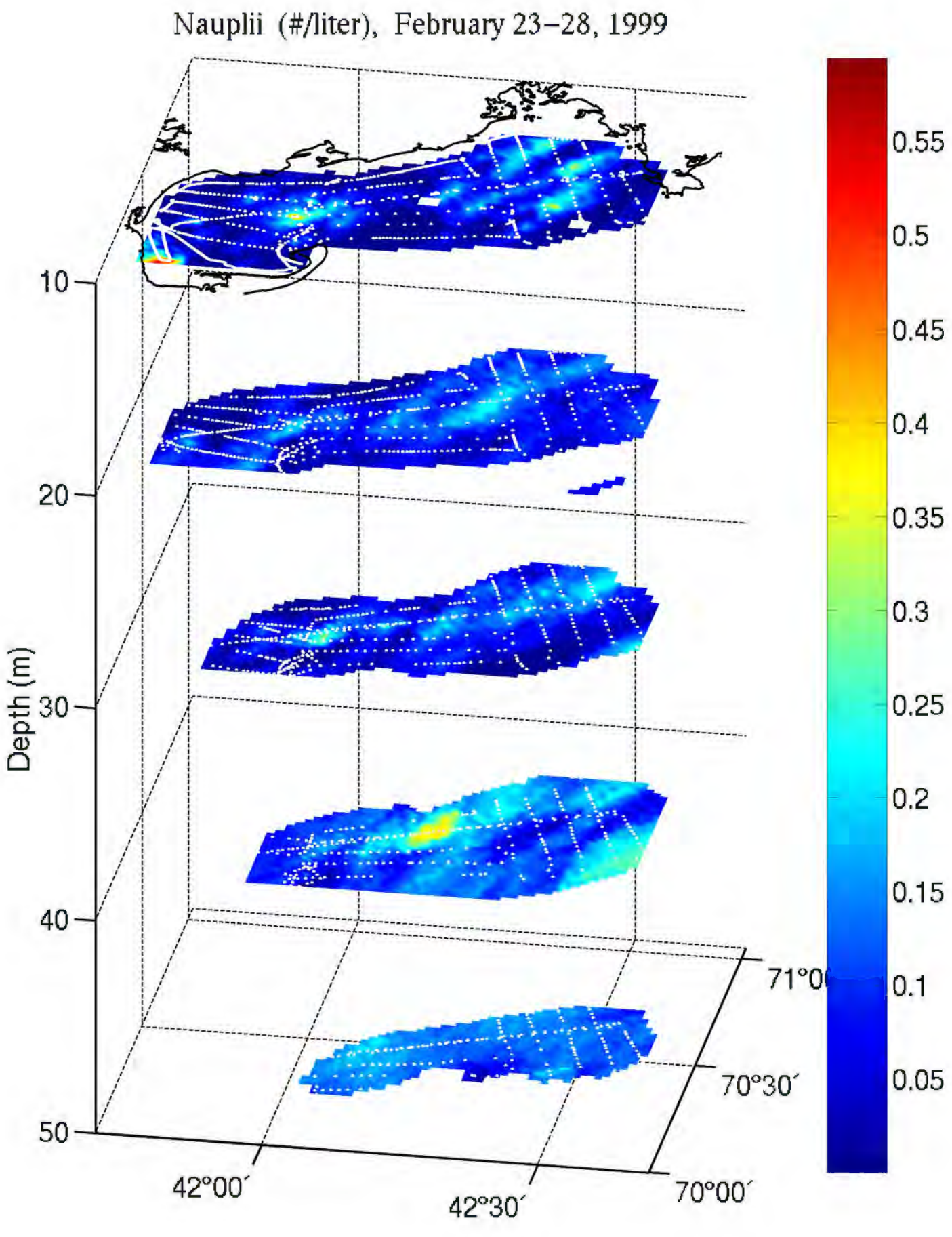
Nauplii (#/liter), February 23–28, 1999
Depth (m)
10
20
30
40
50
42°00´
42°30´
70°00´
70°30´
71°0
0.55
0.5
0.45
0.4
0.35
0.3
0.25
0.2
0.15
0.1
0.05

Pseudocalanus
with eggs

| = 1.0 mm

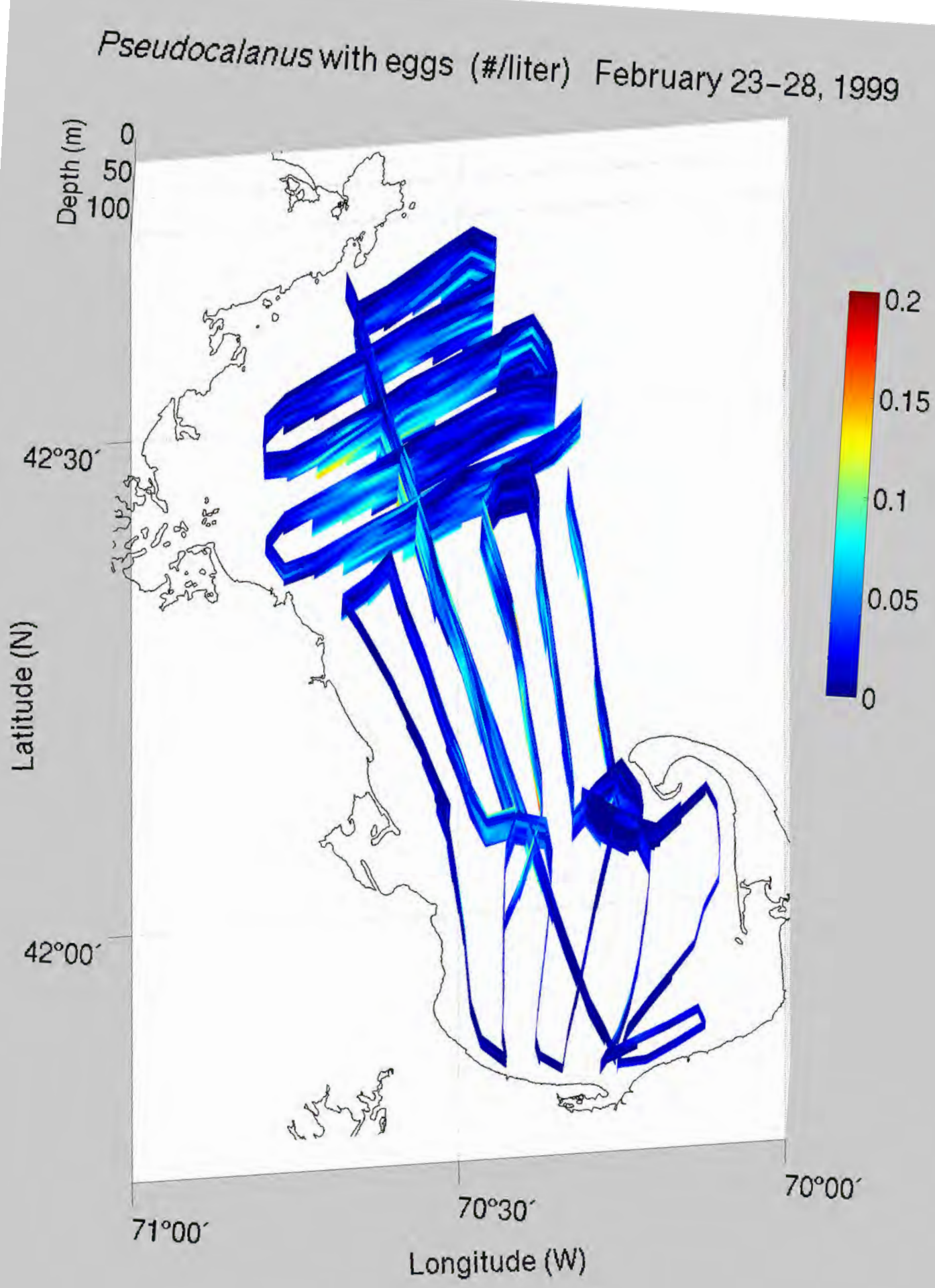
Pseudocalanus with eggs (#/liter) February 23–28, 1999
Depth (m)
0
50
100
42°30´
42°00´
Latitude (N)
71°00´
70°30´
70°00´
Longitude (W)
0.2
0.15
0.1
0.05
0

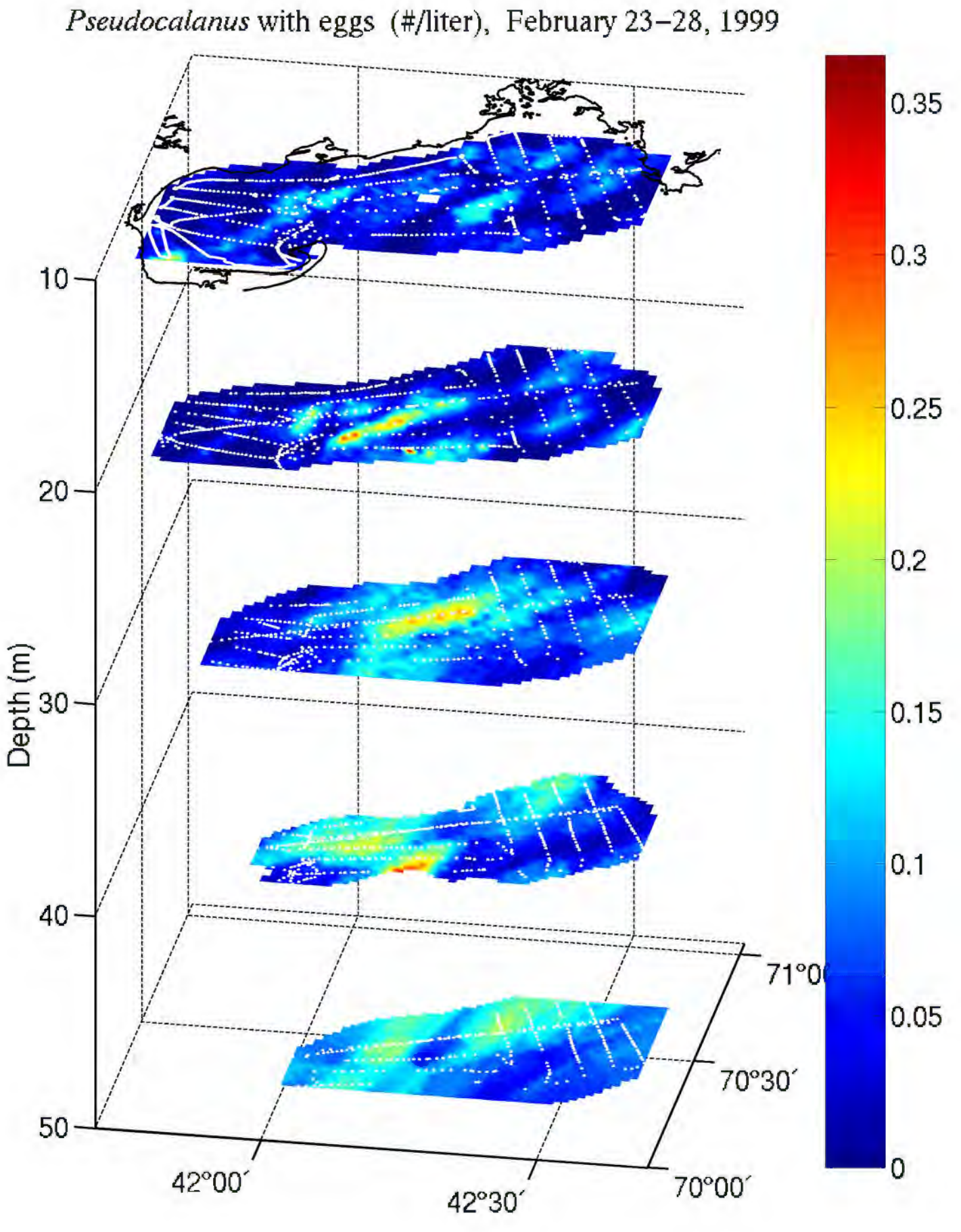
Pseudocalanus with eggs (#/liter), February 23–28, 1999
Depth (m)
10
20
30
40
50
42°00´
42°30´
70°00´
70°30´
71°0
0.35
0.3
0.25
0.2
0.15
0.1
0.05
0

Polychaetes

| = 1.0 mm

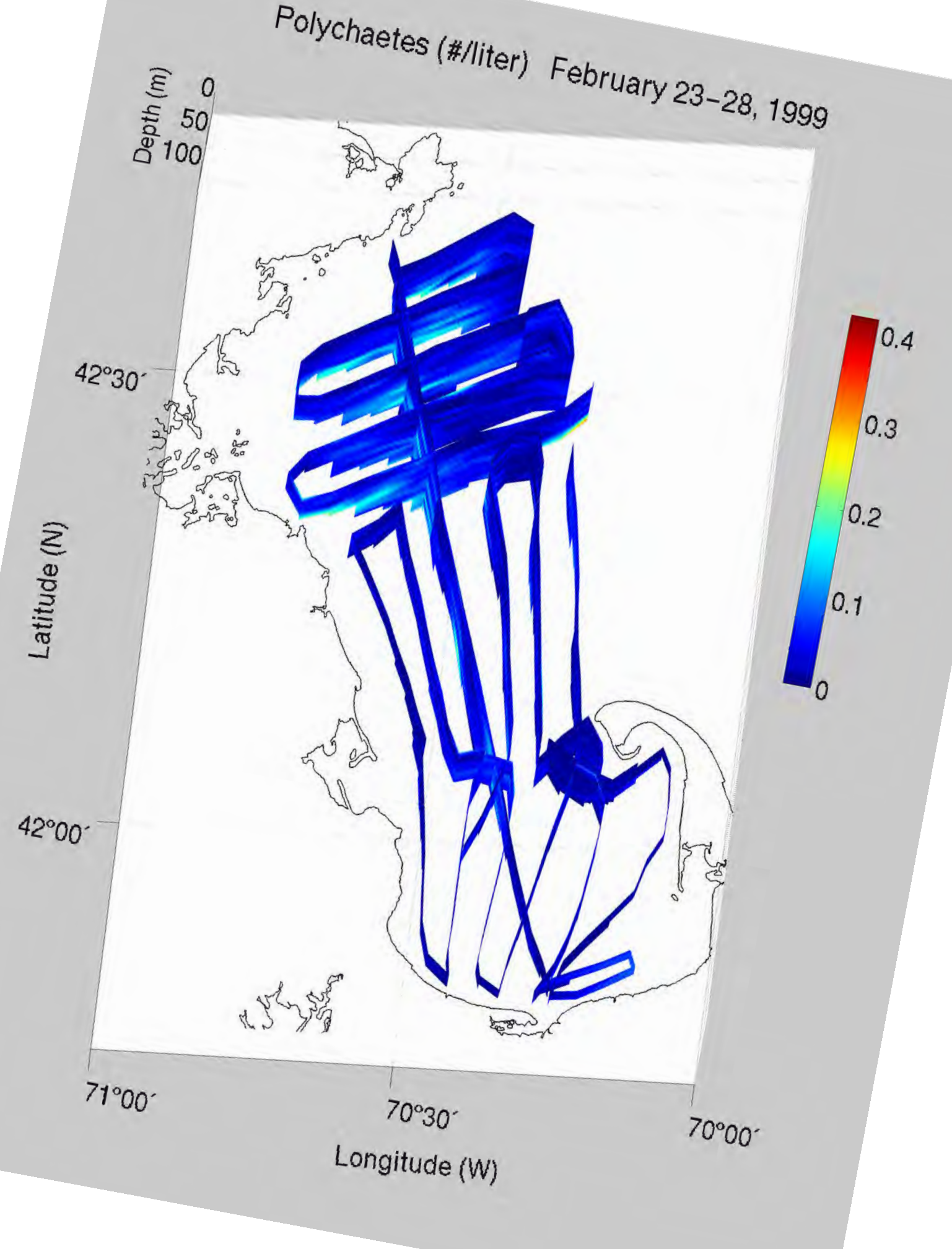
Polychaetes (#/liter) February 23–28, 1999
Depth (m)
0
50
100
42°30´
42°00´
Latitude (N)
71°00´
70°30´
70°00´
Longitude (W)
0.4
0.3
0.2
0.1
0

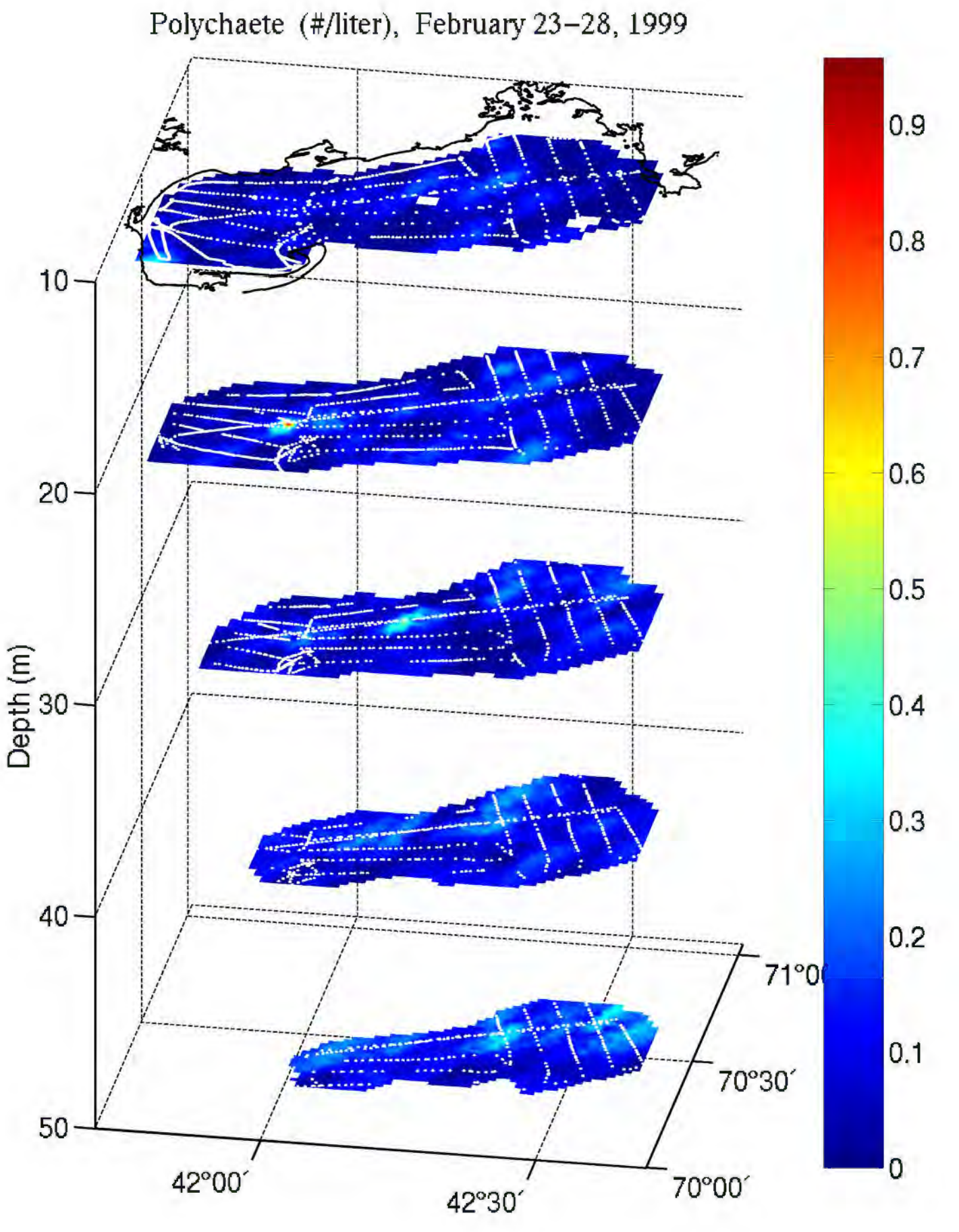
Polychaete (#/liter), February 23–28, 1999
Depth (m)
10
20
30
40
50
42°00´
42°30´
70°00´
70°30´
71°0
0.9
0.8
0.7
0.6
0.5
0.4
0.3
0.2
0.1
0

Pteropods

| = 1.0 mm

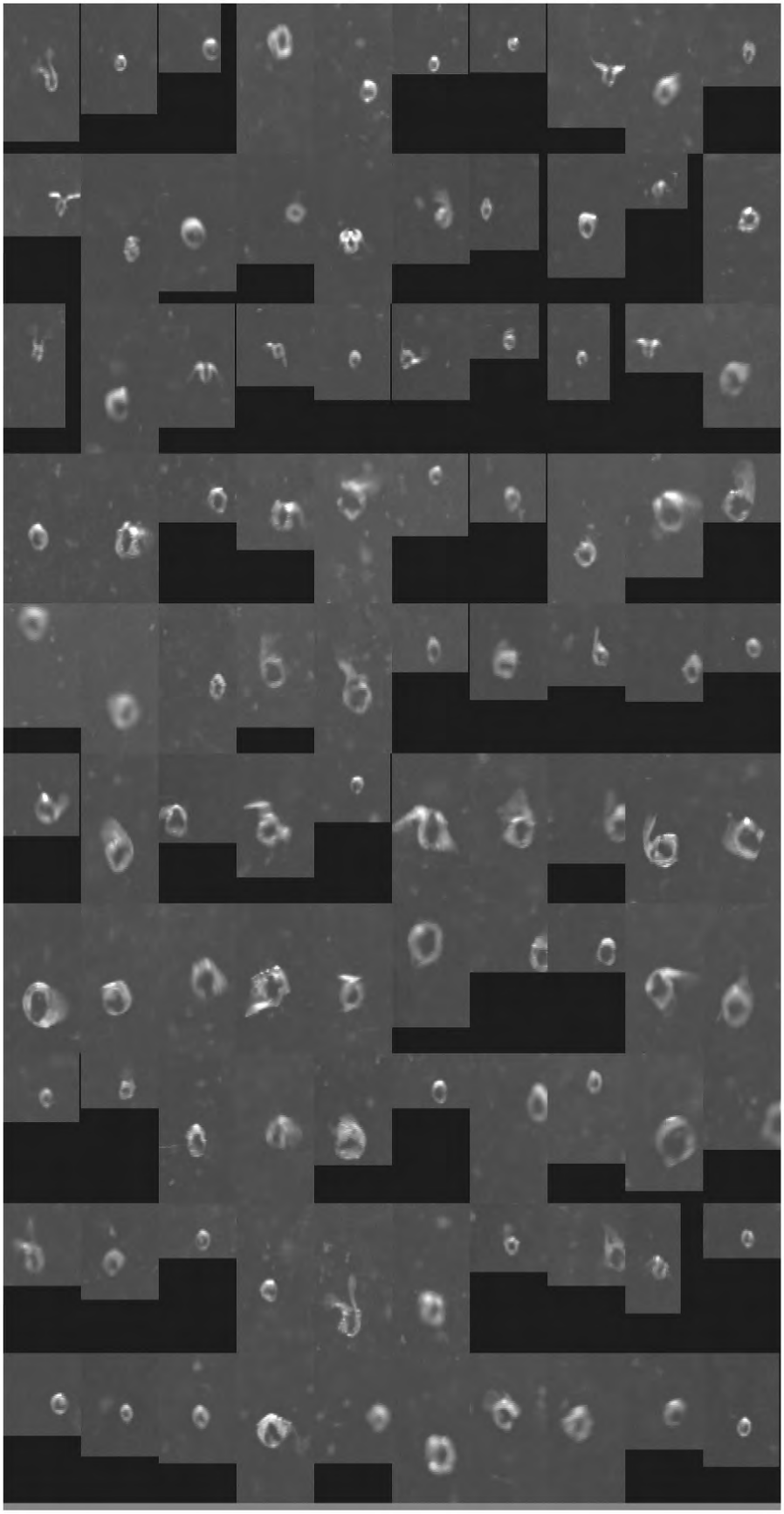

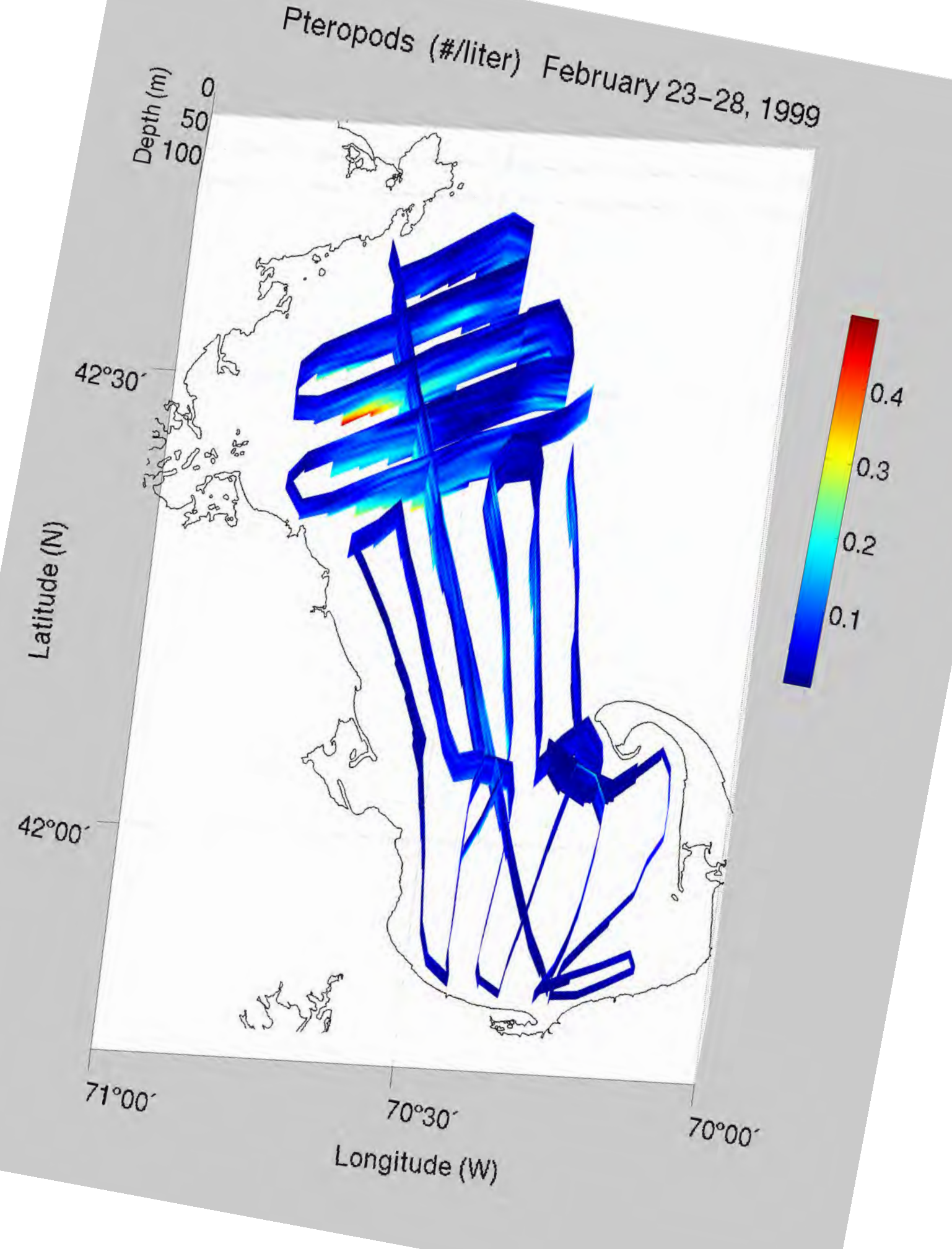
Pteropods (#/liter) February 23–28, 1999
Depth (m)
0
50
100
42°30´
42°00´
Latitude (N)
71°00´
70°30´
70°00´
Longitude (W)
0.4
0.3
0.2
0.1

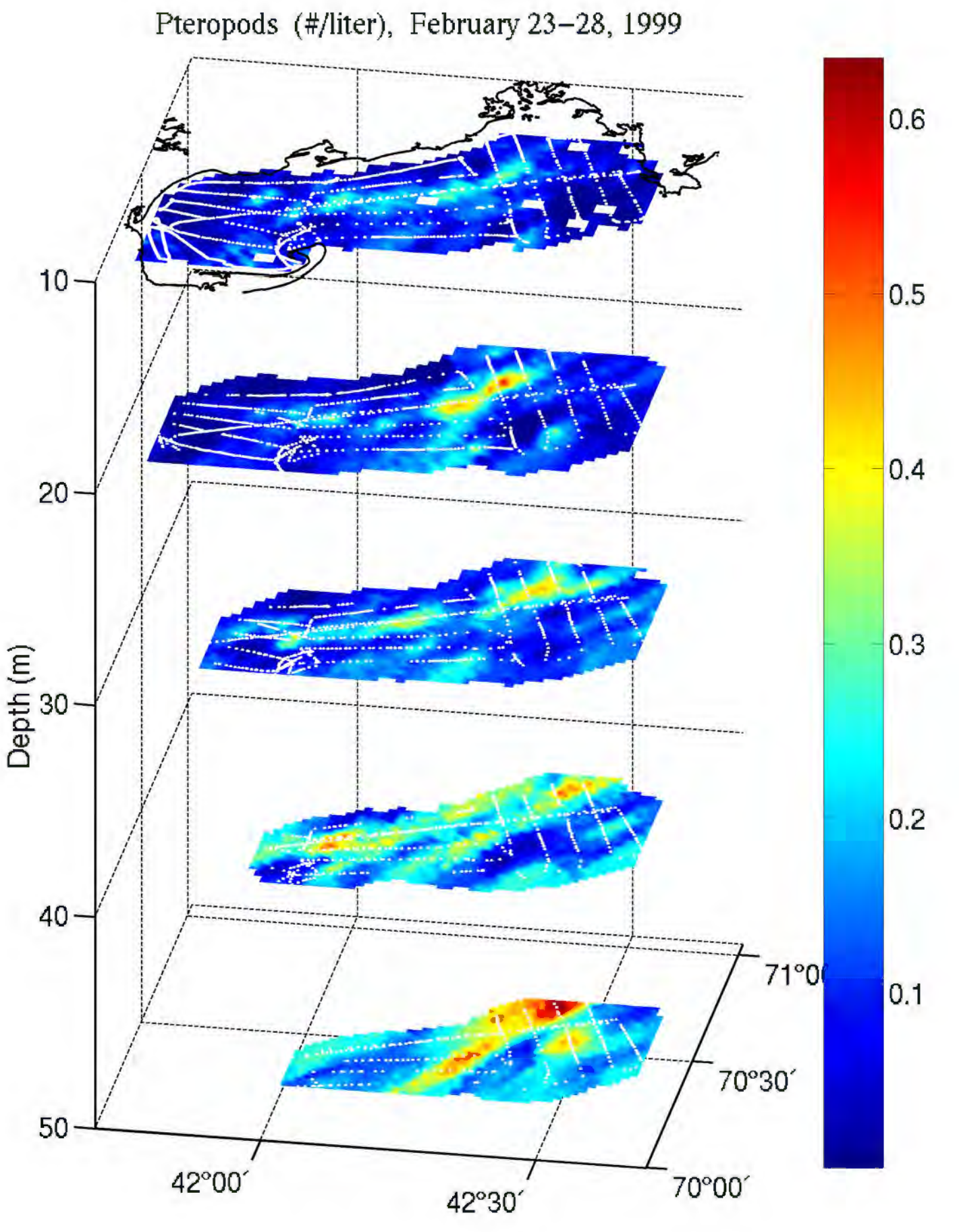
Pteropods (#/liter), February 23–28, 1999
Depth (m)
10
20
30
40
50
42°00´
42°30´
70°00´
70°30´
71°0
0.6
0.5
0.4
0.3
0.2
0.1

Marine Snow

| = 1.0 mm

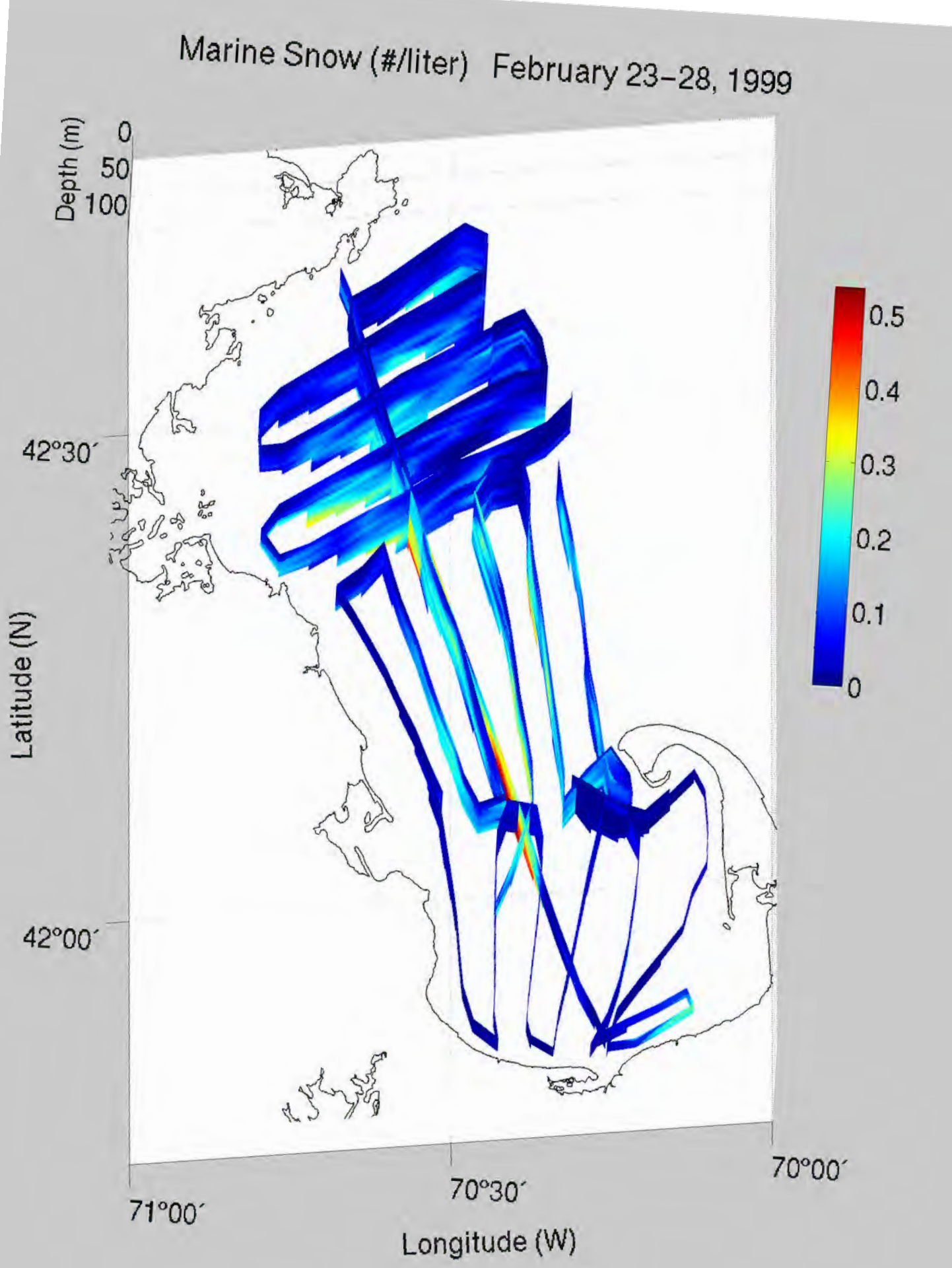
Marine Snow (#/liter) February 23–28, 1999
Depth (m)
0
50
100
42°30´
42°00´
Latitude (N)
0.5
0.4
0.3
0.2
0.1
0
71°00´
70°30´
70°00´
Longitude (W)

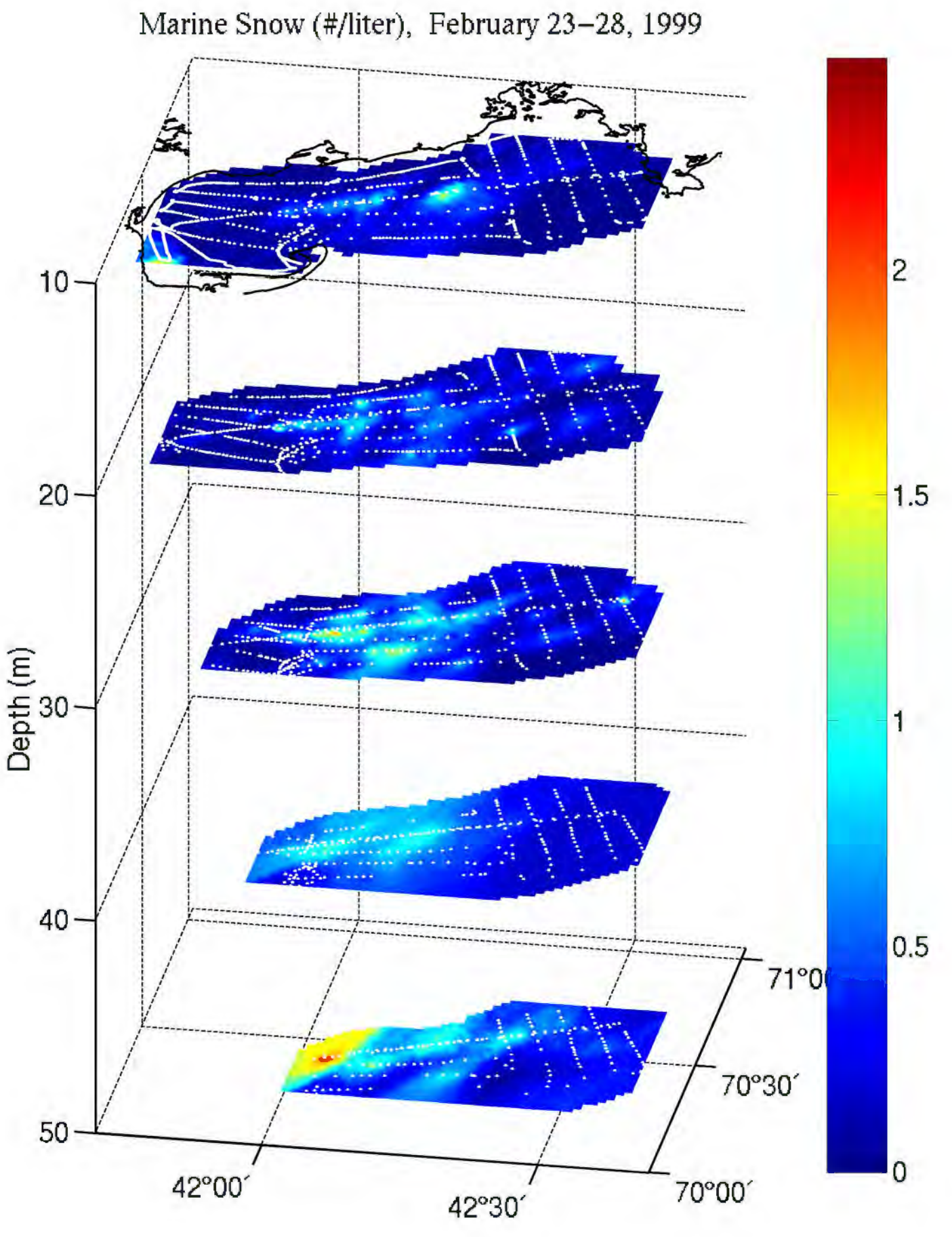
Marine Snow (#/liter), February 23–28, 1999
Depth (m)
10
20
30
40
50
42°00´
42°30´
70°00´
70°30´
71°0
2
1.5
1
0.5
0

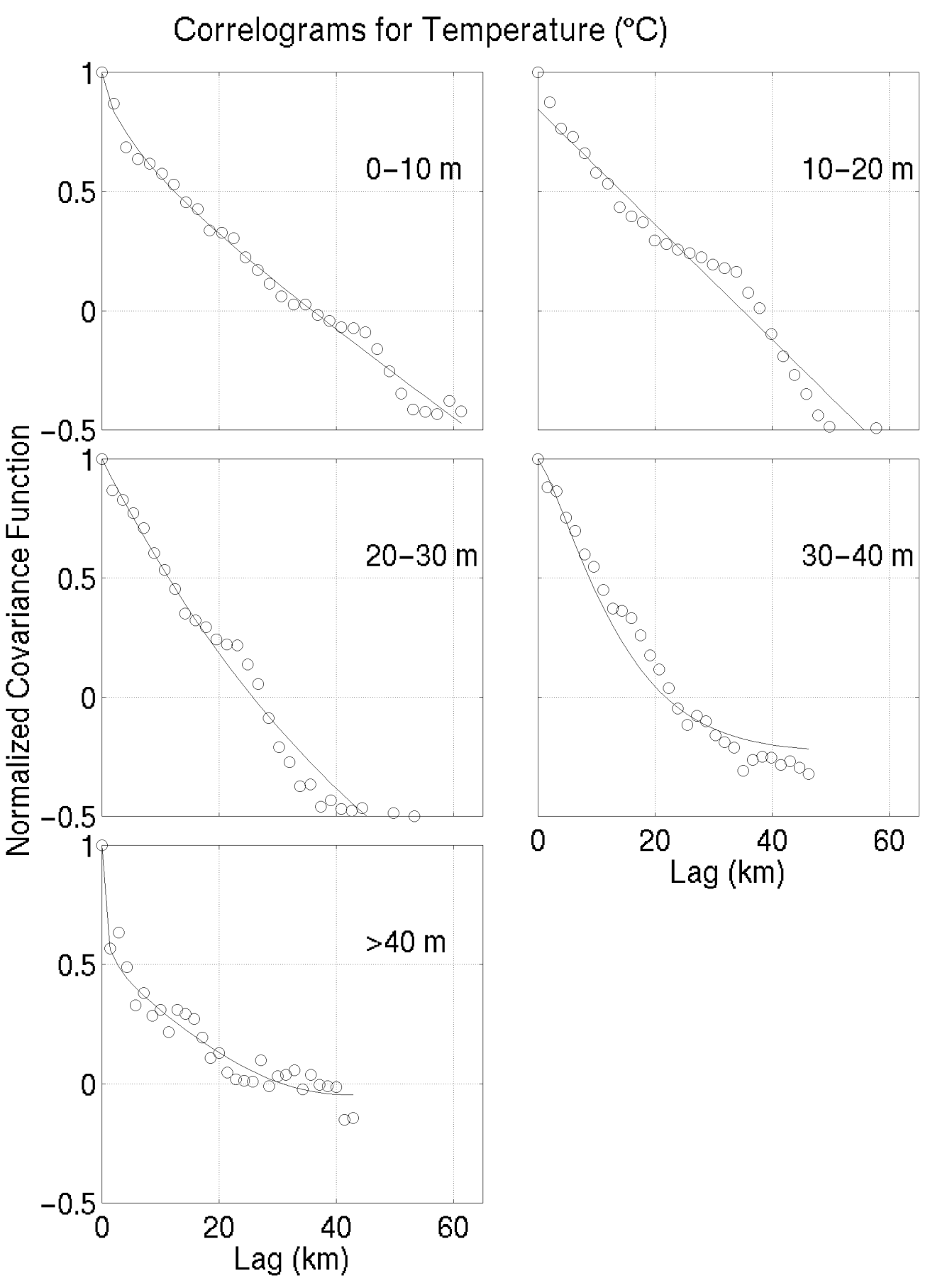
Correlograms for Temperature (°C)
Normalized Covariance Function
0–10 m
10–20 m
20–30 m
30–40 m
>40 m
1
0.5
0
−0.5
0
20
40
60
Lag (km)

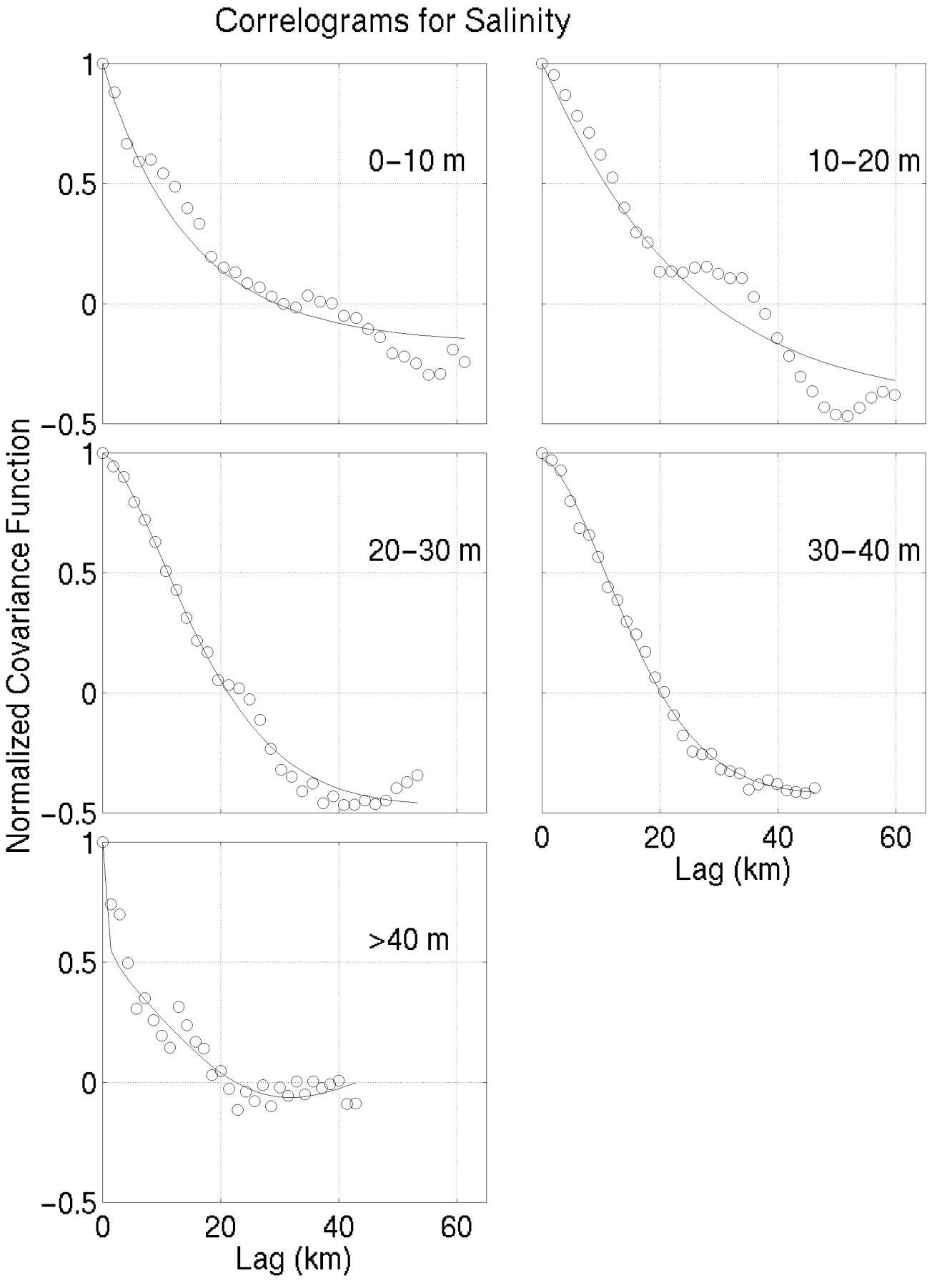
Correlograms for Salinity
Normalized Covariance Function
0–10 m
10–20 m
20–30 m
30–40 m
>40 m
1
0.5
0
−0.5
0
20
40
60
Lag (km)

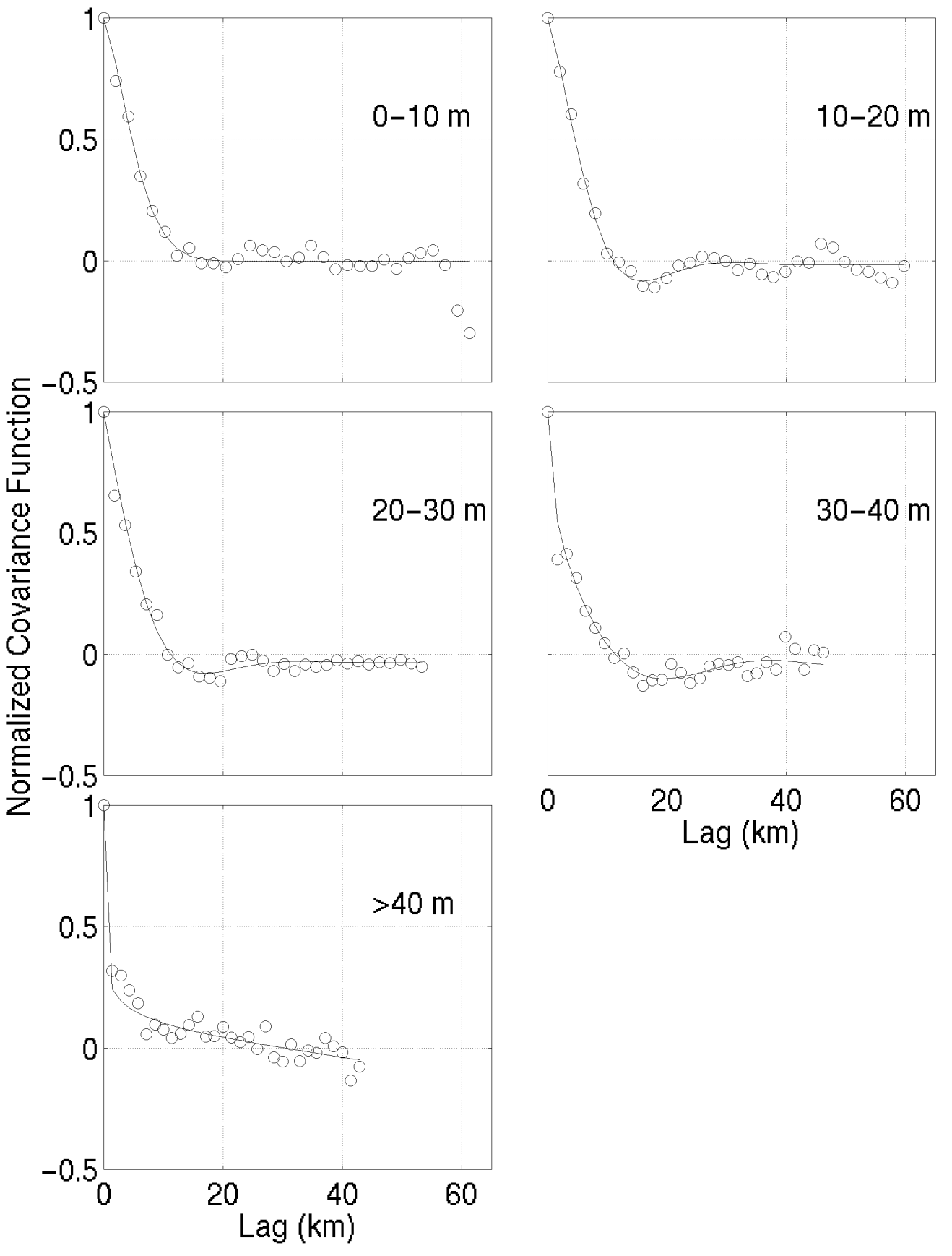
Correlograms for Fluorescence (µgChl/liter)
Normalized Covariance Function
0–10 m
10–20 m
20–30 m
30–40 m
>40 m
1
0.5
0
−0.5
0
20
40
60
Lag (km)

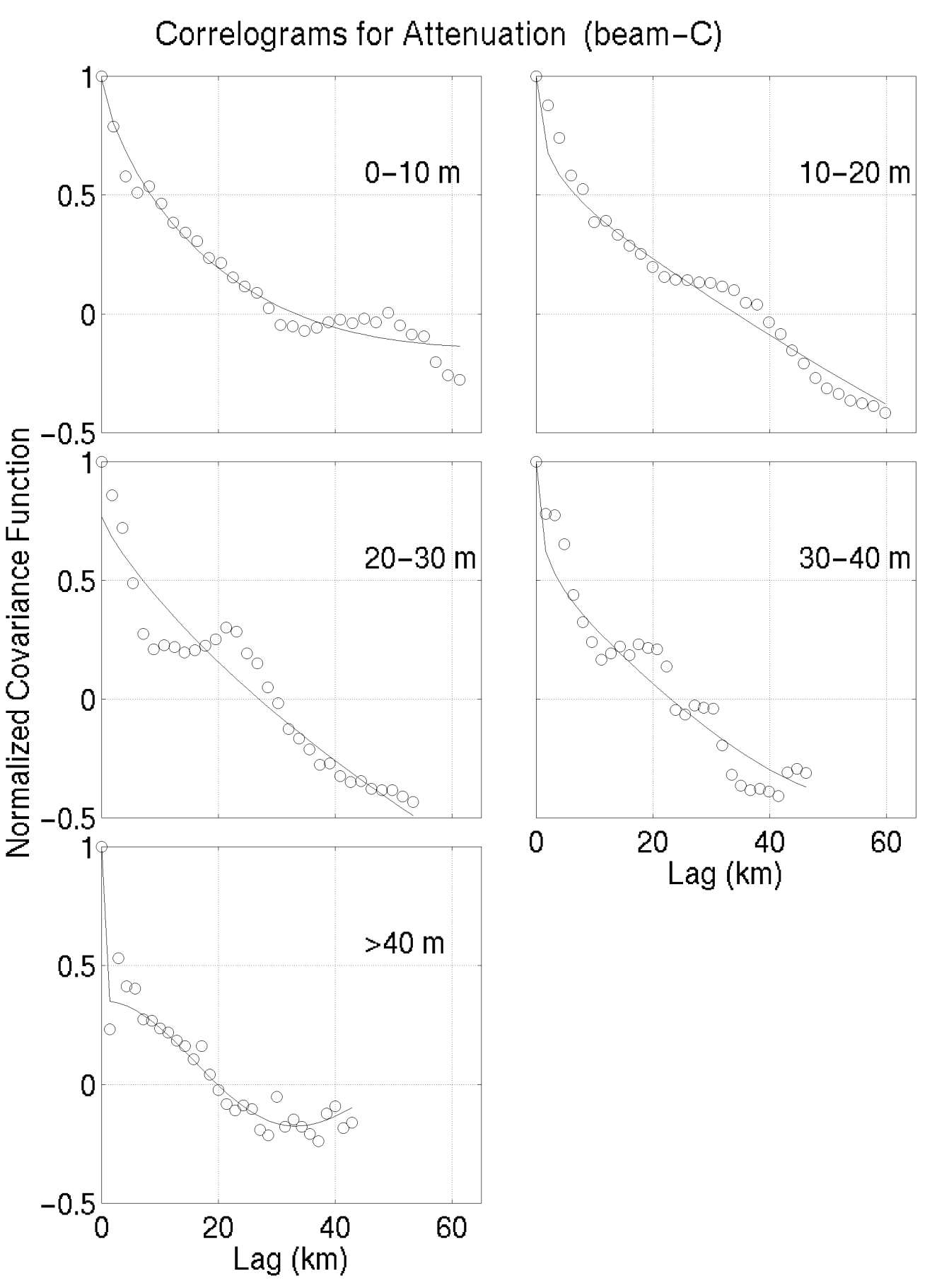
Correlograms for Attenuation (beam−C)
Normalized Covariance Function
0−10 m
10−20 m
20−30 m
30−40 m
>40 m
1
0.5
0
−0.5
0
20
40
60
Lag (km)

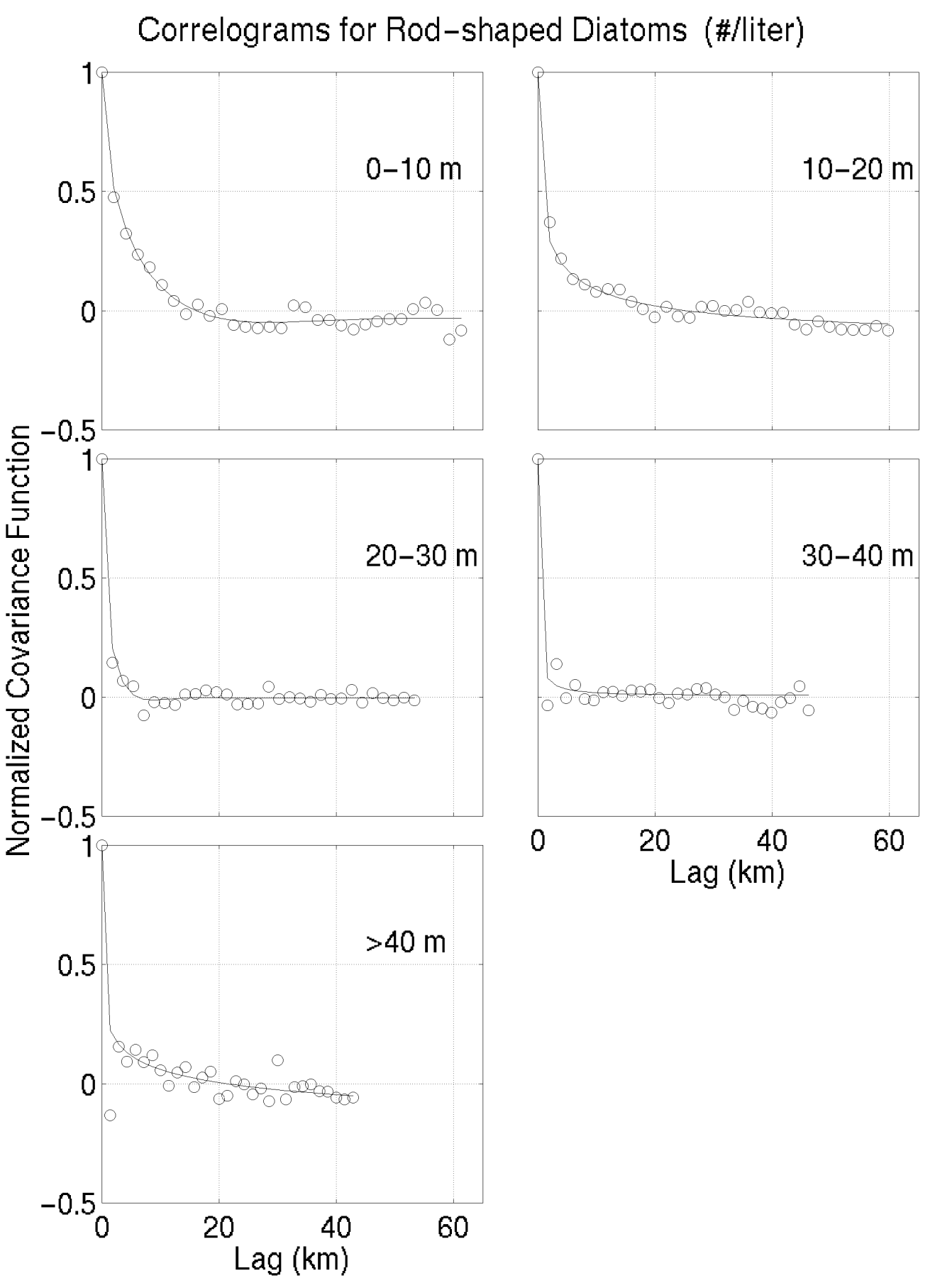
Correlograms for Rod−shaped Diatoms (#/liter)
Normalized Covariance Function
0−10 m
10−20 m
20−30 m
30−40 m
>40 m
1
0.5
0
−0.5
0
20
40
60
Lag (km)

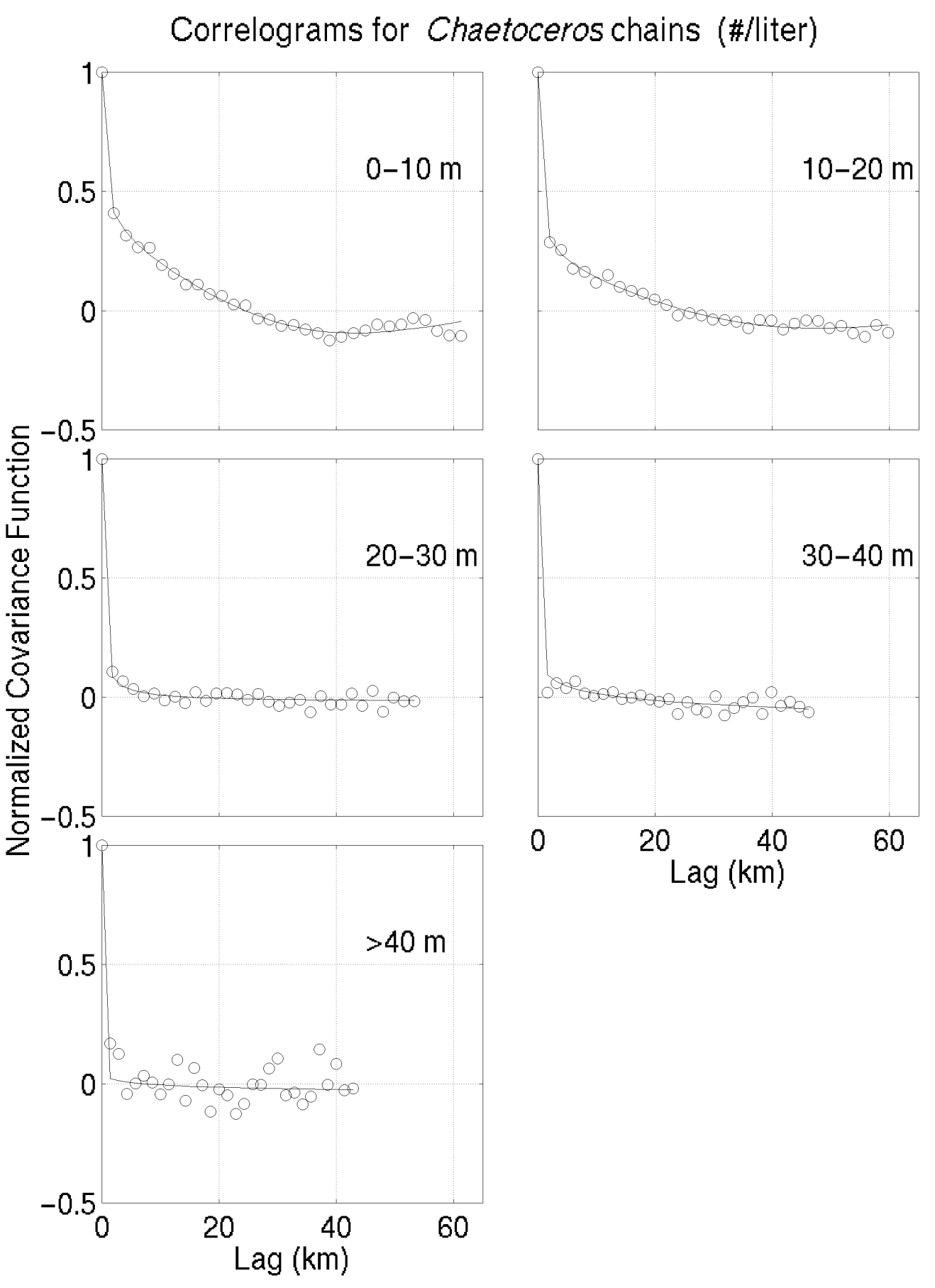
Correlograms for *Chaetoceros* chains (#/liter)
Normalized Covariance Function
0–10 m
10–20 m
20–30 m
30–40 m
>40 m
1
0.5
0
−0.5
0
20
40
60
Lag (km)

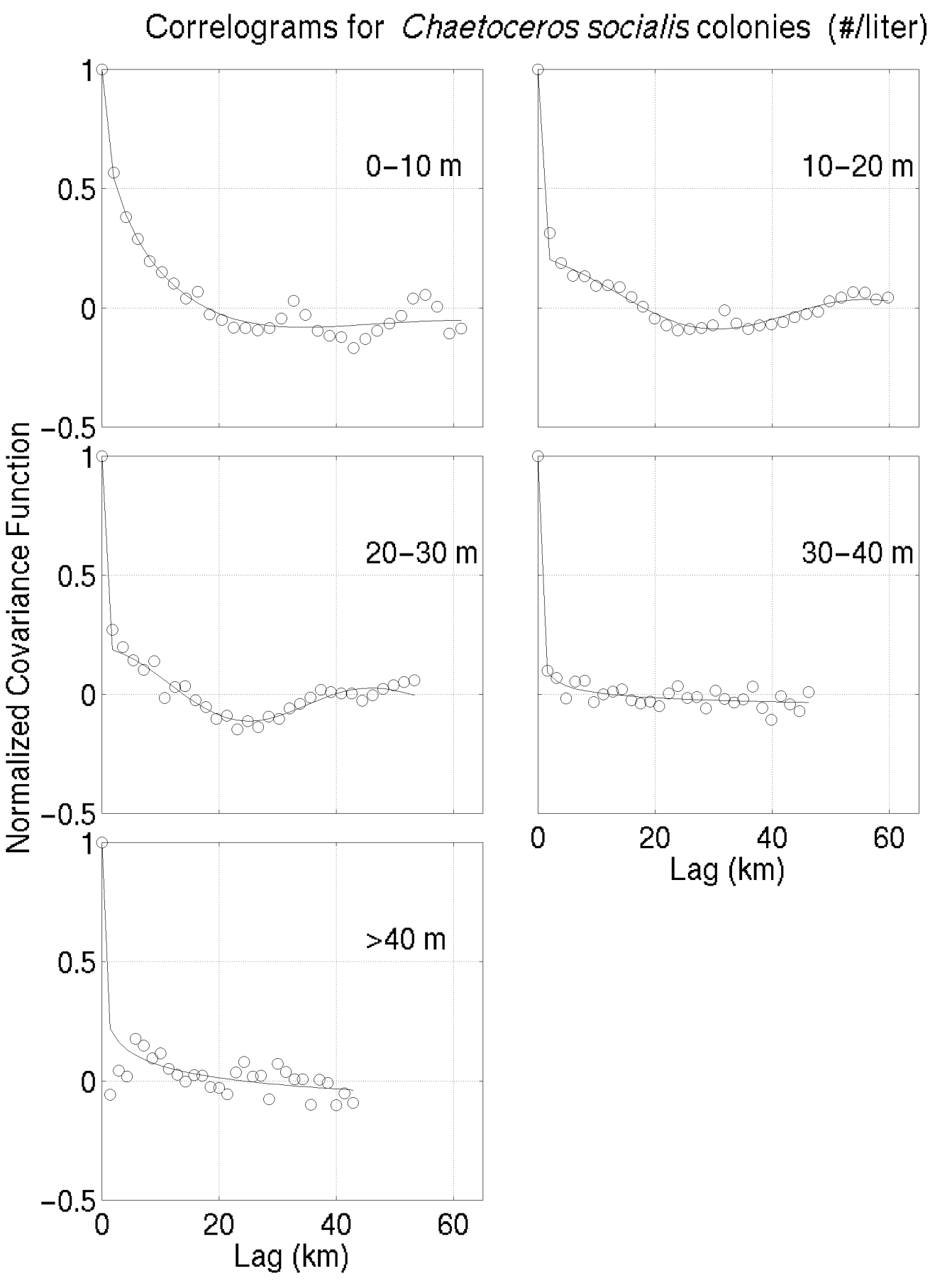
Correlograms for *Chaetoceros socialis* colonies (#/liter)
Normalized Covariance Function
0–10 m
10–20 m
20–30 m
30–40 m
>40 m
1
0.5
0
−0.5
0
20
40
60
Lag (km)

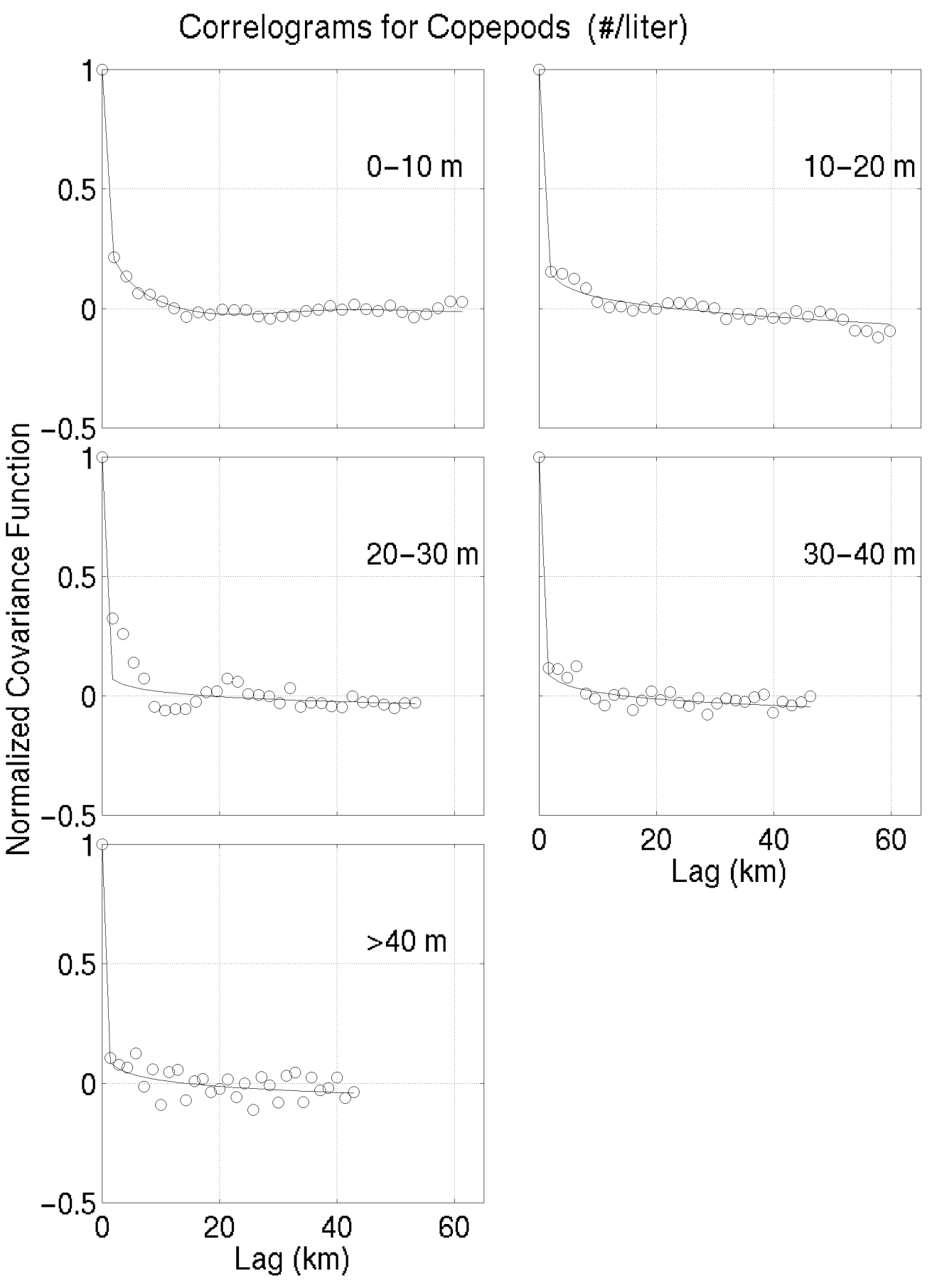
Correlograms for Copepods (#/liter)
Normalized Covariance Function
0–10 m
10–20 m
20–30 m
30–40 m
>40 m
1
0.5
0
−0.5
0
20
40
60
Lag (km)

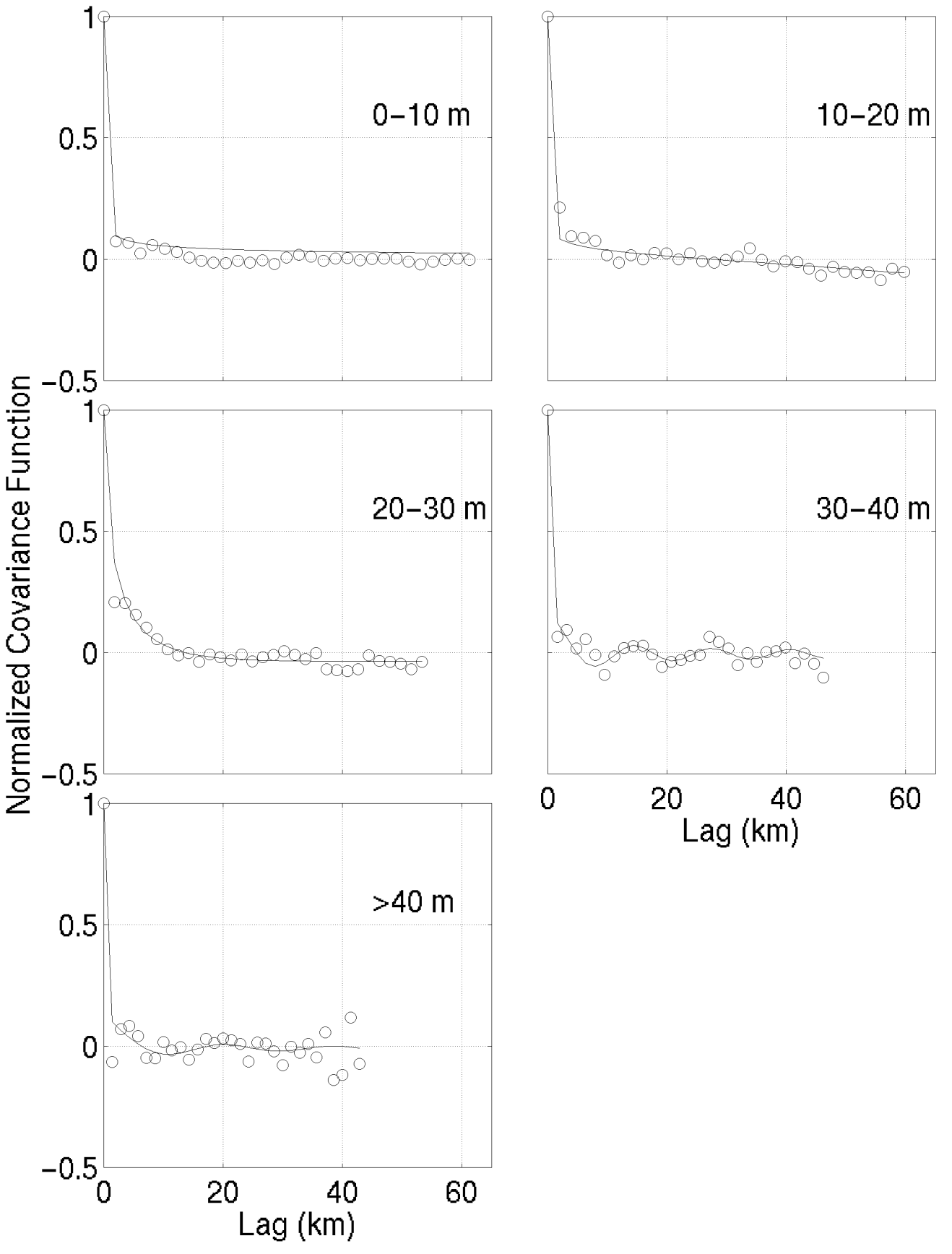
Correlograms for Unidentified Disks (#/liter)
Normalized Covariance Function
0–10 m
10–20 m
20–30 m
30–40 m
>40 m
1
0.5
0
−0.5
0
20
40
60
Lag (km)

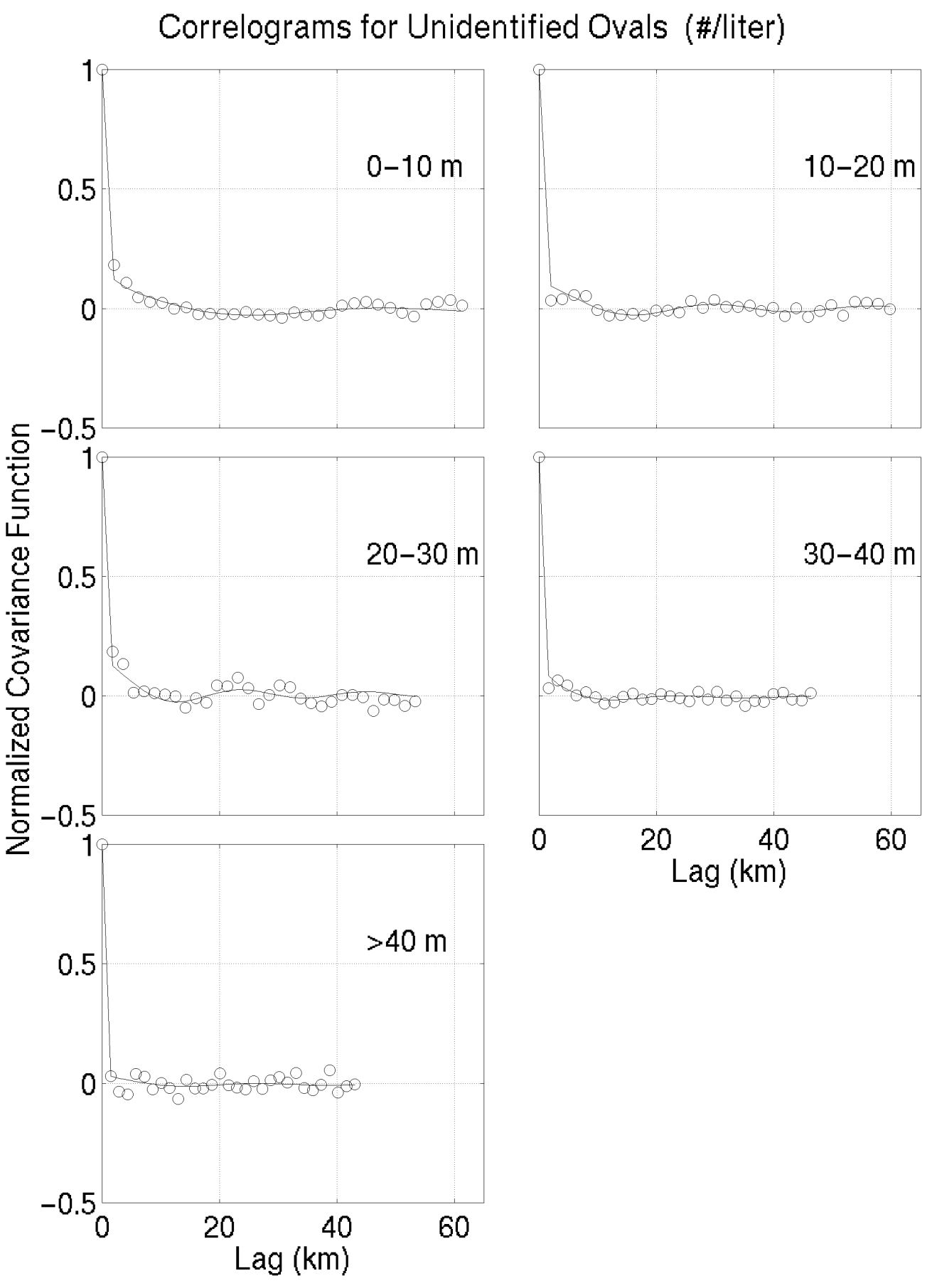
Correlograms for Unidentified Ovals (#/liter)
Normalized Covariance Function
0–10 m
10–20 m
20–30 m
30–40 m
>40 m
1
0.5
0
−0.5
0
20
40
60
Lag (km)

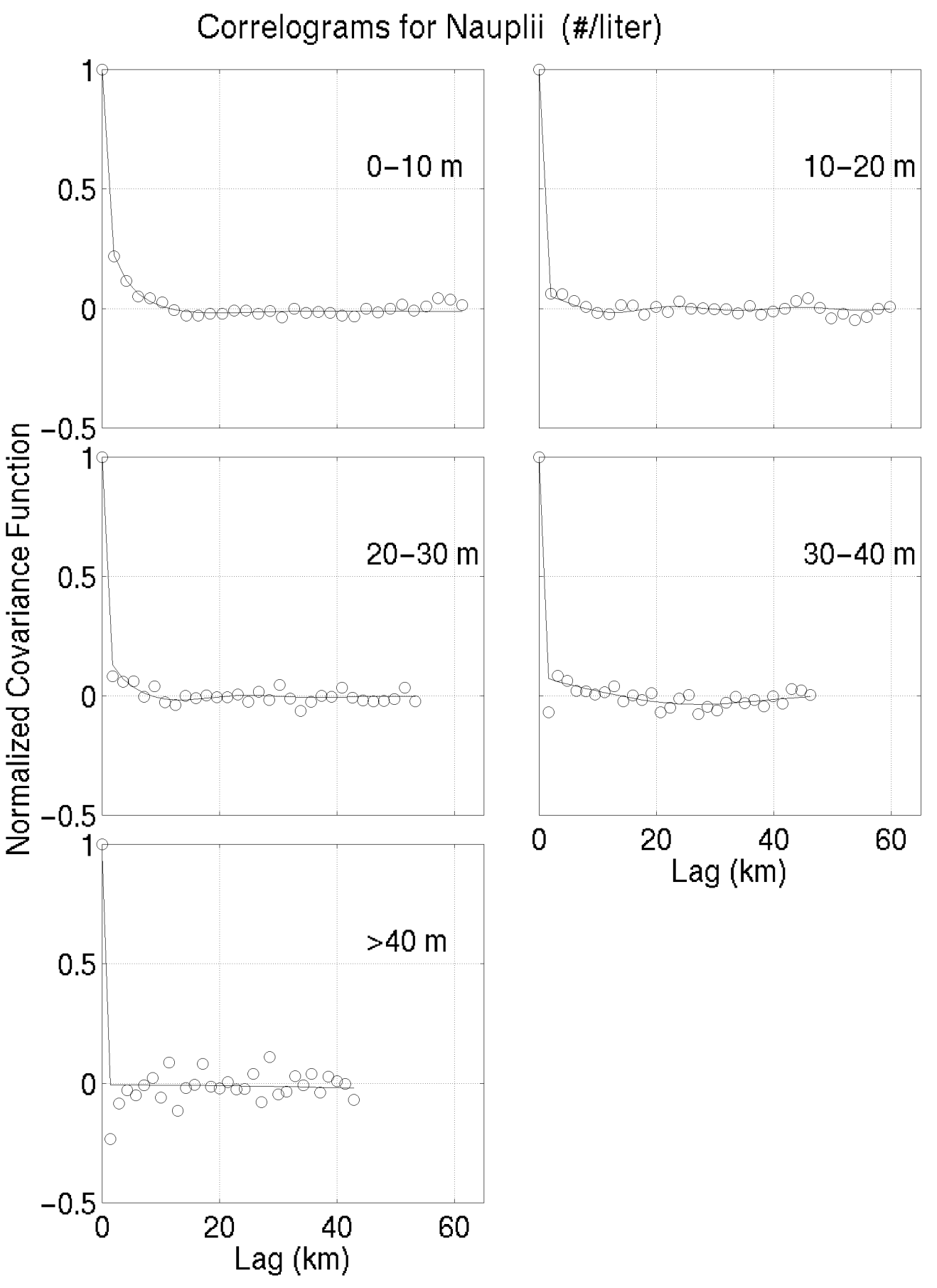
Correlograms for Nauplii (#/liter)
Normalized Covariance Function
0–10 m
10–20 m
20–30 m
30–40 m
>40 m
1
0.5
0
−0.5
0
20
40
60
Lag (km)

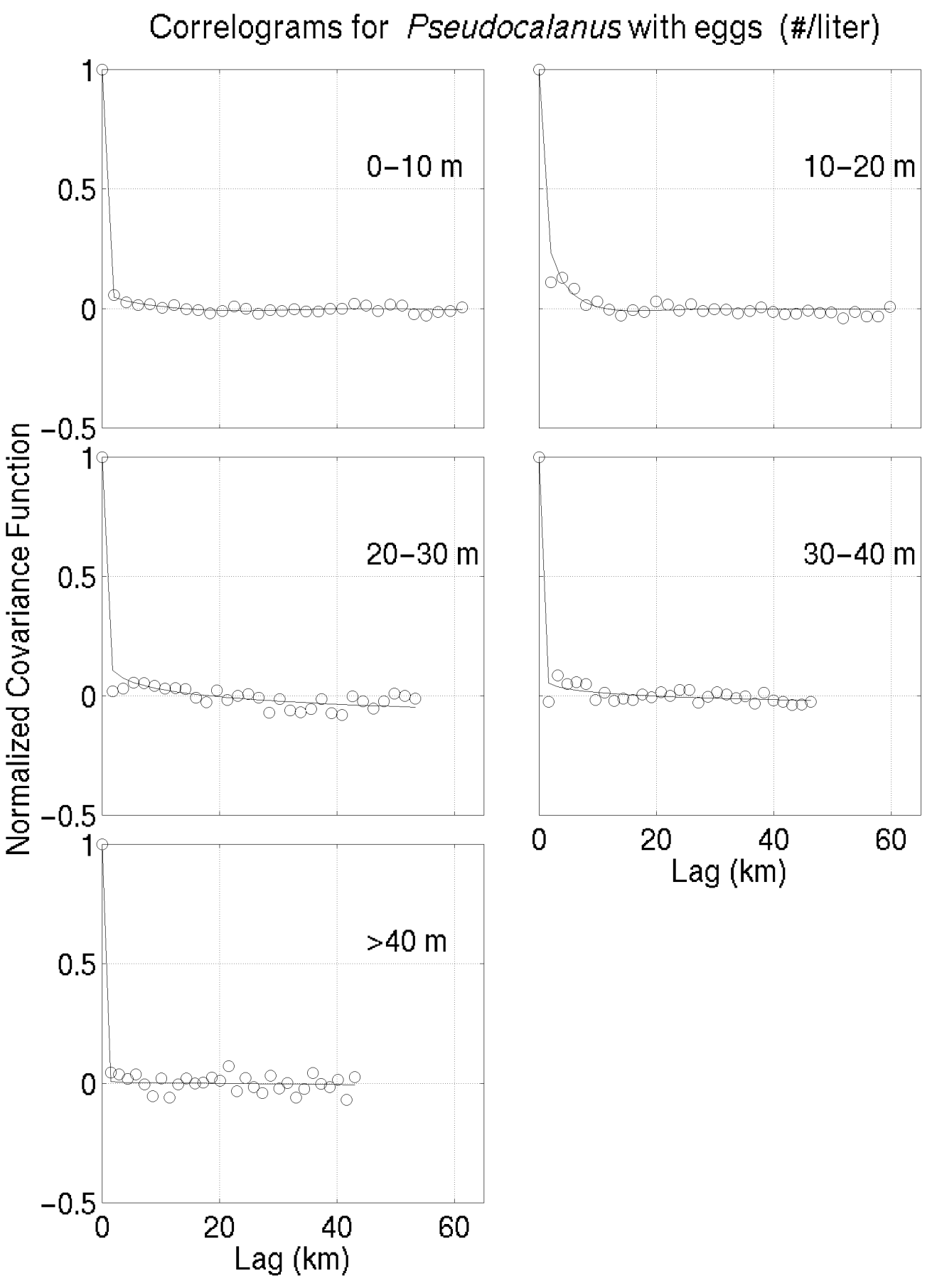
Correlograms for *Pseudocalanus* with eggs (#/liter)
Normalized Covariance Function
0–10 m
10–20 m
20–30 m
30–40 m
>40 m
1
0.5
0
−0.5
0
20
40
60
Lag (km)

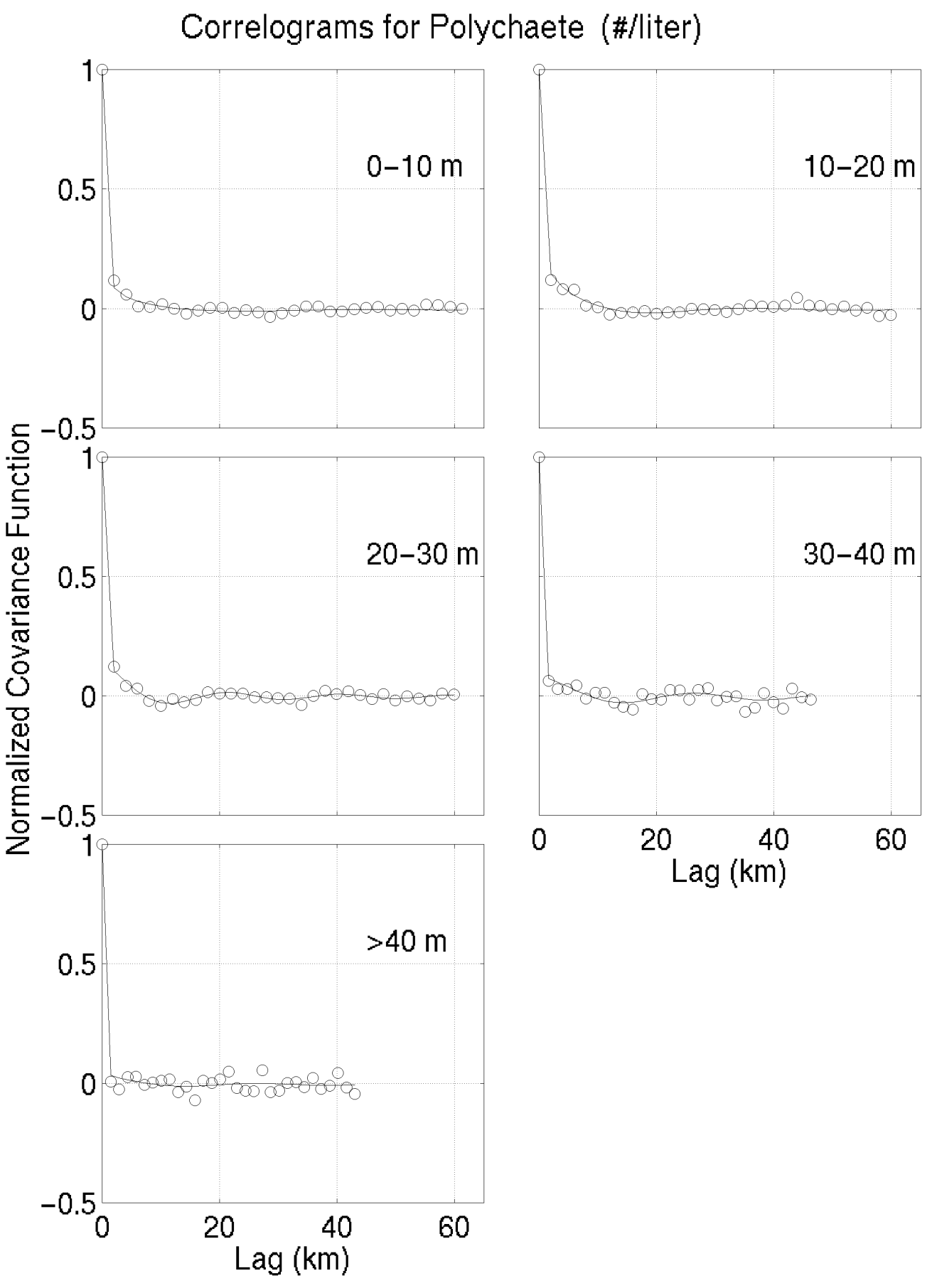
Correlograms for Polychaete (#/liter)
Normalized Covariance Function
0–10 m
10–20 m
20–30 m
30–40 m
>40 m
1
0.5
0
−0.5
0
20
40
60
Lag (km)

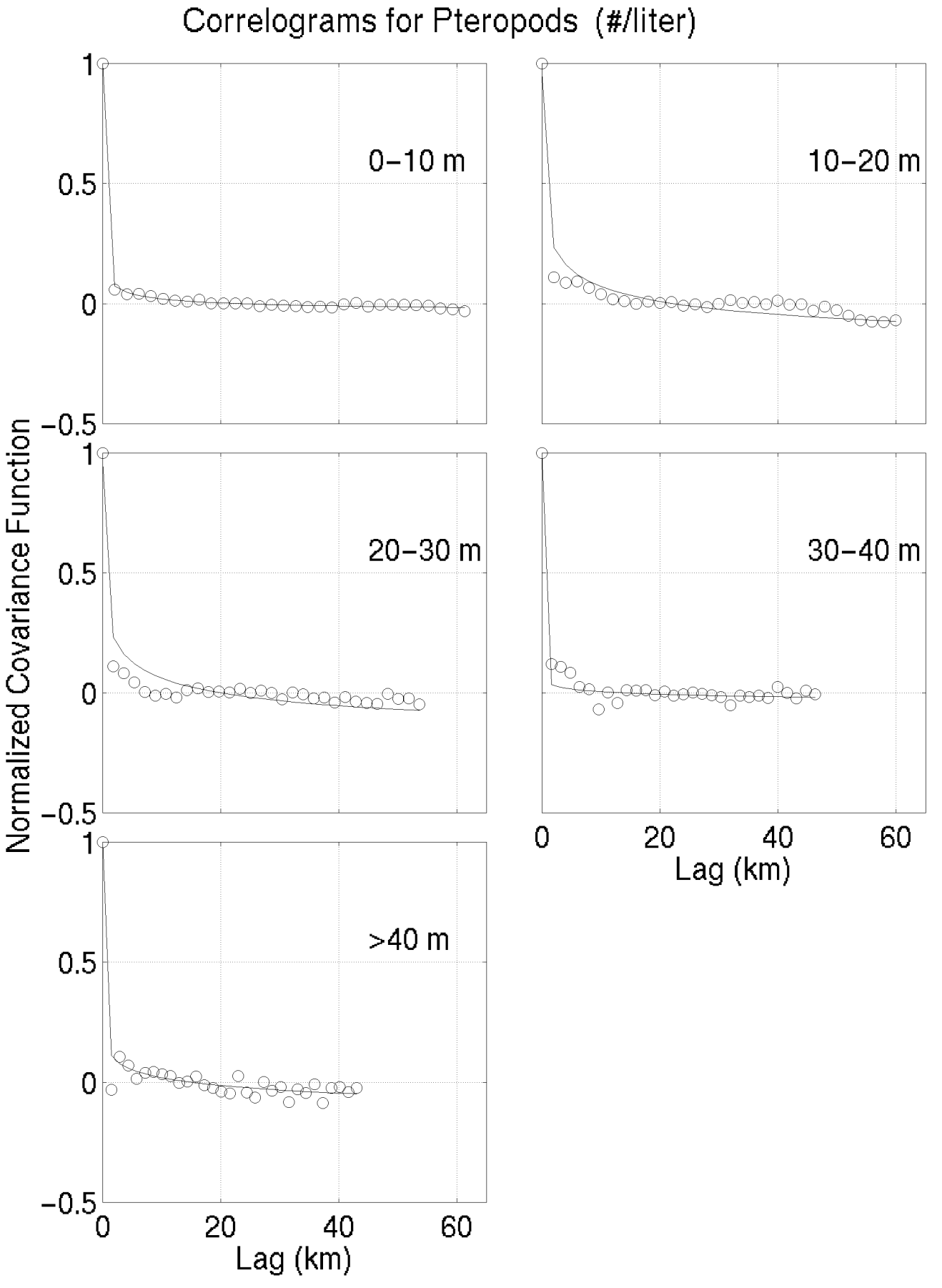
Correlograms for Pteropods (#/liter)
Normalized Covariance Function
0–10 m
10–20 m
20–30 m
30–40 m
>40 m
1
0.5
0
−0.5
0
20
40
60
Lag (km)

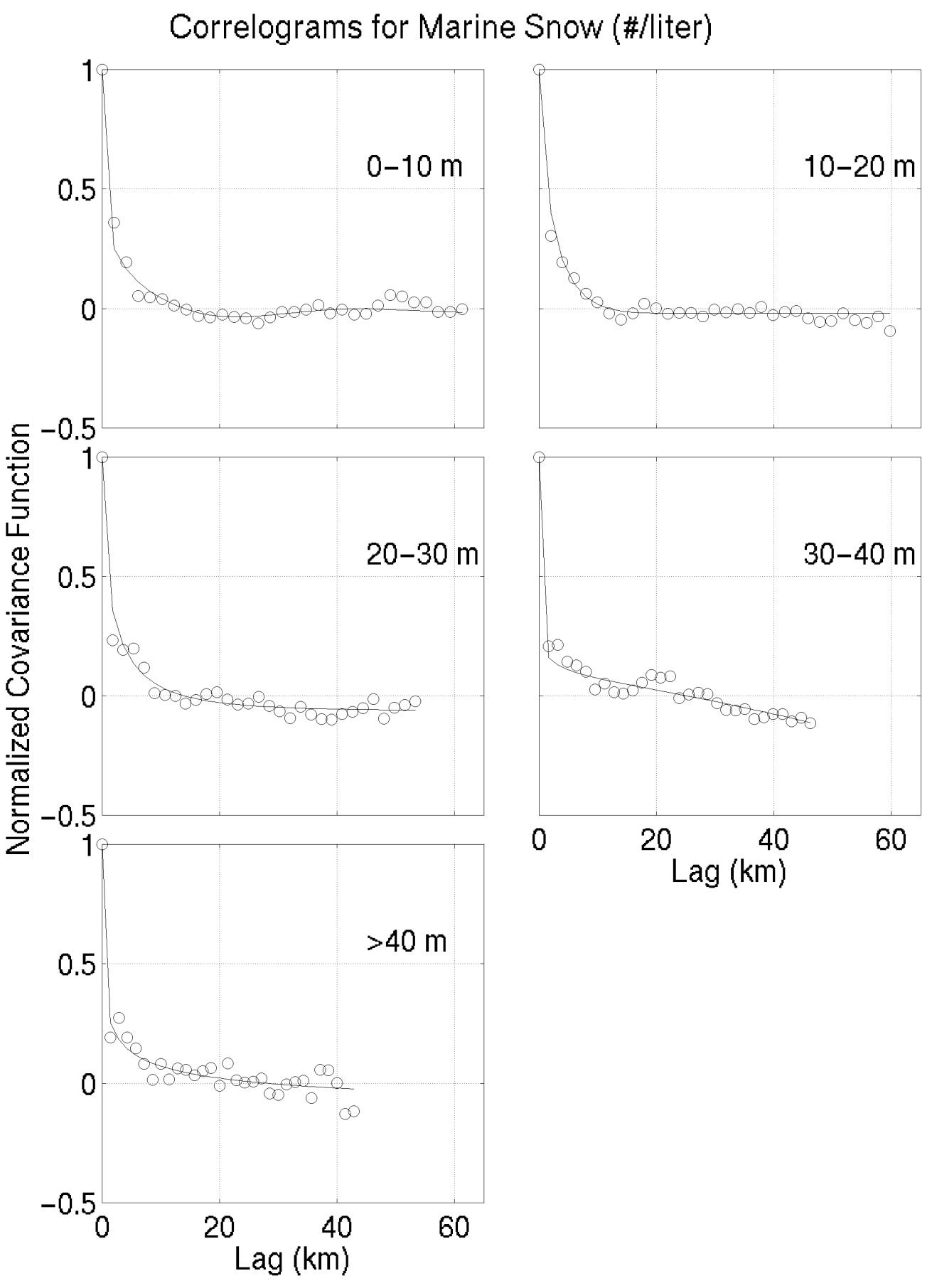
Correlograms for Marine Snow (#/liter)
Normalized Covariance Function
0–10 m
10–20 m
20–30 m
30–40 m
>40 m
1
0.5
0
−0.5
0
20
40
60
Lag (km)

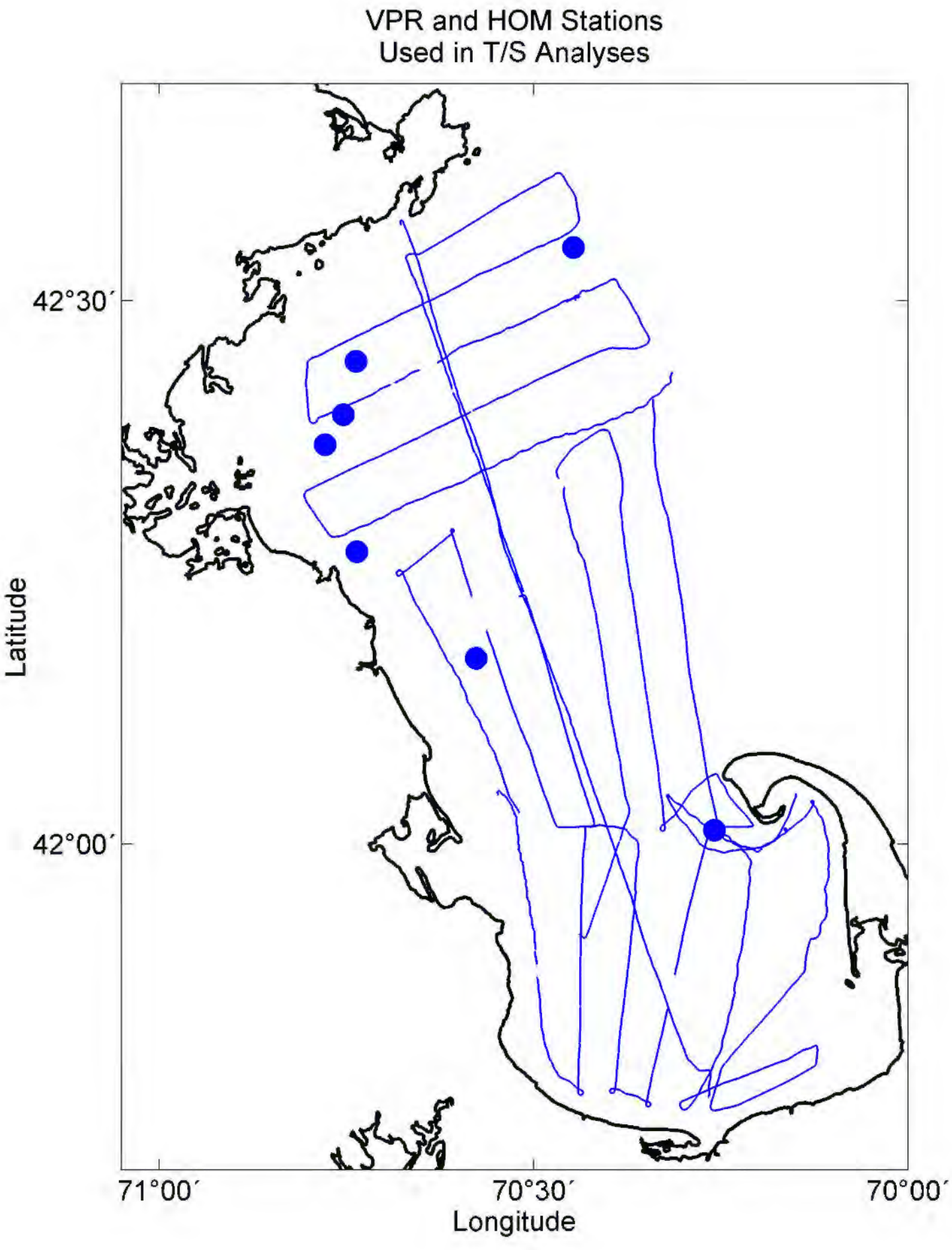
VPR and HOM Stations
Used in T/S Analyses
42°30´
42°00´
Latitude
71°00´
70°30´
70°00´
Longitude

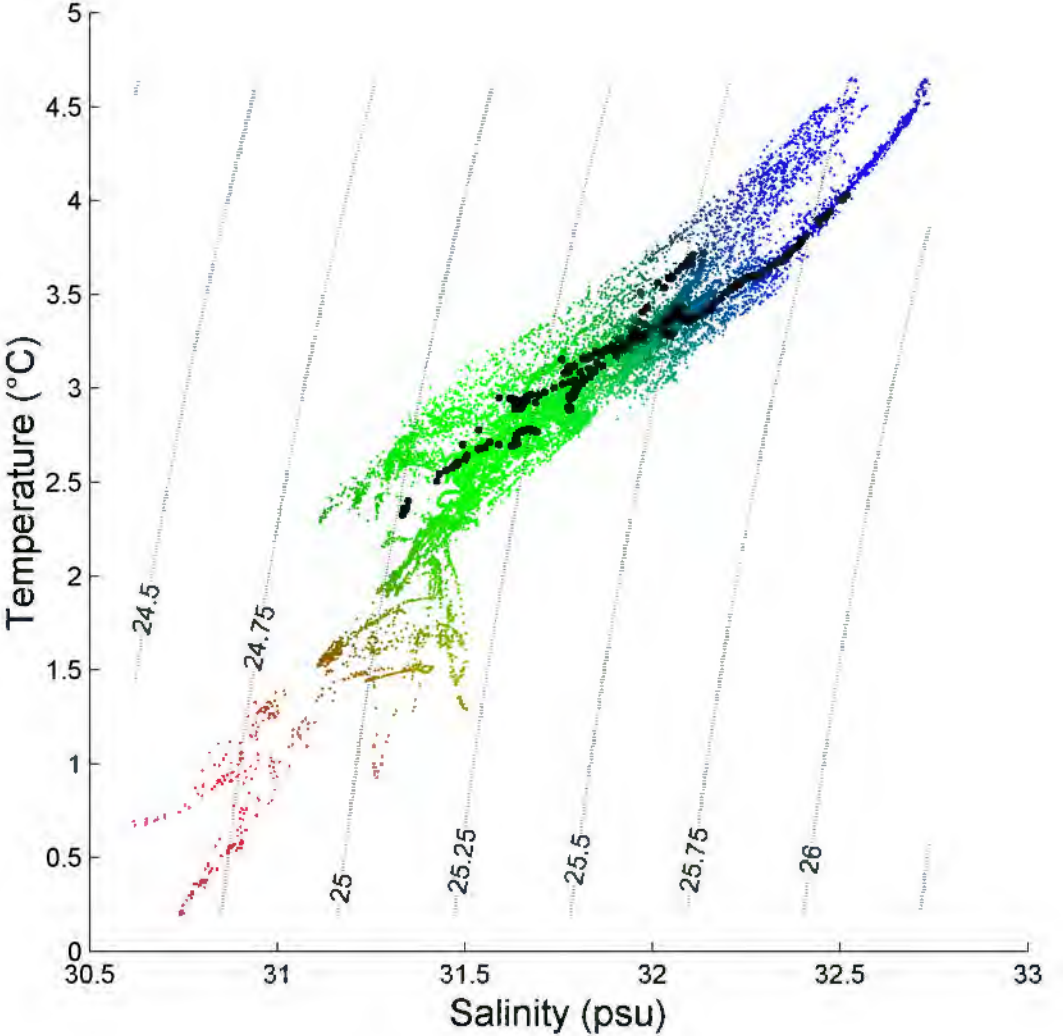
Temperature (°C)
Salinity (psu)
5
4.5
4
3.5
3
2.5
2
1.5
1
0.5
0
30.5
31
31.5
32
32.5
33
24.5
24.75
25
25.25
25.5
25.75
26

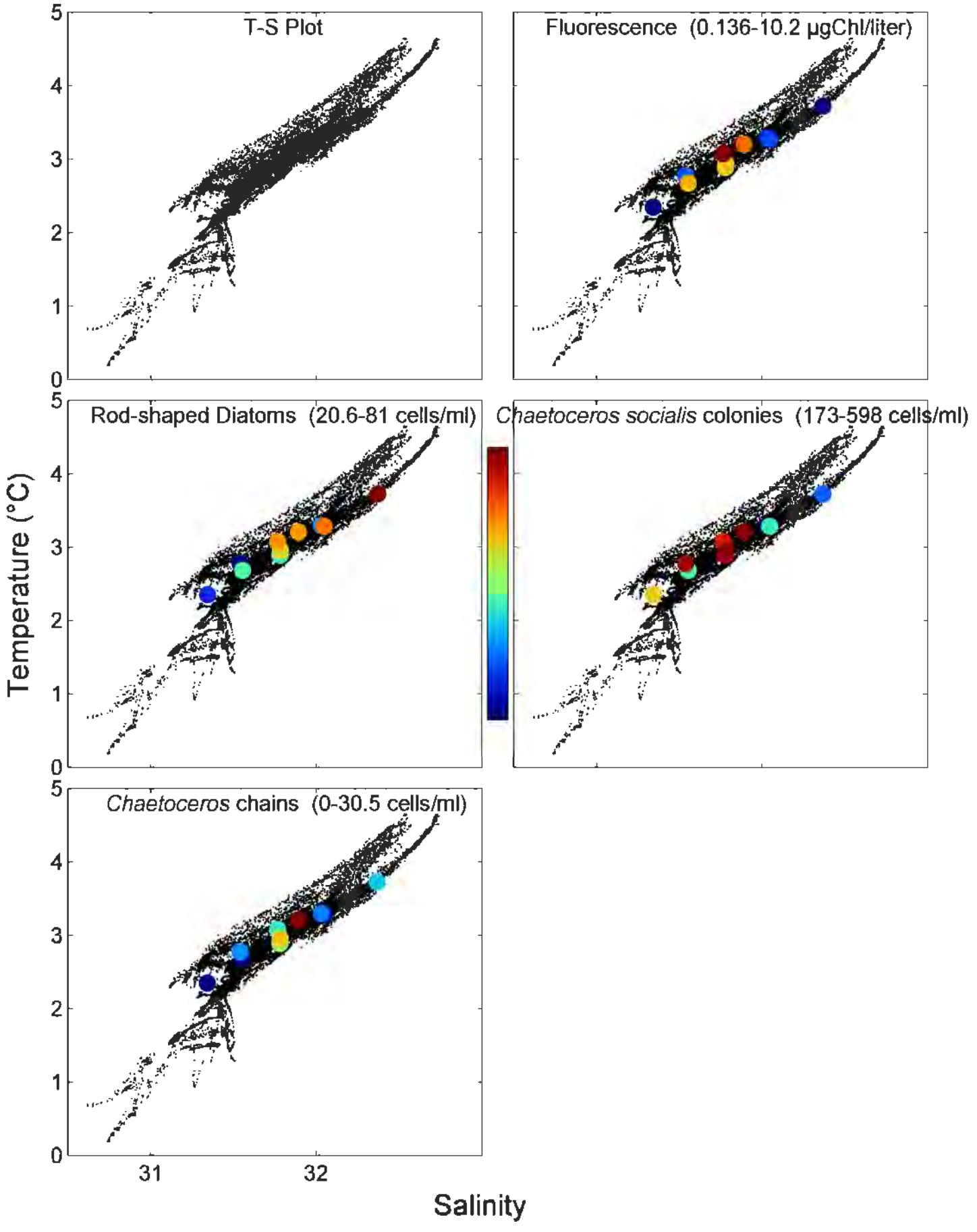
T-S Plot
Fluorescence (0.136-10.2 µgChl/liter)
Rod-shaped Diatoms (20.6-81 cells/ml)
Chaetoceros socialis colonies (173-598 cells/ml)
Chaetoceros chains (0-30.5 cells/ml)
Temperature (°C)
Salinity
0
1
2
3
4
5
31
32

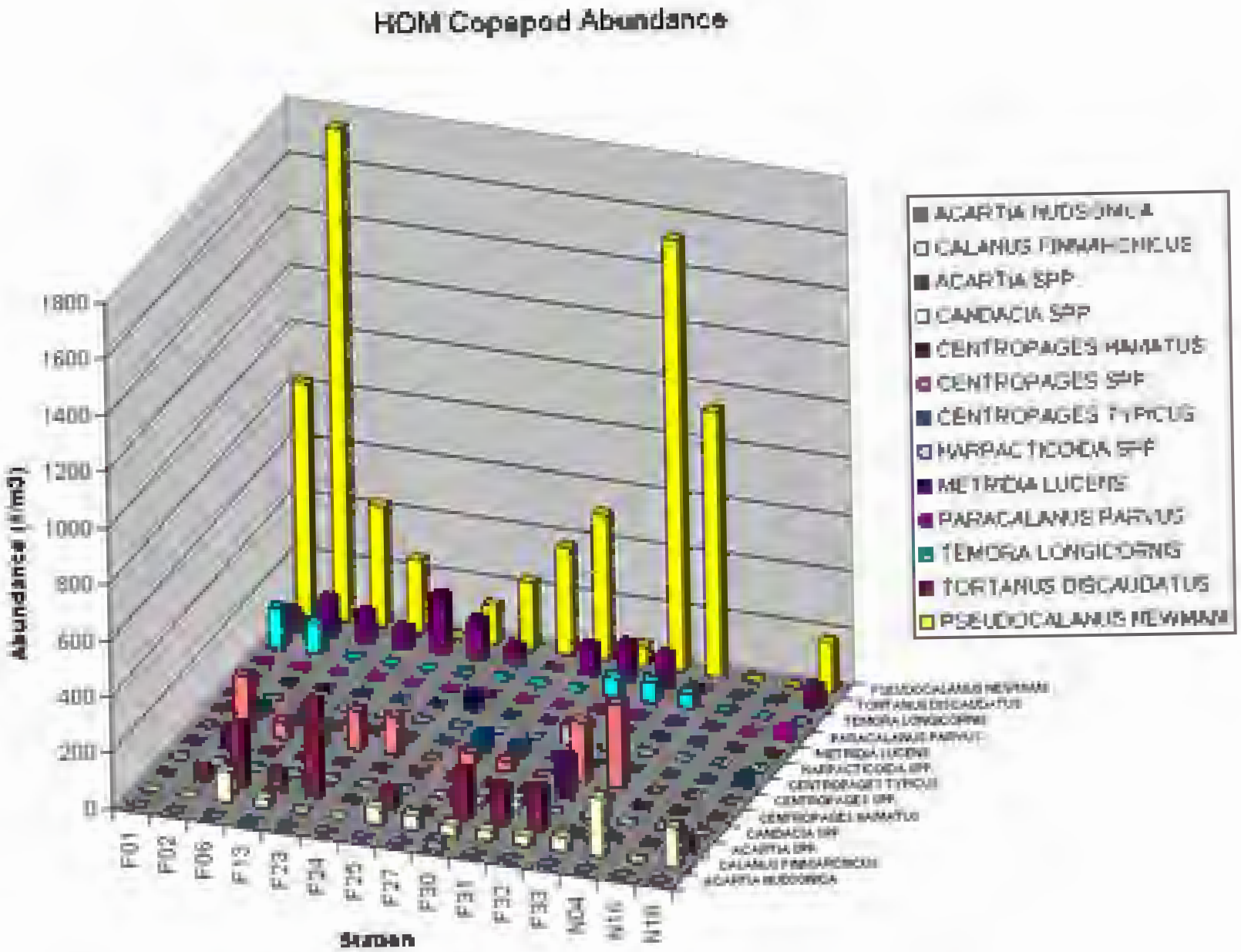
HOM Copepod Abundance
Abundance (#/m3)
1800
1600
1400
1200
1000
800
600
400
200
0
F01
F02
F06
F13
F23
F24
F25
F27
F30
F31
F32
F33
N04
N16
N18
Station
ACARTIA HUDSONICA
CALANUS FINMARCHICUS
ACARTIA SPP
CANDACIA SPP
CENTROPAGES HAMATUS
CENTROPAGES SPP
CENTROPAGES TYPICUS
HARPACTICOIDA SPP
METRIDIA LUCENS
PARACALANUS PARVUS
TEMORA LONGICORNIS
TORTANUS DISCAUDATUS
PSEUDOCALANUS NEWMANI

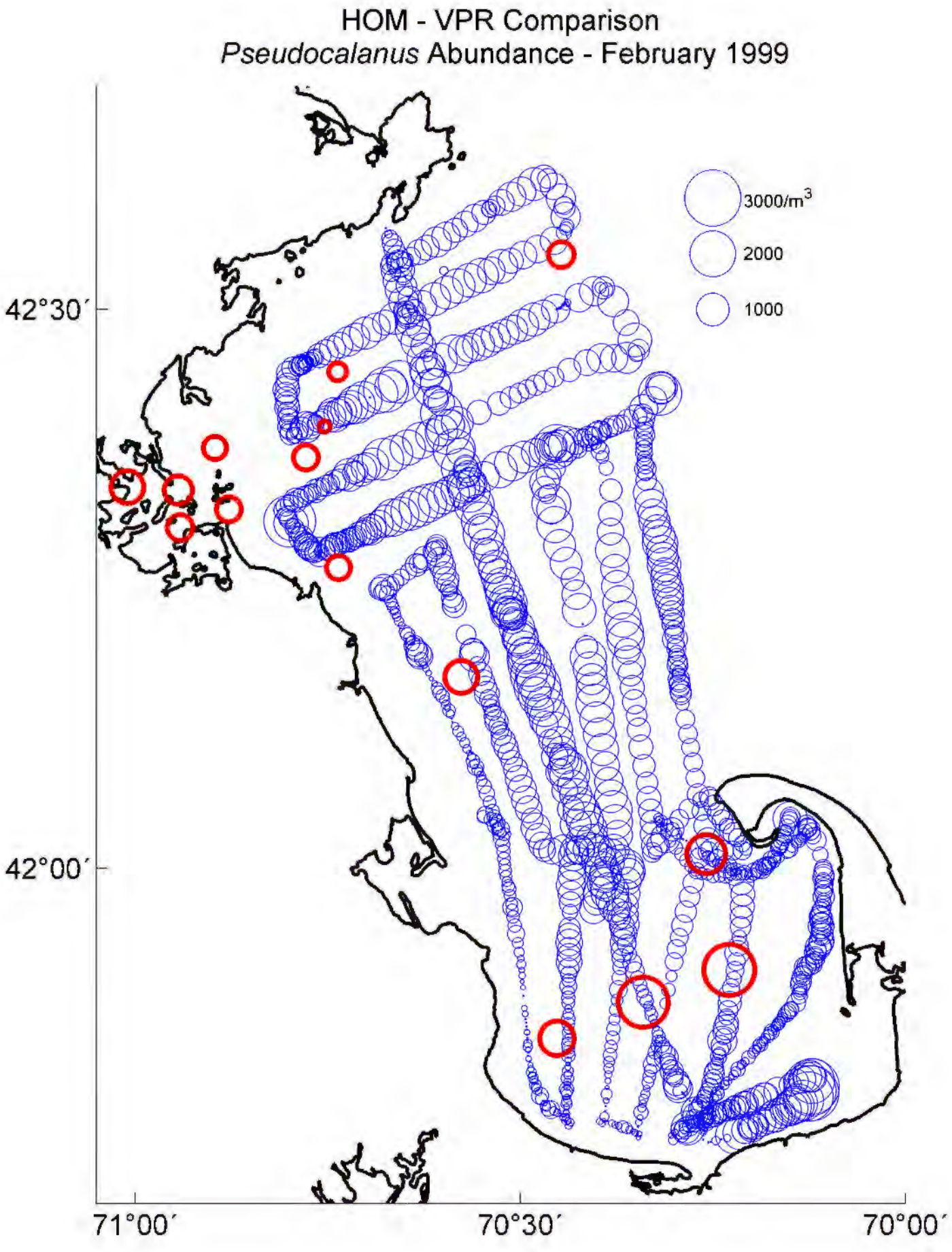
HOM - VPR Comparison
Pseudocalanus Abundance - February 1999
3000/m3
2000
1000
42°30´
42°00´
71°00´
70°30´
70°00´

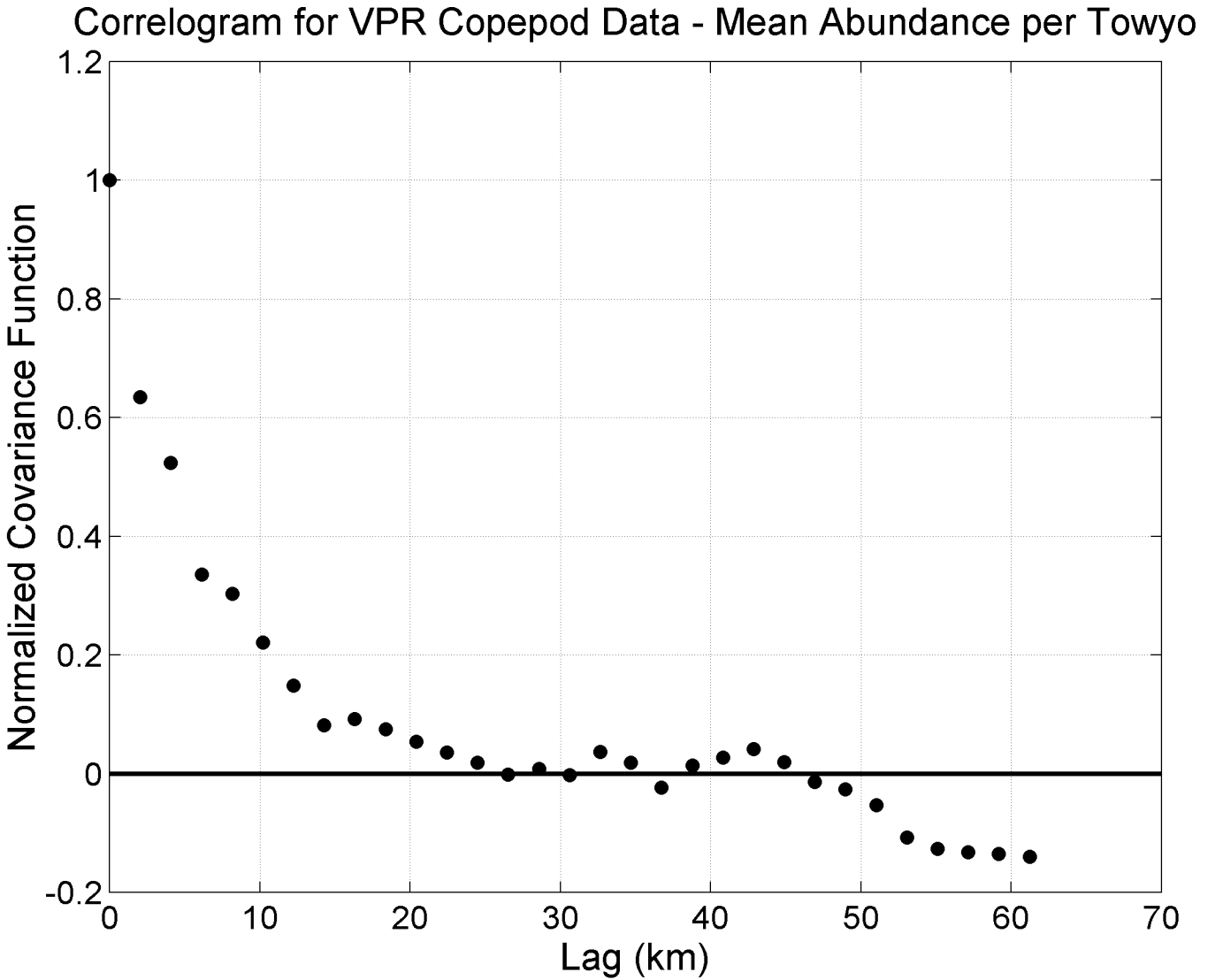
Correlogram for VPR Copepod Data - Mean Abundance per Towyo
Normalized Covariance Function
Lag (km)
1.2
1
0.8
0.6
0.4
0.2
0
-0.2
0
10
20
30
40
50
60
70

Massachusetts Water Resources Authority
Charlestown Navy Yard
100 First Avenue
Boston, MA 02129
(617) 242-6000
http://www.mwra.state.ma.us